Potent Irreversible Inhibitors of LasR Quorum Sensing in *Pseudomonas aeruginosa*

Kevin T. O'Brien[‡], Joseph G. Noto[‡], Luke Nichols-O'Neill, Lark J. Perez*

Department of Chemistry and Biochemistry, Rowan University, Glassboro, NJ 08028

* Corresponding Author Tel. 856 2564502 Email: perezla@rowan.edu

Supporting Information

Table of Contents.

A. Primary bioassay data for all new compounds

A.1. LasR Reporter Strain Bioassay

The LasR reporter strain bioassay was performed as described previously [O'Loughlin, C.T., Miller, L.C., Siryaporn, A.; Drescher, K.; Semmelhack, M.F. and Bassler, B.L. **2013** *Proc. Nat. Acad. Sci.* USA. A quorum-sensing inhibitor blocks *Pseudomonas aeruginosa* virulence and biofilm formation. *110*, 17981-17986] with modifications. Briefly, the assays were performed in *E. coli* strain BL21 DE3 Gold (Agilent) carrying a plasmid containing *lasR* (maintained with 100 µg/mL ampicillin) and a plasmid containing the *rsaL* promoter-driving expression of *gfp* (maintained with 50 µg/mL of kanamycin.) The reporter strain described above was kindly supplied by Bonnie L. Bassler (Princeton University). This *E. coli* strain was grown overnight at 37°C in Luria broth (LB) (Fisher) with the appropriate antibiotics. The overnight culture was subcultured 1:40 for bioassay analysis. The native LasR agonist, *N*-3-oxo-dodecanoyl-L-homoseriene lactone was used as a positive control for all agonist assays and was employed at a constant concentration of 50nM for all antagonist assays. The previously described antagonist, (*S*)-2-(4-bromophenyl)-*N*-(2-oxotetrahydrofuran-3-yl) acetamide was used as the positive control for antagonism [Geske, G. D.; O'Neill, J. C.; Miller, D. M.; Mattmann, M. E.; Blackwell, H. E. Modulation of Bacterial Quorum Sensing with Synthetic Ligands: Systematic Evaluation of N-Acylated Homoserine Lactones in Multiple Species and New Insights Into Their Mechanisms of Action. *J. Am. Chem. Soc.* **2007**, *129*, 13613–13625]. Compounds were added to the diluted overnight reporter strain in 96-well black microplates with clear bottoms (Corning) at the starting concentrations described and titrated by serial dilution. Plates were incubated with shaking at 37°C for 4-6h and were evaluated for fluorescence (ex485/em538) and absorbance (A_{600}) using a Molecular Devices SpectraMax M5 microplate reader. Dose-response curves were fit to the data using standard nonlinear regression data fitting settings in GraphPad Prism 6. All data points on the dose response curves define mean a with error bars describing the standard deviation.

A.1.1. Antagonism dose-response curves for compounds **12, 13, 15-18, and 24-30.**

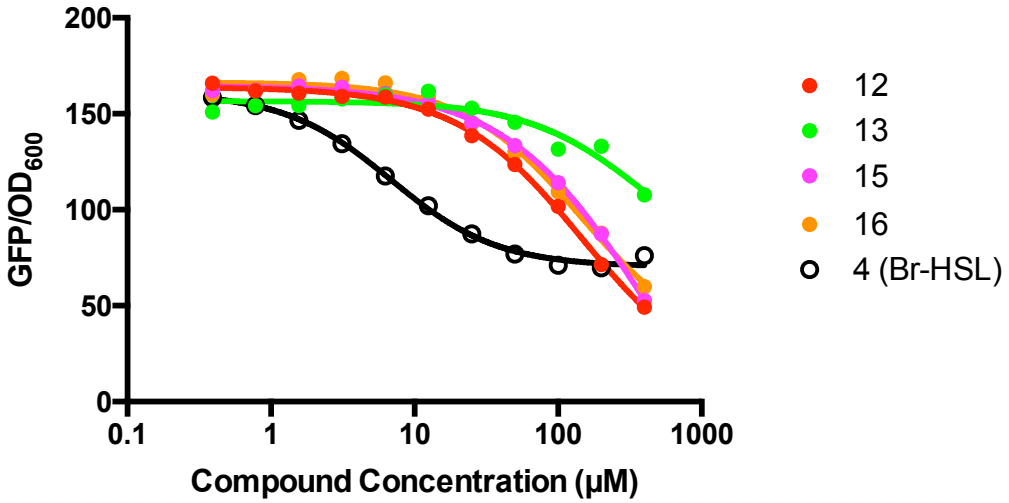

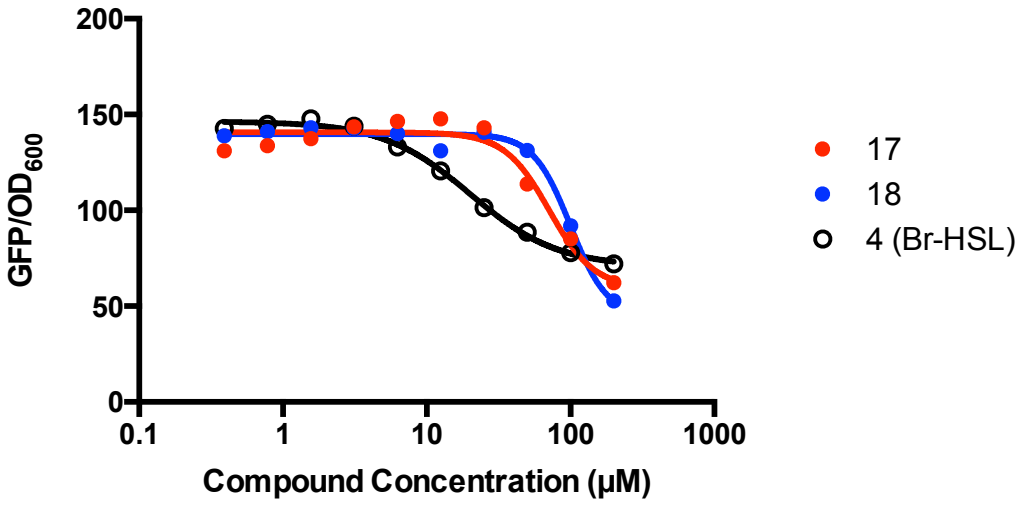
200
150
100
50
0
GFP/OD600
0.1
1
10
100
1000
Compound Concentration (μM)
17
18
4 (Br-HSL)

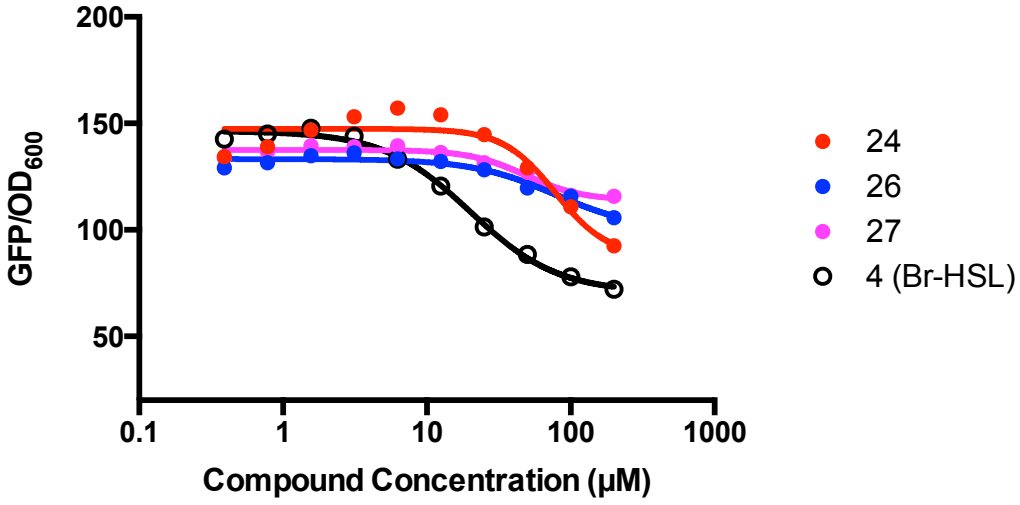
200
150
100
50
GFP/OD600
0.1
1
10
100
1000
Compound Concentration (μM)
24
26
27
4 (Br-HSL)

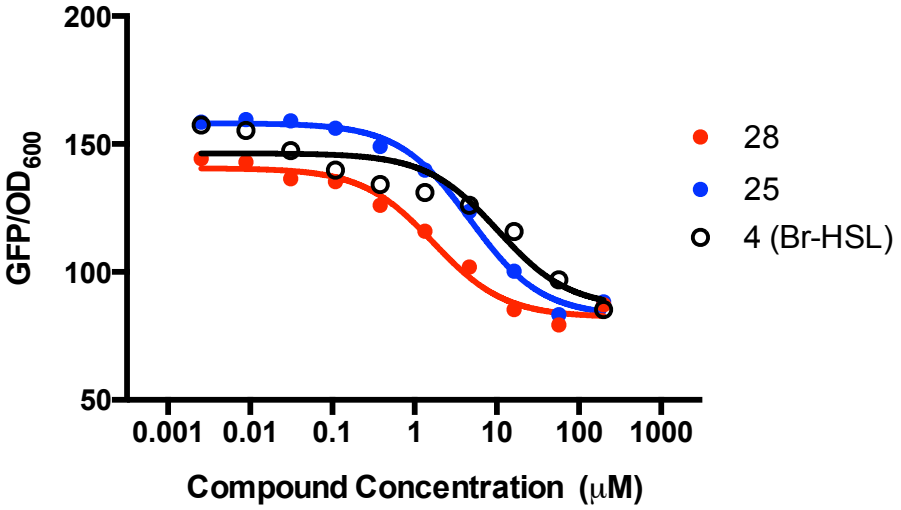
200
150
100
50
GFP/OD600
0.001
0.01
0.1
1
10
100
1000
Compound Concentration (μM)
28
25
4 (Br-HSL)

A.2. LasR Agonism Bioassay

A.2.1 Primary data for Table 2: Dose-response curves for compounds **27, 29, and 30**

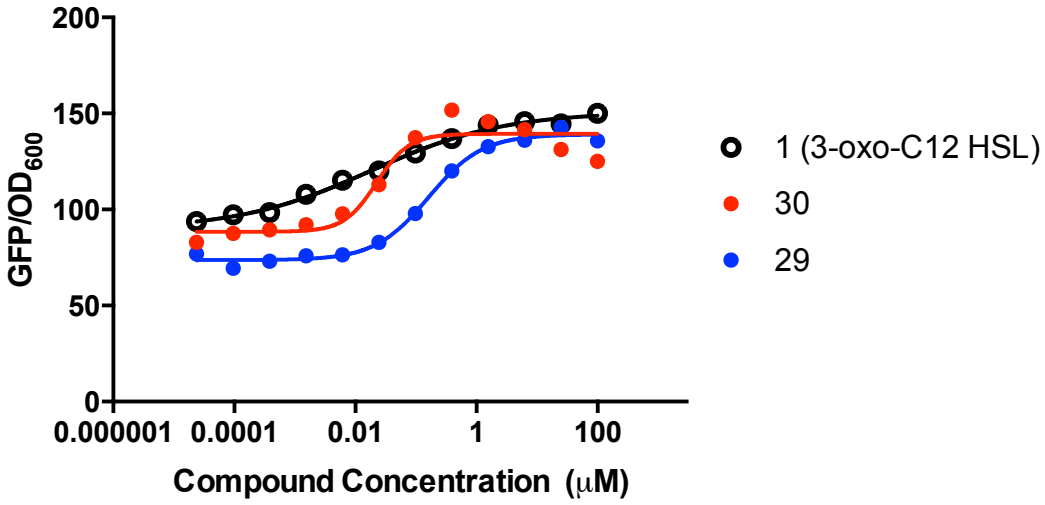

B. Competition Binding Assay for Analogs 16 and 25.

Competition binding assays were performed using the standard LasR reporter assay procedure. The diluted overnight reporter was inoculated with the designated concentration of antagonist **16**, **25**, **28** or BrHSL which was assayed as a positive control for *reversible* inhibition and was plated in 96-well black microplates with clear bottoms (Corning). The native LasR agonist was added at the starting concentrations described and titrated by serial dilution. Plates were incubated with shaking at 37°C for 4-6h and were evaluated for fluorescence (ex485/em538) and absorbance (A_{600}) using a Molecular Devices SpectraMax M5 microplate reader. Dose-response curves were fit to the data using standard nonlinear regression data fitting settings in GraphPad Prism 6. All data points on the dose response curves define mean a with error bars describing the standard deviation.

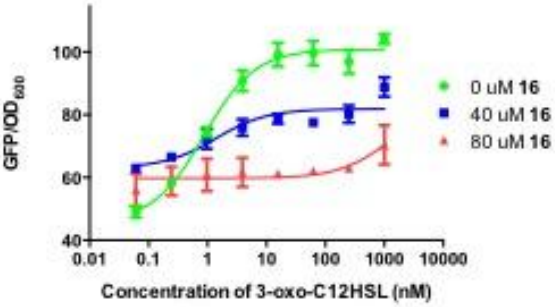

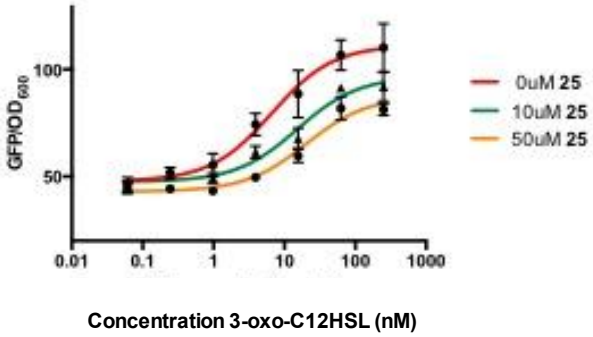

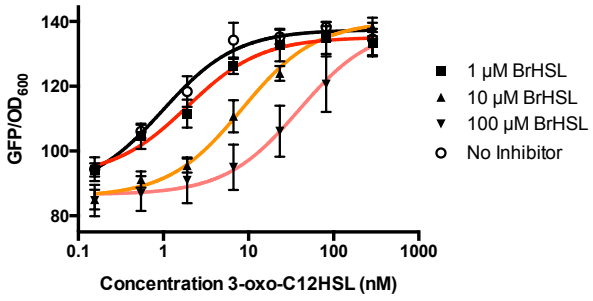

C. Virulence Factor Assays

C.1. Pyocyanin Assay

Evaluation of the effect of lead inhibitor **28** on pyocyanin expression was performed using wild-type *Pseudomonas aeruginosa* strains PAO1 (ATCC 10145) and PA14 [Rahme, L. G.; Stevens, E. J.; Wolfort, S. F.; Shao, J.; Tompkins, R. G.; Ausubel, F. M. Common Virulence Factors for Bacterial Pathogenicity in Plants and Animals. *Science* **1995**, *268*, 1899–1902] following the established procedures [O'Loughlin, C. T.; Miller, L. C.; Siryaporn, A.; Drescher, K.; Semmelhack, M. F.; Bassler, B. L. A Quorum-Sensing Inhibitor Blocks Pseudomonas Aeruginosa Virulence and Biofilm Formation. Proceedings of the National Academy of Sciences **2013**, 110, 17981–17986 and Essar D.W., Eberly L., Hadero A., Crawford I.P. Identification and characterization of genes for a second anthranilate synthase in Pseudomonas aeruginosa: interchangeability of the two anthranilate synthases and evolutionary implications. J. Bacteriol. **1990** *172*, 884–900] with modifications. Overnight cultures were prepared in Luria broth at 37^{o}C and were diluted 1:1000 into 5mL of fresh *Pseudomonas* broth [Essar D.W. *et. al.* J. Bacteriol. **1990** *172*, 884-900]. Antagonist **28** was added at the indicated concentrations and the cultures were incubated with vigorous shaking (380 r.p.m.) for 12 h. At which time an aliquot of the culture was taken for determination of OD_{600}. The cultures were centrifuged at 13.0 x 1000g for 18 minutes and were filtered through a 0.2 μm syringe-driven filter (Millipore). An aliquot of the cell-free supernatants were directly evaluated for pyocyanin levels by evaluating A_{695} as described in O'Loughlin *et al*. A 3.0 mL portion of the cell-free supernatants was extracted with 2.0 mL $CHCl_3$ and the resulting organic layer was separated and acidified with 0.5 mL 0.1 M HCl. An aliquot of the resulting acidified aqueous layer was evaluated for pyocyanin level by measurement of A_{520} as described in Essar *et al.* The experiment was performed in triplicate and all data is displayed as the mean with error bars representing the standard deviation.

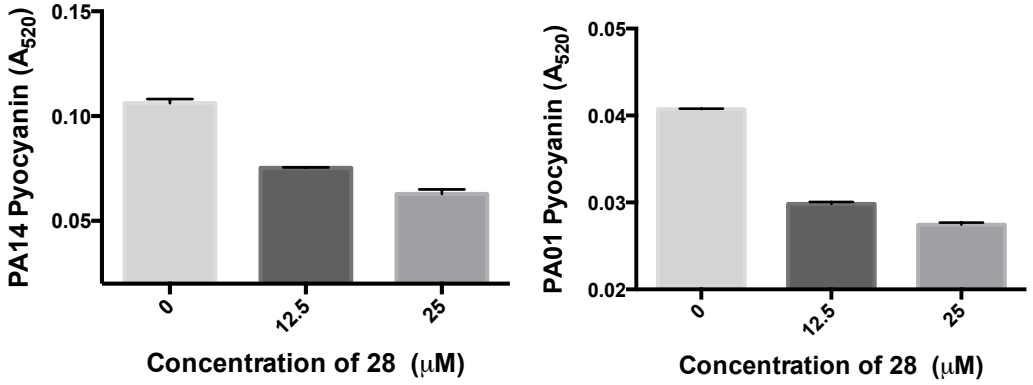

C.2. Crystal Violet Biofilm Formation Assay

Evaluation of the effect of lead inhibitor **28** on static biofilm formation was evaluated using the crystal violet staining method with *P. aeruginosa* strain PA14 [Rahme, L.G. *et. al.* Science **1995**, *268*, 1899] following the established procedure [O'Toole, G.A. Microtiter Dish Biofilm Formation Assay **2011**, J. Vis. Exp. *47* 2437]. Briefly, overnight cultures of PA14 were diluted 1:100 into M63 minimal media supplemented with $MgSO_4$, glucose and casamino acids as described previously. Compounds

were added at the indicated concentrations in a 96-well microplate before static incubation at 37°C for 48 hours. After incubation, the plates were thoroughly rinsed to remove planktonic cells and the adherent cells were quantified by staining with crystal violet and measurement of A_{550}. The assay was performed with five replicates for each compound concentration. After exclusion of the highest and lowest absorbance readings the remaining triplicate readings are described as mean with error bars representing standard deviation.

C.3. Confocal Fluorescence Microscopy Assay

Evaluation of the effect of lead inhibitor **28** on static biofilm formation was evaluated by confocal fluorescence microscopy with *P. aeruginosa* strain PA14 [Rahme, L.G. *et. al.* Science **1995**, *268*, 1899] following the established procedure [Müsken, M.; Di Fiore, S.; Römling, U.; Häussler, S. A 96-Well-Plate–Based Optical Method for the Quantitative and Qualitative Evaluation of *Pseudomonas aeruginosa* Biofilm Formation and Its Application to Susceptibility Testing. *Nat Protoc* **2010**, *5*, 1460–1469]. Briefly, overnight cultures of PA14 were diluted 1:100 into the designated media. Compounds were added at the indicated concentrations in 96-well microplates with optical grade glass bottoms (Corning) before static incubation at 37 °C for 36 hours. After incubation the samples were treated with 1.4 µM SYTO-9 nucleic acid stain and were maintained in the dark for 15 minutes before imaging on a Nikon Eclipse TI confocal microscope equipped with a 20X lens. Images were acquired from a central point in each well of the microplate. Each compound concentration was evaluated in duplicate and the experiment was repeated three times.

We note that under the different media conditions employed for biofilm growth (see media composition described below, a modified low background fluorescence media), we observe striking differences in biofilm morphology see supporting confocal images in comparison to biofilm images collected after growth in LB media described in the manuscript. In the presence of our lead inhibitor (**28**) we similarly observe significant reduction in overall biofilm biomass and mean biofilm thickness.

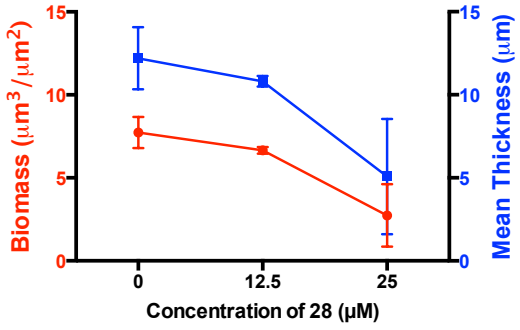

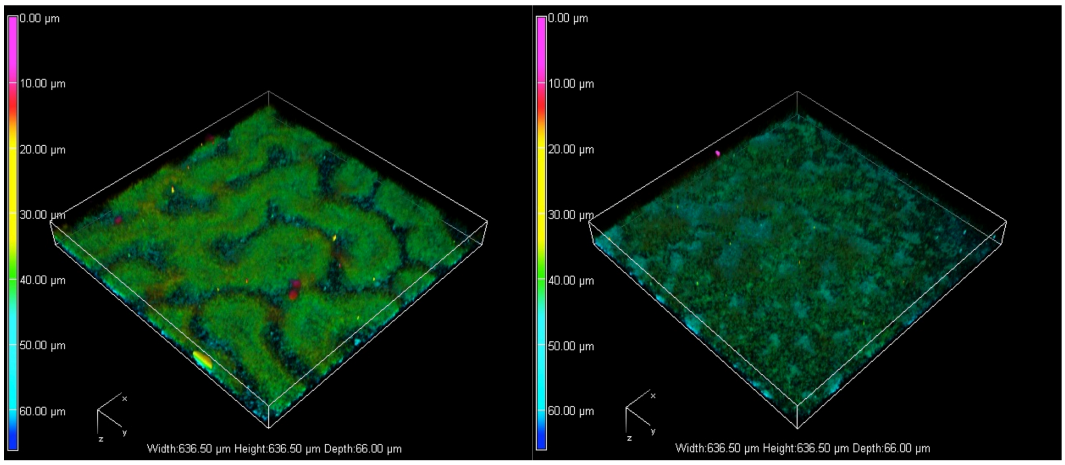

0 µM **28** 12.5 µM **28**

Composition of defined media used in the collection of this series of confocal fluorescence microscopy images:

Reagent	Molarity
KH_2PO_4	8.08 mM
K_2HPO_4	6.20 mM
NaCl	17.0 mM
D-Glucose	140.0 µM
Thiamine	66.5 nM
Biotin	41.0 nM
$(NH_4)_2SO_4$	75.7 mM
$MgSO_4$	1.0 µM
$CaCl_2$	500.0 pM
$MnCl_2$	100.0 pM
H_3BO_3	500.0 pM
$CuSO_4$	10.0 pM
$(NH_4)_6Mo_7O_{24}$	1.0 pM
Casamino acids	5 g/L

D. Molecular Modeling

D.1. Docking of Ligand 28 using SwissDock

Docking of **28** was performed using the SwissDock docking server [Grosdidier, A.; Zoete, V.; Michielin, O. SwissDock, a Protein-Small Molecule Docking Web Service Based on EADock DSS. *Nucleic Acids Research* 2011, *39*, W270–W277.]. SwissDock requires the input of two different file types, one .pdb file for the protein target, and one .mol file for molecule to be docked. The file for the target receptor LasR was prepared using the 3IX4 crystal structure [Zou, Y.; Nair, K.S. Molecular Basis for the Recognition of Structurally Distinct Autoinducer Mimics by the *Pseudomonas aeruginosa* LasR Quorum Sensing Signaling Receptor. *Chemistry & Biology* 2009, 16, 913-914.]. The ligand was manually removed from the pdb file by opening the text pdb file and deleting all atoms associated with the ligand. Ligands **28** was drawn into ChemBioDraw 13.0 and saved as a .mol file. The .mol file was converted into a .mol2 file using OpenBabel file converter program. SwissDock allows only a few parameters to be altered, namely the docking type and specification of the region of interest within the protein. The docking type selected for these experiments was the very fast parameter, as the ligands contain less than fifteen rotatable bonds, the fast binding modes were deemed sufficient. No region of interest was specific for these experiments. The .mol2 file of **28** and the pdb file of 3IX4 LasR were submitted to the SwissDock docking server. The SwissDock docking server is based on EADock DSS docking software [Grosdidier, A.; Zoete, V.; Michielin, O.; Fast docking using the CHARMM force field with EADock DSS. *J. Comput. Chem. 2011*]. Initially a range of 5000 to 15000 binding modes are generated in near cavities of the protein or on the surface of the protein. As each of the binding modes are generated the CHARMM force field energies are calculated on a grid and a ranking of the most favorable binding modes is generated on the basis of the calculated energies [Brooks, B.R.; Brooks, C.L. III; Mackerell, A.D.; Nilsson, L.; Petrella, R.J.;, Roux, B.; Won, Y.; Archontis, G.; Bartels, C.; Boresch, S.; *et al.* CHARMM: the biomolecular simulation program. *J. Comput. Chem.,* 2009, 30, 1545-1614.]. The energy of solvation is taken into consideration using FACTS implicit solvation model [Haberthur, U.; Caflisch, A.; FACTS: fast analytical continuum treatment of solvation. *J. Comput. Chem.*, 2008, 29, 701-715. The most favorable binding modes are dumped into the output result file. The output zip file was extracted and the ligand clusters text file was opened. The poses with the most favorable free energies and relevant binding locations were copied from the cluster text file and pasted into the LasR pdb file. The three most favorable poses were nearly superimposable with the coordinates of the ligand-binding site of TP1 within the binding pocket of LasR. The free energy of binding and the total free energy of the protein ligand complex were recorded. Cluster 0 pose 0 (lowest energy) was the pose that was used to create the images found in Figure 3. The images disclosed herein were visualized using VMD molecular graphics system and PyMOL molecular graphics system.

Tabulated Binding Data

Compound[a]	$\Delta G_{FullFitness}$	$\Delta G_{binding}$
28_0	-1086.36	-9.66
28_1	-1086.35	-9.66
28_2	-1001.54	-6.76
25_0	-1050.01	-8.54
25_1	-1035.54	-6.46
25_2	-1031.52	-6.96

[a]subscript values indicate pose number

Three lowest energy poses for **28** highlighting key amino acid interactions with LasR W60, D73 and C79.

Pose #0:

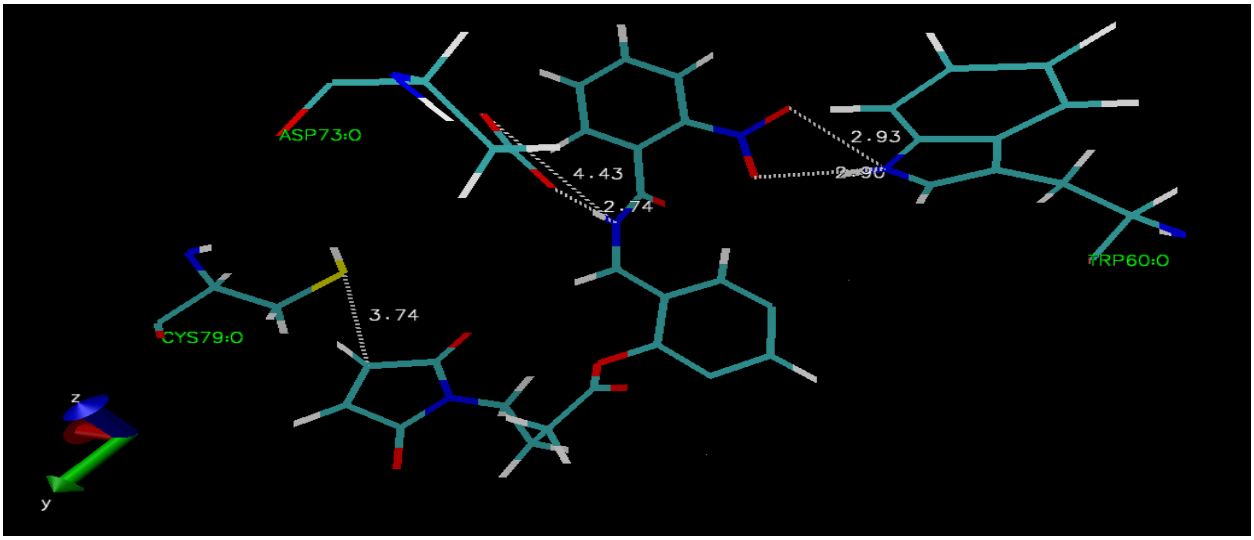

Pose #1:

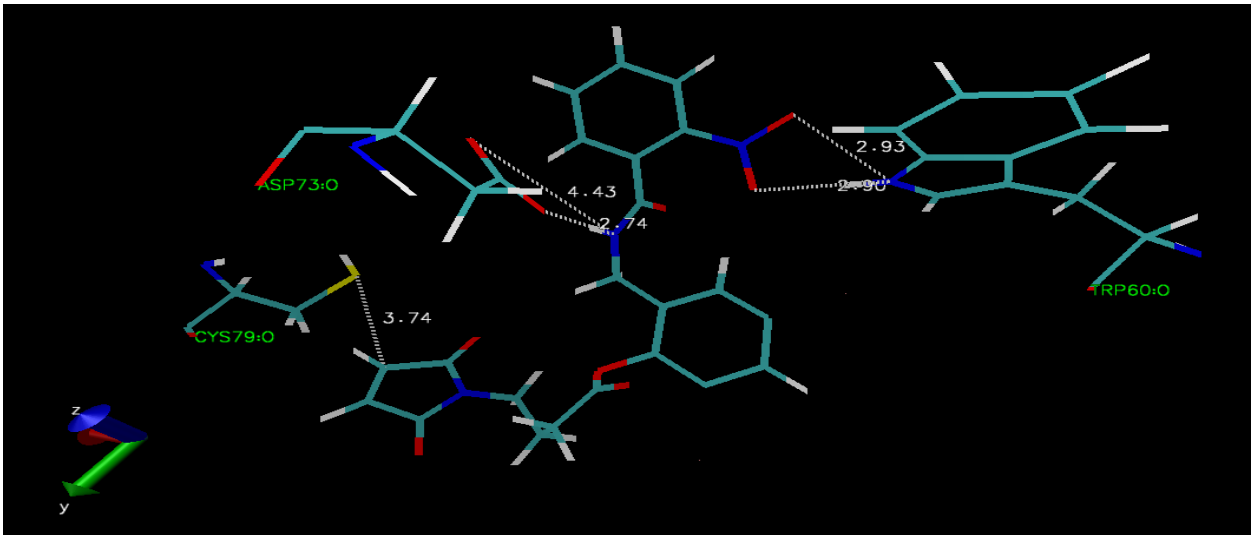

Pose #2:

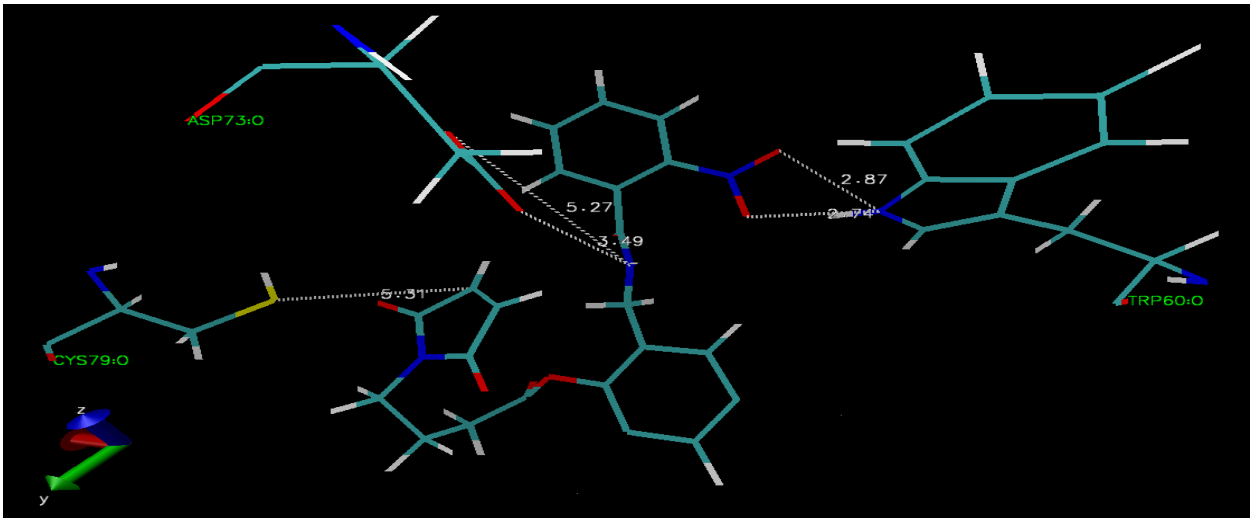

Three lowest energy poses for **25** highlighting key amino acid interactions with LasR W60, D73 and C79.

Pose #0:

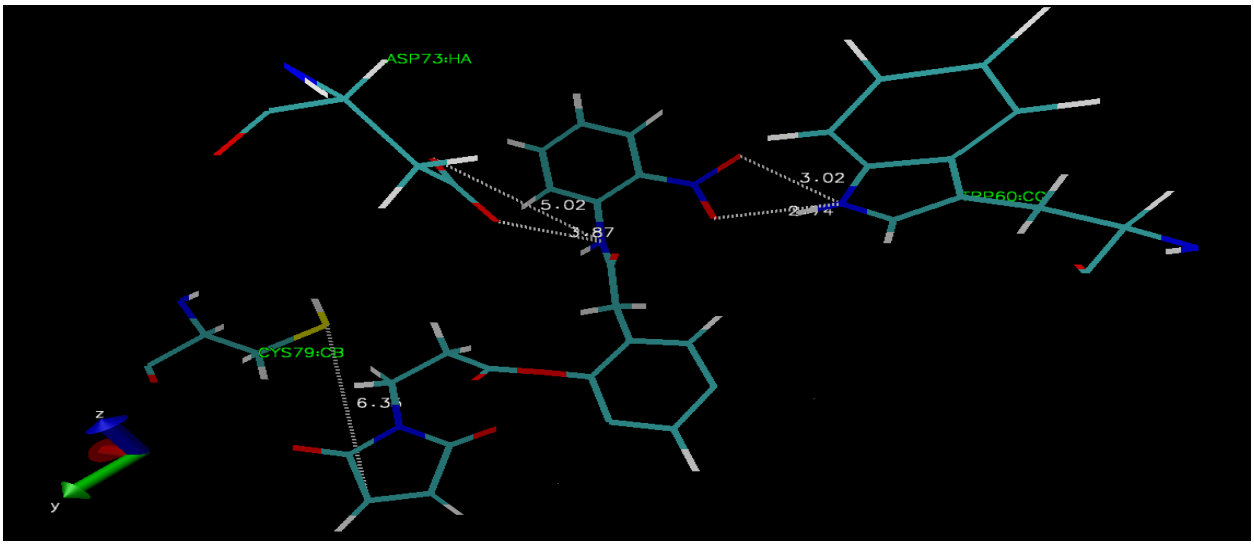

Pose #1:

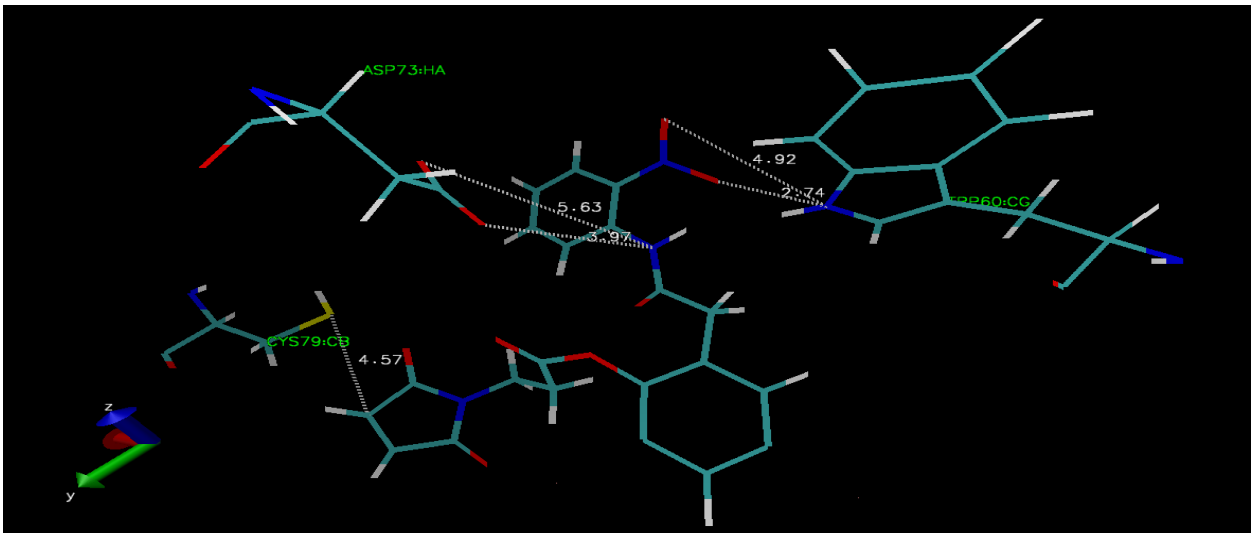
ASP73:HA
4.92
2.74
5.63
3.97
CYS79:CB
4.57
z
y

Pose #2:

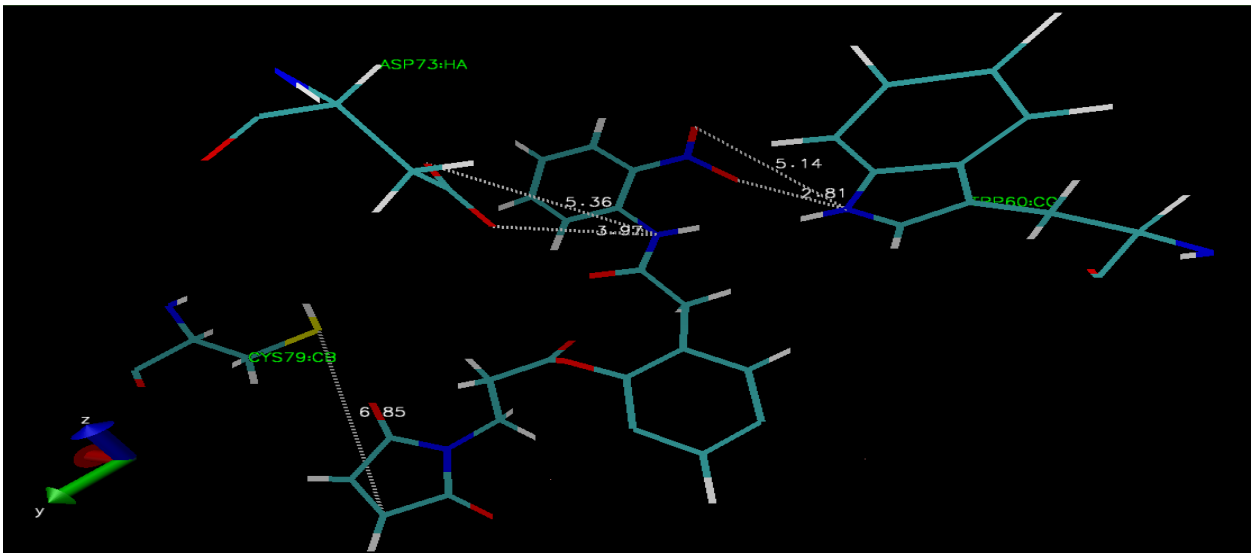
ASP73:HA
5.14
2.81
5.36
3.97
CYS79:CB
6.85
z
y

D.2. Pharmacophore Model

Pharmacophore model generation was carried out using the software Ligand Scout. Ligand Scout version 3.03b [inteligand.com, Wolber, G.; Langer, T. LigandScout: 3-D Pharmacophores Derived From Protein-Bound Ligands and Their Use as Virtual Screening Filters. *J. Chem. Inf. Model.* **2005**, *45*, 160–169.] was used following the standard settings for "Best" fit pharmacophore modeling. The "Training Set" consisted of a single low energy conformer of **28** within the HSL-binding pocket of LasR as identified above. Ligands **24–27** were prepared as .mol files using ChemBioDraw 14.0. The .mol files were imported into Ligand Scout, 500 unique conformers for each of the ligands was generated as "Test Set" compounds to provide 10 best fit models which served as the pharmacophore model.

E. Compound synthesis and tabulated compound data

E.1. General Experimental.

Unless otherwise noted, all reactions were performed in flame-dried glassware under an atmosphere of nitrogen or argon using dried reagents and solvents. All chemicals were purchased from commercial vendors and used without further purification. Anhydrous solvents were purchased from commercial vendors.

Flash chromatography was performed using standard grade silica gel 60 230-400 mesh from SORBENT Technologies or was performed using a Biotage Flash Purification system equipped with Biotage SNAP columns. Silica gel was loaded into glass columns as a slurry. All purifications were performed using gradients of mixtures of ethyl acetate and hexanes. Analytical thin-layer chromatography was carried out using Silica G TLC plates, 200 µm with UV_{254} fluorescent indicator (SORBENT Technologies), and visualization was performed by staining and/or by absorbance of UV light.

NMR spectra were recorded using a Varian Mercury Plus spectrometer (400 MHz for ^{1}H-NMR; 100 MHz for ^{13}C-NMR). Chemical shifts are reported in parts per million (ppm) and were calibrated according to residual protonated solvent. Low-resolution LC-MS data was collected using an Agilent 1100-Series LC/MSD Trap LC-MS equipped with a Phenomenex Kinetex 2.6 µm C18-UPLC column using a gradient of water to acetonitrile with 0.1% formic acid in positive ionization mode. High-resolution mass spectral analysis was performed using an Agilent 1200-series electrospray ionization – time-of-flight (ESI-TOF) mass spectrometer in the positive ESI mode.

All final compounds were evaluated to be of greater then 90% purity by analysis of ^{1}H-NMR, ^{13}C-NMR, HRMS and/or LC-MS data.

C.2. Compound Synthesis

General Procedures:

Typical procedure for the synthesis of analogs **11, 12, S5, and S6** (for specific details see below).

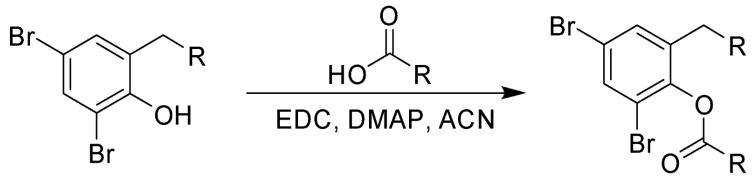

To a solution of the phenol (1.0 eq) in ACN (0.05 M) at room temperature was added the carboxylic acid (2.0 eq), 1-Ethyl-3-(3-dimethylaminopropyl)carbodiimide (4.0 eq), and catalytic 4-dimethylaminopyridine. The mixture was stirred at room temperature overnight. The reaction mixture was concentrated to dryness and resuspended in ethyl acetate (0.05 M). The mixture was quenched with HCl (0.5 M), washed with brine (0.5 M), and dried over Na_2SO_4. The organic phase was concentrated on silica and purified by silica gel chromatography.

Typical procedure for the synthesis of intermediates **S2, S3, and S4** (for specific details see below).

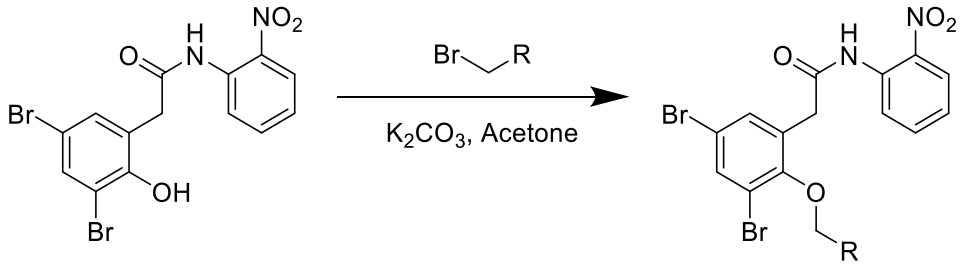

To a solution of the phenol (1.0 eq) in ACN (0.1 M) at room temperature was added potassium carbonate (1.2 eq) and the alkyl bromide (1.2 eq). The reaction mixture was heated to reflux and allowed to stir overnight. Silica gel was added directly to the reaction vessel, the mixture was concentrated *in vacuo*, and the material was purified by silica gel chromatography.

Typical procedure for the synthesis of analogs **15 and 16** (for specific details see below).

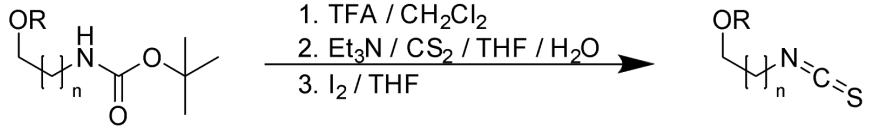

To a solution of the Boc protected amine (1.0 eq) in dichloromethane (0.1 M) at 0 °C under N_2 was slowly added neat TFA (0.1 M). The mixture was allowed to warm to room temperature for 2 h. Upon completion, the suspension was concentrated to dryness *in vacuo*. The material was resuspended in tetrahydrofuran (0.1 M) and H_2O (0.1 M) before the addition of triethylamine (7.2 eq) and carbon disulfide (9.0 eq). The mixture was allowed to stir at room temperature overnight. Iodine (1.1 eq) was dissolved in tetrahydrofuran (0.1 M) and cooled to 0 °C. To the iodine suspension at 0 °C was added the reaction mixture dropwise. The mixture was allowed to stir and warm to room temperature over a period of two hours. Upon completion, the reaction mixture was quenched with HCl (1.0 eq) and Na_2SO_3 (2.0 eq). The solution was extracted with ethyl acetate three times and the organic phases were dried over Na_2SO_4. The crude product was purified by silica gel chromatography.

Typical procedure for the synthesis of analogs **24, and 26-30** (for specific details see below)

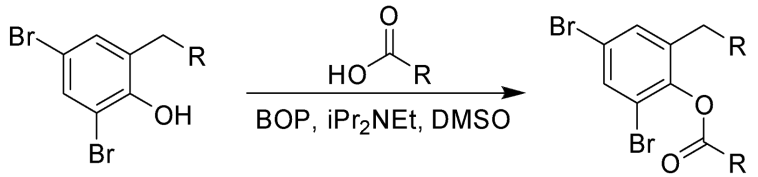

To a solution of the phenol (1.0 eq) in DMSO (0.02 M) at room temperature under N_2 was added the carboxylic acid (1.5 eq), iPr_2NEt (3.0 eq), and BOP (1.5 eq). The mixture was allowed to stir at room temperature overnight. To the reaction mixture was added 50 mL of H_2O and 50 mL of EtOAc upon completion. The organic phase was collected and the water layer was extracted three times with 50 mL

of EtOAc. Organic layers were pooled and washed with HCl, Na_2CO_3, and NaCl. The resulting solution was dried over Na_2SO_4, concentrated to dryness *in vacuo*, and purified by silica gel chromatography.

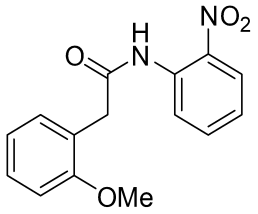

2-(2-methoxyphenyl)-*N*-(2-nitrophenyl)acetamide, 6. To a solution of 2-methoxyphenyl acetic acid (6.75 g, 40.62 mmol) and 2-nitroaniline (3.76 g, 27.22 mmol) in ACN (91 mL, 0.3 M) was slowly added $SOCl_2$ (2.96 mL, 40.62 mmol). The mixture was heated to reflux and allowed to stir for three hours. Upon completion the reaction was concentrated to dryness. The material was resuspended in CH_2Cl_2, washed with 1 M NaOH (40 mL), 1 M HCl (40 mL), saturated $NaHCO_3$ (40 mL), saturated NaCl (40 mL), and dried over Na_2SO_4. The crude product was purified by silica gel chromatography to provide 2-(2-methoxyphenyl)-*N*-(2-nitrophenyl)acetamide (7.17 g, 92.0% yield). ^{1}H-NMR (400 MHz, $CDCl_3$) δ 10.36 (s, 1H), 8.76 (dd, *J*=8.8, 1.6 Hz, 1H), 8.14 (dd, *J*=8.8, 1.6 Hz, 1H), 7.62-7.58 (m, 1H), 7.37-7.31 (m, 2H), 7.15-7.11 (m, 1H), 7.02-6.93 (m, 2H), 3.91 (s, 3H), 3.82 (s, 2H). ^{13}C-NMR (100 MHz, $CDCl_3$) δ 170.6, 157.1, 136.4, 135.6, 134.8, 131.3, 129.4, 125.5, 122.9, 122.3, 122.0, 121.0, 110.7, 55.3, 40.5.

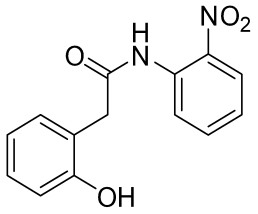

2-(2-hydroxyphenyl)-*N*-(2-nitrophenyl)acetamide, S1. To a solution of 2-(2-methoxyphenyl)-*N*-(2-nitrophenyl)acetamide (6.93 g, 24.21 mmol) in CH_2Cl_2 (161.4 mL, 0.15 M) at -78 °C was slowly added BBr_3 (2.33 mL, 24.21 mmol). The mixture was allowed to stir and the temperature was maintained below -30 °C for 4h. Upon completion, the reaction mixture was cooled to -78 °C and quenched with saturated $NaHCO_3$ (30 mL). The organic phase was collected, washed with brine, and dried over Na_2SO_4. The crude product was purified by silica gel chromatography to provide 2-(2-hydroxyphenyl)-*N*-(2-nitrophenyl)acetamide (3.98 g, 60.5 % yield). ^{1}H-NMR (400 MHz, $CDCl_3$) δ 10.60 (s, 1H), 8.72 (dd, *J* = 8.8, 1.2 Hz, 1H), 8.16 (dd, *J* = 8.4, 1.6 Hz, 1H), 7.62 (td, *J* = 8.8, 1.6 Hz, 1H), 7.48 (s, 1H), 7.24 – 7.16 (m, 3H), 6.96 – 6.91 (m, 2H), 3.84 (s, 2H). ^{13}C-NMR (100 MHz, $CDCl_3$) δ 171.8, 154.8, 136.7, 135.9, 134.2, 131.2, 129.5, 125.7, 123.8, 122.5, 121.1, 120.4, 116.9, 41.7.

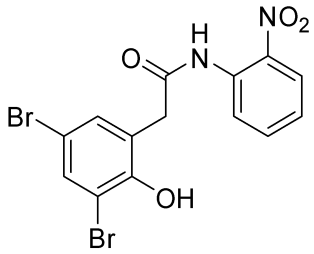

2-(3,5-dibromo-2-hydroxyphenyl)-*N*-(2-nitrophenyl)acetamide, 7. To a solution of 2-(2-hydroxyphenyl)-*N*-(2-nitrophenyl)acetamide (2.36 g, 8.67 mmol) in acetic acid (173.4 mL, 0.05 M) at room temperature was added dropwise a solution of Br_2 (1.33 mL, 26.0 mmol). The reaction mixture was allowed to stir at room temperature for 1h. The reaction was quenched by the addition of H_2O (50 mL). The slurry was filtered and the filtrate was discarded. The crude product was purified by silica gel chromatography to provide 2-(3,5-dibromo-2-hydroxyphenyl)-*N*-(2-nitrophenyl)acetamide (3.15 g, 84.5 % yield). ^{1}H-NMR (400 MHz, $CDCl_3$) δ 10.58 (s, 1H), 8.74 (d, *J* = 8.4 Hz, 1H), 8.19 (d, *J* = 8.4 Hz, 1H), 7.64 (t, *J* = 8.8 Hz, 1H), 7.59 (d, *J* = 2.4 Hz, 1H), 7.37 (d, *J* = 2.0 Hz, 1H), 7.19 (t, *J* = 8.0 Hz, 1H), 6.76 (s, 1H), 3.83 (s, 2H). ^{13}C-NMR (100 MHz, $CDCl_3$) δ 169.5, 150.2, 136.5, 136.0, 134.3, 134.0, 133.4, 125.8, 123.7, 123.3, 122.3, 112.9, 111.8, 41.0. ESI-MS calculated for $C_{14}H_{11}Br_2N_2O_4$ 428.9 ($M+H^+$), observed 429.0 ($M+H^+$).

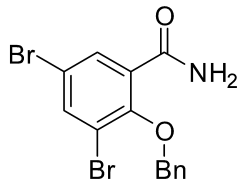

2-(benzyloxy)-3,5-dibromobenzamide, **9**. To a solution of 3,5-dibromo-2-hydroxybenzamide, **8** (21.51g, 72.93 mmol) in acetone (729.3 mL, 0.1 M) was added K_2CO_3 (12.09g, 87.48 mmol), and benzyl bromide (10.41 mL, 87.52 mmol). The reaction mixture was heated to reflux and allowed to stir overnight. Upon completion, the solution was filtered and the filtrate was concentrated to dryness. The crude product was recrystallized in acetone to provide 2-(benzyloxy)-3,5-dibromobenzamide (12.5 g, 44.5 % yield). ^{1}H-NMR (400 MHz, $CDCl_3$) δ 8.18 (d, *J* = 2.4 Hz, 1H), 7.89 (d, *J* = 2.4 Hz, 1H), 7.53-7.41 (m, 5H), 5.88 (bs, 1H), 5.01 (s, 2H).

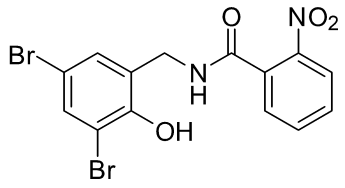

***N*-(3,5-dibromo-2-hydroxybenzyl)-2-nitrobenzamide, 10.** To a solution 2-(benzyloxy)-3,5-dibromobenzamide, **8** (4.90 g, 12.73 mmol) in THF (31.8 mL, 0.4 M) at room temperature was added BH_3 DMS (3.63 mL, 38.25 mmol). The mixture was allowed to stir at room temperature for 1 h then heated to reflux overnight. The reaction was cooled to 0 °C then slowly quenched with 30 mL MeOH. The

solution was heated to reflux and allowed to react for 30 min before cooling the mixture to room temperature and concentrating the solution to dryness. The resulting residue was dissolved in 60 mL MeOH and 40 mL HCl (1 M) was added. The resulting suspension was heated to reflux for 1 h at which time the majority of the material had dissolved. The insoluble material was removed by filtration while hot and the solution was allowed to crystalize at room temperature providing (2-(benzyloxy)-3,5-dibromophenyl)methanamine hydrochloride. To a solution of 2-nitrobenzoic acid (534.8 mg, 3.2 mmol) in CH_2Cl_2 (32 mL, 0.1 M) at 0 °C was added dropwise $(COCl)_2$ (549 µL, 6.4 mmol), followed by catalytic DMF. The mixture was allowed to stir for 1 h and warm to room temperature. The solution was concentrated to dryness and resuspended in ACN (32 mL, 0.1 M). (2-(benzyloxy)-3,5-dibromophenyl)methanamine hydrochloride (655 mg, 1.61 mmol) was dissolved in ACN (32 mL, 0.05 M). To this solution was added Et_3N (1.56 mL, 11.2 mmol) and catalytic DMAP. This solution of (2-(benzyloxy)-3,5-dibromophenyl)methanamine hydrochloride in ACN was transferred to the suspension containing 2-nitrobenzoyl chloride and was allowed to stir at room temperature overnight. Upon completion, the reaction was concentrated to dryness and resuspended in CH_2Cl_2. The suspension was washed with 1 M NaOH (20 mL), 1 M HCl (20 mL), saturated $NaHCO_3$ (20 mL), and saturated NaCl (20 mL), then dried over Na_2SO_4. The crude product was purified by silica gel chromatography to provide *N*-(2-(benzyloxy)-3,5-dibromobenzyl)-2-nitrobenzamide (354 mg, 42.5 % yield). ^{1}H-NMR (400 MHz, DMSO-d_6) δ 9.32 (t, *J* = 6.0 Hz, 1H), 8.06 (d, *J* = 7.6 Hz, 1H), 7.82 (td, *J* = 7.6, 1.2 Hz, 1H), 7.74-7.67 (m, 2H), 7.65 (d, *J* = 2.4 Hz, 1H), 7.42 (d, *J* = 2.4 Hz, 1H), 4.45 (d, *J* = 5.2 Hz, 2H). 13C-NMR (100 MHz, DMSO-d_6) δ 166.3, 152.7, 147.8, 134.9, 133.7, 132.4, 132.0, 131.3, 131.2, 130.1, 124.7, 113.4, 111.9, 38.5. ESI-MS calculated for $C_{14}H_{11}Br_2N_2O_4$ 428.9 ($M+H^+$), observed 429.1 ($M+H^+$).

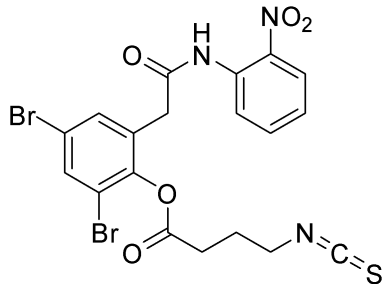

2,4-dibromo-6-{2-[(2-nitrophenyl)amino]-2-oxoethyl}phenyl-4-isothiocyanatobutanoate, 11. To a solution of 2-(3,5-dibromo-2-hydroxyphenyl)-N-(2-nitrophenyl)acetamide (49.9 mg, 0.116 mmol) in ACN (2.32 mL, 0.05 M) at room temperature was added 4-isothiocyanatobutanoic acid (67.4 mg, 0.464 mmol), 1-Ethyl-3-(3-dimethylaminopropyl)carbodiimide (72.0 mg, 0.464 mmol), and a catalytic amount of 4-dimethylaminopyridine. The reaction mixture was allowed to stir overnight at room temperature. The reaction was concentrated in vacuo and resuspended in EtOAc. The reaction was quenched with 1 M HCl (20 mL), washed with brine (20 mL) and the organic layer was dried over Na_2SO_4. The mixture was concentrated *in vacuo* and purified using silica gel chromatography to provide 2,4-dibromo-6-{2-[(2-nitrophenyl)amino]-2-oxoethyl}phenyl-4-isothiocyanatobutanoate (12.9 mg, 20%). ^{1}H-NMR (400 MHz, $CDCl_3$) δ 10.32 (s, 1H), 8.70 (dd, *J* = 8.8, 1.2 Hz, 1H), 8.19 (dd, *J* = 8.4, 1.6 Hz, 1H), 7.76 (d, *J* = 2.4 Hz, 1H), 7.65 (td, *J* = 6.4, 1.6 Hz, 1H), 7.56 (d, *J* = 2.4 Hz, 1H), 7.20 (td, *J* = 8.0, 1.6 Hz, 1H), 3.69 (s, 2H), 3.68 (t, *J* = 6.4 Hz, 2H), 2.83 (t, *J* = 7.2 Hz, 2H), 2.10 (p, *J* = 6.8 Hz, 2H). ^{13}C-NMR (100 MHz, $CDCl_3$) δ 169.3, 167.5,

146.3, 136.4, 136.0, 135.5, 134.2, 133.4, 131.2, 130.2, 125.8, 123.8, 122.0, 120.3, 118.5, 44.0, 40.9, 30.3, 24.7. ESI-MS calculated for $C_{19}H_{16}Br_2N_3O_5S$ 555.9 ($M+H^+$), observed 556.0 ($M+H^+$). HRMS (ESI-TOF) calculated for $C_{19}H_{16}Br_2N_3O_5S$ 555.9172 ($M+H^+$), observed 555.91411 ($M+H^+$).

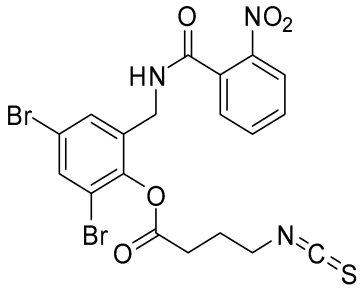

2,4-dibromo-6-((2-nitrobenzamido)methyl)phenyl 4-isothiocyanatobutanoate, 12. Prepared following the procedure for the synthesis of **11** using *N*-(3,5-dibromo-2-hydroxybenzyl)-2-nitrobenzamide (31.8 mg, 0.074 mmol), 4-isothiocyanatobutanoic acid (43.2 mg, 0.298 mmol), 1-Ethyl-3-(3-dimethylaminopropyl)carbodiimide (46.2 mg, 0.298 mmol) and DMAP (catalytic). The crude product was purified using silica gel chromatography to provide 2,4-dibromo-6-((2-nitrobenzamido)methyl)phenyl 4-isothiocyanatobutanoate (9.5 mg, 23 % yield). ^{1}H-NMR (400 MHz, $(CD_3)_2CO$) δ 8.28 (bs, 1H), 8.04 (dd, *J* = 8.0, 1.2 Hz, 1H), 7.84 (d, *J* = 2.4 Hz, 1H), 7.82 – 7.77 (m, 2H), 7.72 (dt, *J* = 8.0, 1.2 Hz, 1H), 7.66 (dd, *J* = 7.6, 1.6 Hz, 1H), 4.57 (d, *J* = 6.0 Hz, 2H), 3.84 (t, *J* = 6.8 Hz, 2H), 2.95 (t, *J* = 6.8 Hz, 2H), 2.17 (p, *J* = 7.6, 6.4 Hz, 2H). ^{13}C-NMR (100 MHz, $(CD_3)_2CO$) δ 170.7, 166.8, 147.1, 136.7, 135.2, 134.5, 133.6, 133.1, 131.9, 130.0, 127.3, 125.3, 122.5, 120.2, 118.8, 45.1, 39.4, 31.4, 25.9. ESI-MS calculated for $C_{19}H_{16}Br_2N_3O_5S$ 555.9 ($M+H^+$), observed 555.9 ($M+H^+$).

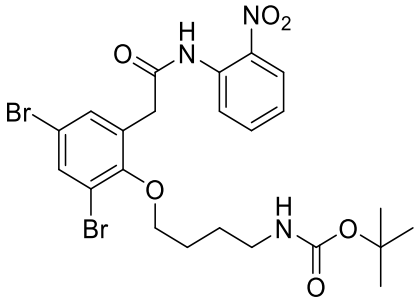

***tert*-butyl (4-(2,4-dibromo-6-(2-((2-nitrophenyl)amino)-2-oxoethyl)phenoxy)butyl)carbamate, S2.** To a solution of 2-(3,5-dibromo-2-hydroxyphenyl)-N-(2-nitrophenyl)acetamide (255.0 mg, 0.593 mmol) in acetone (5.9 mL, 0.1 M) at room temperature was added K_2CO_3 (98.0 mg, 0.709 mmol) and *tert*-Butyl *N*-(4-bromobutyl)carbamate (179.4 mg, 0.711 mmol). The reaction was heated to reflux at 60 °C and allowed to stir overnight. Silica gel was added directly to the reaction vessel upon completion and the mixture was concentrated *in vacuo*. The material was purified by silica gel chromatography to provide *tert*-butyl (4-(2,4-dibromo-6-(2-((2-nitrophenyl)amino)-2-oxoethyl)phenoxy)butyl)carbamate (149.0 mg, 41.8 % yield). ^{1}H-NMR (400 MHz, $CDCl_3$) δ 10.35 (s, 1H), 8.66 (d, *J* = 8.4 Hz, 1H), 8.13 (dd, *J* = 8.4, 1.2 Hz,

1H), 7.63 (d, *J* = 1.6 Hz, 1H), 7.59 (t, *J* = 8.4 Hz, 1H), 7.42 (d, *J* = 2.0 Hz, 1H), 7.14 (t, *J* = 8.4 Hz, 1H), 4.74 (s, 1H), 3.96 (t, *J* = 6.4 Hz, 2H), 3.77 (s, 2H), 3.16 (q, *J* = 6.4 Hz, 2H), 1.85 (p, *J* = 7.2 Hz, 2H), 1.67 (p, *J* = 7.2 Hz, 2H), 1.39 (s, 9H). ^{13}C-NMR (100 MHz, $CDCl_3$) δ 168.6, 155.9, 153.8, 136.4, 135.7, 135.6, 134.2, 133.2, 130.7, 125.6, 123.5, 122.1, 118.5, 117.3, 78.9, 73.4, 40.1, 29.5, 28.3, 27.2, 26.4.

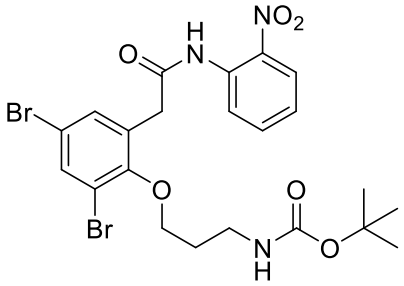

***tert*-butyl (3-(2,4-dibromo-6-(2-((2-nitrophenyl)amino)-2-oxoethyl)phenoxy)propyl)carbamate, S3.** Prepared according to the procedure given for the synthesis of **S2** using 2-(3,5-dibromo-2-hydroxyphenyl)-N-(2-nitrophenyl)acetamide (315.0 mg, 0.732 mmol), K_2CO_3 (111.8 mg, 0.809 mmol), and *tert*-butyl (3-bromopropyl)carbamate (204.0 mg, 0.857 mmol). The crude product was purified by silica gel chromatography to provide *tert*-butyl (3-(2,4-dibromo-6-(2-((2-nitrophenyl)amino)-2-oxoethyl)phenoxy)propyl)carbamate (263.0 mg, 55.4 % yield). ^{1}H-NMR (400 MHz, $CDCl_3$) δ 10.38 (s, 1H), 8.67 (d, *J* = 8.0 Hz, 1H), 8.15 (dd, *J* = 8.0, 1.6 Hz, 1H), 7.66 (d, *J* = 2.4 Hz, 1H), 7.61 (t, *J* = 7.6 Hz, 1H), 7.44 (d, *J* = 2.4 Hz, 1H), 7.16 (t, *J* = 8.4 Hz, 1H), 5.02 (bs, 1H), 4.01 (t, *J* = 5.6 Hz, 2H), 3.79 (s, 2H), 3.36 (q, *J* = 6.0 Hz, 2H), 2.01 (p, *J* = 6.0 Hz, 2H), 1.40 (s, 9H). ^{13}C-NMR (100 MHz, $CDCl_3$) δ 169.1, 156.4, 154.0, 136.9, 136.1, 136.0, 134.6, 133.7, 131.2, 126.0, 123.9, 122.5, 118.9, 117.9, 79.4, 71.6, 40.5, 37.7, 30.5, 28.6.

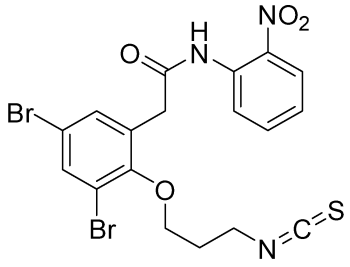

2-(3,5-dibromo-2-(3-isothiocyanatopropoxy)phenyl)-*N*-(2-nitrophenyl)acetamide, 15. To a solution of *tert*-butyl (3-(2,4-dibromo-6-(2-((2-nitrophenyl)amino)-2-oxoethyl)phenoxy)propyl)carbamate, **S3** (25.8 mg, 0.044 mmol) in CH_2Cl_2 (940 µL) at 0 °C under N_2 was slowly added neat TFA (440 µL). The mixture was allowed to stir and warm to room temperature for approximately three hours before concentration *in vacuo*. The material was resuspended in THF (940 µL) and H_2O (940 µL), before the addition of Et_3N (44.2 µL, 0.317 mmol) and CS_2 (24.0 µL, 0.396 mmol). The mixture was allowed to stir at room temperature overnight. A mixture of I_2 (12.4 mg, 0.049 mmol) in THF (940 µL) was cooled to 0 °C and the reaction mixture was added to this solution dropwise. The mixture was allowed to stir and warm to room temperature over a period of 2 h. Upon completion, the reaction mixture was quenched with HCl

and Na_2SO_3. The resulting suspension was extracted three times with EtOAc (20 mL) and the organic phase was concentrated to dryness *in vacuo*. The crude product was purified by silica gel chromatography to provide 2-(3,5-dibromo-2-(3-isothiocyanatopropoxy)phenyl)-*N*-(2-nitrophenyl)acetamide (9.3 mg, 38.9 % yield). ^{1}H-NMR (400 MHz, $CDCl_3$) δ 10.39 (s, 1H), 8.70 (d, *J* = 8.0 Hz, 1H), 8.17 (dd, *J* = 8.8, 1.2 Hz, 1H), 7.67 (d, *J* = 2.0 Hz, 1H), 7.63 (t, *J* = 6.2 Hz, 1H), 7.46 (d, *J* = 2.4 Hz, 1H), 7.18 (t, *J* = 6.2 Hz, 1H), 4.09 (t, *J* = 5.6 Hz, 2H), 3.86 (t, *J* = 6.0 Hz, 2H), 3.80 (s, 2H), 2.20 (p, *J* = 6.0 Hz, 2H). ^{13}C-NMR (100 MHz, $CDCl_3$) δ 168.5, 135.2, 136.5, 136.0, 135.8, 134.3, 133.4, 130.7, 130.6, 125.7, 123.6, 122.1, 118.5, 118.0, 69.4, 41.7, 40.2, 30.3. ESI-MS calculated for $C_{18}H_{16}Br_2N_3O_4S$ 527.9 ($M+H^+$), observed 528.1 ($M+H^+$).

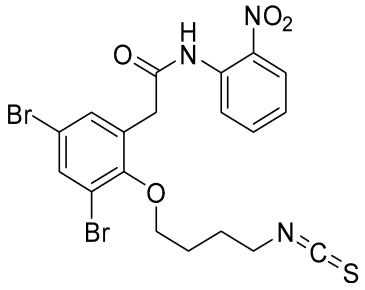

2-(3,5-dibromo-2-(4-isothiocyanatobutoxy)phenyl)-*N*-(2-nitrophenyl)acetamide, 16. Prepared according to the procedure given for the preparation of **15** using *tert*-butyl (4-(2,4-dibromo-6-(2-((2-nitrophenyl)amino)-2-oxoethyl)phenoxy)butyl)carbamate, **S2** (23.8 mg, 0.041 mmol), TFA (400 µL), Et_3N (14 µL, 0.100 mmol), CS_2 (22.0 µL, 0.12 mmol), and I_2 (11.0 mg, 0.043 mmol). The crude product was purified by silica gel chromatography to provide 2-(3,5-dibromo-2-(4-isothiocyanatobutoxy)phenyl)-*N*-(2-nitrophenyl)acetamide (2.4 mg, 10.8 % yield). ^{1}H-NMR (400 MHz, $CDCl_3$) δ 10.40 (s, 1H), 8.72 (dd, *J* = 8.4, 1.2 Hz, 1H), 8.19 (dd, *J* = 8.4, 1.2 Hz, 1H), 7.70 (d, *J* = 2.4 Hz, 1H), 7.65 (td, *J* = 8.0, 1.6 Hz, 1H), 7.46 (d, *J* = 2.4 Hz, 1H), 7.22-7.17 (m, 1H), 4.02 (t, *J* = 5.2 Hz, 2H), 3.79 (s, 2H), 3.64 (t, *J* = 6.0 Hz, 2H), 1.97 (p, *J* = 2.8 Hz, 4H). ^{13}C-NMR (100 MHz, $CDCl_3$) δ 168.6, 153.7, 136.4, 136.0, 135.9, 134.4, 133.4, 130.7, 130.2, 125.8, 123.7, 122.1, 118.6, 117.7, 72.7, 44.9, 40.3, 27.1, 26.7. ESI-MS calculated for $C_{19}H_{18}Br_2N_3O_4S$ 541.9 ($M+H^+$), observed 541.8 ($M+H^+$).

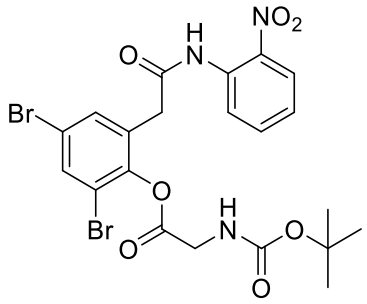

2,4-dibromo-6-(2-((2-nitrophenyl)amino)-2-oxoethyl)phenyl (*tert*-butoxycarbonyl)glycinate, S5. Prepared following the procedure for the synthesis of **11** using 2-(3,5-dibromo-2-hydroxyphenyl)-N-(2-nitrophenyl)acetamide (100 mg, 0.233 mmol), N-(tert-Butoxycarbonyl)glycine (81.6 mg, 0.466 mmol), 1-Ethyl-3-(3-dimethylaminopropyl)carbodiimide (72.3 mg, 0.466 mmol) and DMAP (catalytic). The crude product was purified using silica gel to provide2,4-dibromo-6-(2-((2-nitrophenyl)amino)-2-oxoethyl)phenyl (*tert*-butoxycarbonyl)glycinate (49.0 mg, 36% yield). ^{1}H-NMR (400 MHz, $CDCl_3$) δ 10.32 (s, 1H), 8.63 (d, *J*=8.4 Hz, 1H), 8.18 (dd, *J*=8.0, 1.2 Hz, 1H), 7.74 (d, *J*=2.0 Hz, 1H), 7.63 (t, *J*=7.2 Hz, 1H), 7.56 (d, *J*=2.0 Hz, 1H), 7.22-7.17 (m, 1H), 5.15 (s, 1H), 4.22 (d, *J*=5.6 Hz, 2H), 3.73 (s, 2H), 1.42 (s, 9H).

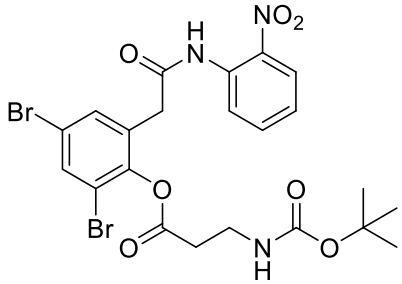

2,4-dibromo-6-(2-((2-nitrophenyl)amino)-2-oxoethyl)phenyl 3-((*tert*-butoxycarbonyl)amino)propanoate, S6. Prepared following the procedure for the synthesis of **11** using 2-(3,5-dibromo-2-hydroxyphenyl)-N-(2-nitrophenyl)acetamide (100 mg, 0.233 mmol), Boc-β-alanine-OH (88.2 mg, 0.466 mmol),), 1-Ethyl-3-(3-dimethylaminopropyl)carbodiimide (72.3 mg, 0.466 mmol) and DMAP (catalytic). The crude product was purified using silica gel chromatography to provide 2,4-dibromo-6-(2-((2-nitrophenyl)amino)-2-oxoethyl)phenyl 3-((*tert*-butoxycarbonyl)amino)propanoate (65 mg, 46% yield). ^{1}H-NMR (400 MHz, $CDCl_3$) δ 10.33 (s, 1H), 8.67 (dd, *J*=8.8, 1.2 Hz, 1H), 8.18 (dd, *J*=6.8, 1.2 Hz, 1H), 7.76 (d, *J*=2.4 Hz, 1H), 7.66-7.62 (m, 1H), 7.57 (d, *J*=2.4 Hz, 1H), 7.22-7.17 (m, 1H), 3.70 (s, 2H), 3.50 (q, *J*=6 Hz, 2H), 2.89 (t, *J*=6 Hz, 2H), 1.43 (s, 9H). ^{13}C-NMR (100 MHz, $CDCl_3$) δ 169.5, 167.7, 146.4, 136.5, 135.9, 135.5, 134.2, 133.3, 130.3, 125.8, 123.8, 122.1, 120.3, 118.5, 79.5, 40.8, 37.8, 36.1, 34.5, 28.4.

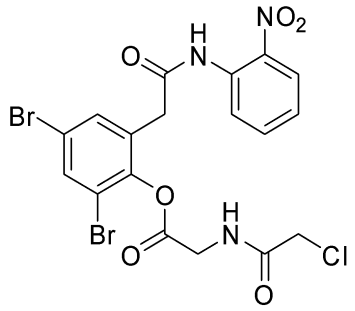

2,4-dibromo-6-(2-((2-nitrophenyl)amino)-2-oxoethyl)phenyl (2-chloroacetyl)glycinate, 17. To a solution of **S5** (19.6 mg, 0.033 mmol) in CH_2Cl_2 (68 µL) at 0 °C was added TFA (10 µL) dropwise. The mixture was allowed to warm to room temperature and stir for 2 h. Upon completion, the reaction mixture was concentrated to dryness. The dry material was dissolved in CH_2Cl_2 (3.34 ml) and cooled to 0 °C, followed by the addition of Et_3N (47 µL, 0.334 mmol) and chloroacetyl chloride (27 µl, 0.334 mmol). The reaction was allowed to stir overnight. Upon completion, the reaction mixture was concentrated to dryness, dissolved in CH_2Cl_2, washed with HCl, $NaHCO_3$, NaCl, and dried over Na_2SO_4. The crude product was purified by silica gel chromatography to yield 2,4-dibromo-6-(2-((2-nitrophenyl)amino)-2-oxoethyl)phenyl (2-chloroacetyl)glycinate (8.8 mg, 47.3 %). ^{1}H-NMR (400 MHz, $CDCl_3$) δ 10.34 (s, 1H), 8.65 (dd, *J* = 8.7, 1.2 Hz, 1H), 8.19 (dd, *J* = 8.5, 1.6 Hz, 1H), 7.76 (d, *J* = 2.2 Hz, 1H), 7.68 – 7.61 (m, 1H), 7.60 (d, *J* = 2.3 Hz, 1H), 7.22 (t, *J* = 8.4 Hz, 1H), 4.41 (d, *J* = 5.6 Hz, 2H), 4.10 (s, 2H), 3.74 (s, 2H). ^{13}C-NMR (100 MHz, $CDCl_3$) δ 167.9, 167.7, 165.0, 146.2, 143.9, 141.5, 135.9, 135.6, 133.8, 127.9, 127.3, 125.9, 123.9, 122.6, 120.2, 47.2, 43.1, 40.6. ESI-MS calculated for $C_{18}H_{15}Br_2ClN_3O_6$ 562.1 ($M+H^+$), observed 561.9 ($M+H^+$).

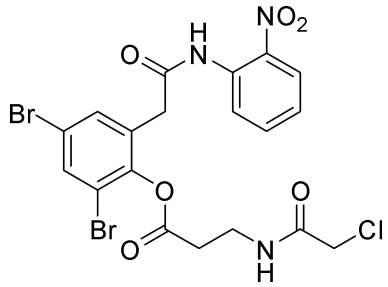

2,4-dibromo-6-(2-((2-nitrophenyl)amino)-2-oxoethyl)phenyl 3-(2-chloroacetamido)propanoate, 18. To a solution of **S6** (27.0 mg, 0.045 mmol) in Et_2O at 0 °C was bubbled HCl gas. HCl gas was generated by the treatment of acetyl chloride (20 mL, 281.27 mmol) with anhydrous methanol (11.4 mL, 281.27 mmol). Once the reaction was complete the contents were concentrated to dryness. The material was dissolved in CH_2Cl_2 and Et_3N (6.28 µL, 0.045 mmol) was added. The solution was cooled to 0 °C, chloroacetyl chloride was added dropwise (3.58 µL, 0.045 mmol), and the reaction was allowed to stir overnight. The reaction was concentrated to dryness, resuspended in CH_2Cl_2, washed with HCl, $NaHCO_3$, brine, and dried over Na_2SO_4. The crude product was purified by silica gel chromatography to yield 2,4-dibromo-6-(2-((2-nitrophenyl)amino)-2-oxoethyl)phenyl 3-(2-chloroacetamido)propanoate (8.2 mg, 31.5 % yield). ^{1}H-NMR (400 MHz, $CDCl_3$) δ 10.35 (s, 1H), 8.67 (dd, *J* = 8.5, 1.4 Hz, 1H), 8.20 (dd, *J* = 8.5, 1.6 Hz,

1H), 7.78 (d, *J* = 2.3 Hz, 1H), 7.65 (ddd, *J* = 8.8, 7.3, 1.6 Hz, 1H), 7.59 (d, *J* = 2.1 Hz, 1H), 7.21 (ddd, *J* = 8.5, 7.2, 1.3 Hz, 1H), 4.05 (s, 2H), 3.76 – 3.66 (m, 4H), 2.98 – 2.91 (m, 2H). ^{13}C-NMR (100 MHz, DMSO-d6) δ 168.6, 167.7, 166.3, 146.1, 142.5, 134.2, 133.9, 133.8, 132.5, 130.8, 125.6, 125.4, 125.0, 118.9, 117.5, 42.6, 37.4, 34.9, 33.1. ESI-MS calculated for $C_{19}H_{17}Br_2ClN_3O_6$ 575.9 ($M+H^+$), observed 575.6 ($M+H^+$).

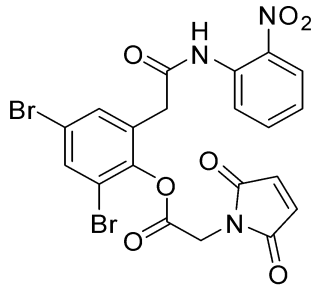

2,4-dibromo-6-(2-((2-nitrophenyl)amino)-2-oxoethyl)phenyl 2-(2,5-dioxo-2,5-dihydro-1*H*-pyrrol-1-yl)acetate, 24. To a solution of 2-(3,5-dibromo-2-hydroxyphenyl)-*N*-(2-nitrophenyl)acetamide (50.0 mg, 0.116 mmol) in DMSO at room temperature under N_2 was added (2,5-dioxo-2,5-dihydro-1*H*-pyrrol-1-yl)acetic acid (30.0 mg, 0.174 mmol), N, N-diisopropylethylamine (61.0 µL, 0.348 mmol), and (Benzotriazol-1-yloxy)tris(dimethylamino)phosphonium hexafluorophosphate (76.9 mg, 0.174 mmol). The mixture was allowed to stir at room temperature overnight. To the reaction mixture was added 50 mL of H_2O and 50 mL of ethyl acetate upon completion. The organic phase was collected and the water layer was extracted three times with 10 mL of ethyl acetate. The organic layers were pooled and washed with HCl, Na_2CO_3, and NaCl. The resulting solution was dried over Na_2SO_4 and concentrated to dryness. The crude product was purified by silica gel chromatography to provide 2,4-dibromo-6-(2-((2-nitrophenyl)amino)-2-oxoethyl)phenyl 2-(2,5-dioxo-2,5-dihydro-1*H*-pyrrol-1-yl)acetate (5.4 mg, 8.2 % yield). ^{1}H-NMR (400 MHz, $CDCl_3$) δ 10.36 (s, 1H), 8.70 (dd, *J* = 8.4, 1.6 Hz, 1H), 8.20 (dd, *J* = 8.4, 1.6 Hz, 1H), 7.74 (d, *J* = 2.4 Hz, 1H), 7.67 – 7.62 (m, 1H), 7.57 (d, *J* = 2.0 Hz, 1H), 7.22 – 7.18 (m, 1H), 6.77 (s, 2H), 4.63 (s, 2H), 3.73 (s, 2H). ^{13}C-NMR (100 MHz, $CDCl_3$) δ 169.3, 167.4, 164.6, 135.8, 135.4, 134.5, 134.3, 133.5, 130.3, 125.7, 125.5, 123.7, 122.4, 120.6, 119.3, 118.0, 40.0, 38.5. ESI-MS calculated for $C_{20}H_{14}Br_2N_3O_7$ 565.9 ($M+H^+$), observed 565.9 ($M+H^+$).

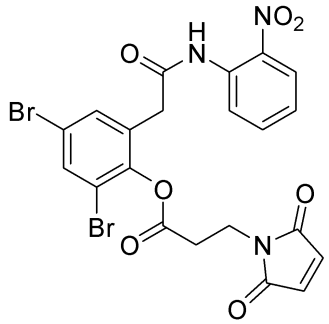

2,4-dibromo-6-(2-((2-nitrophenyl)amino)-2-oxoethyl)phenyl 3-(2,5-dioxo-2,5-dihydro-1*H*-pyrrol-1-yl)propanoate, 25. To a solution of 3-(2,5-dioxo-2,5-dihydro-1*H*-pyrrol-1-yl)propanoic acid (50.0 mg,

0.296 mmol) in CH_2Cl_2 at 0 °C was added $(COCl)_2$ (28 µL, 0.326 mmol). The reaction was allowed to warm to room temperature. To the mixture was added 2-(3,5-dibromo-2-hydroxyphenyl)-*N*-(2-nitrophenyl)acetamide (63.6 mg, 0.148 mmol), Et_3N (0.1 mL, 0.74 mmol), and catalytic DMAP. The reaction was allowed to stir at room temperature overnight. The reaction was quenched with HCl, washed with Na_2CO_3, NaCl, and dried over Na_2SO_4. The crude product was purified by silica gel chromatography to provide 2,4-dibromo-6-(2-((2-nitrophenyl)amino)-2-oxoethyl)phenyl 3-(2,5-dioxo-2,5-dihydro-1*H*-pyrrol-1-yl)propanoate (9.2 mg, 10.7 % yield). ^{1}H-NMR (400 MHz, $CDCl_3$) δ 10.33 (s, 1H), 8.69 (dd, *J* = 8.8, 1.2 Hz, 1 H), 8.19 (dd, *J* = 8.8, 1.6 Hz, 1 H), 7.74 (d, *J* = 2.0 Hz, 1 H), 7.68-7.63 (m, 1 H), 7.57 (d, *J* = 2.4 Hz, 1 H), 7.22-7.18 (m, 1 H), 6.71 (s, 2 H), 3.95 (t, *J* = 7.2 Hz, 2 H), 3.75 (s, 2 H), 3.05 (t, *J* = 6.4 Hz, 2 H). ^{13}C-NMR (100 MHz, $CDCl_3$) δ 170.3, 167.9, 167.7, 146.2, 136.6, 136.0, 135.4, 134.3, 133.4, 130.5, 125.8, 123.7, 122.3, 120.3, 118.4, 40.4, 33.2, 32.2, 29.7. ESI-MS calculated for $C_{21}H_{16}Br_2N_3O_7$ 579.9 ($M+H^+$), observed 579.9 ($M+H^+$). HRMS (ESI-TOF) calculated for $C_{21}H_{16}Br_2N_3O_7$ 579.9355, observed 579.9344.

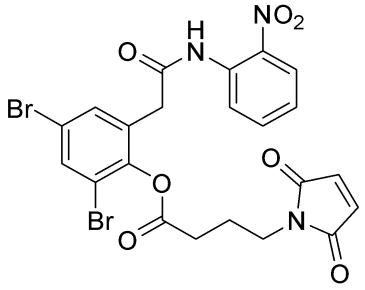

2,4-dibromo-6-(2-((2-nitrophenyl)amino)-2-oxoethyl)phenyl 4-(2,5-dioxo-2,5-dihydro-1*H*-pyrrol-1-yl)butanoate, 26. Prepared according to the procedure given for the preparation of **24** using 2-(3,5-dibromo-2-hydroxyphenyl)-*N*-(2-nitrophenyl)acetamide (150.1 mg, 0.349 mmol), 4-(2,5-dioxo-2,5-dihydro-1*H*-pyrrol-1-yl)butanoic acid (96.0 mg, 0.524 mmol), N, N-diisopropylethylamine (187 µL, 1.05 mmol), and (Benzotriazol-1-yloxy)tris(dimethylamino)phosphonium hexafluorophosphate (231.8 mg, 0.524 mmol). The crude product was purified by silica gel chromatography to provide 2,4-dibromo-6-(2-((2-nitrophenyl)amino)-2-oxoethyl)phenyl 4-(2,5-dioxo-2,5-dihydro-1*H*-pyrrol-1-yl)butanoate (50.0 mg, 24.1 % yield). ^{1}H-NMR (400 MHz, $CDCl_3$) δ 10.31 (s, 1H), 8.66 (dd, *J* = 8.4 Hz, 1.6 Hz, 1H), 8.16 (dd, *J* = 8.8, 1.6 Hz, 1H), 7.72 (d, *J* = 2.4 Hz, 1H), 7.63 (td, *J* = 8.8, 1.6 Hz, 1H), 7.59 (d, *J* = 2.0 Hz, 1H), 7.18 (td, *J* = 8.8, 1.6 Hz, 1H), 6.70 (s, 2H), 3.81 (s, 2H), 3.67 (t, *J* = 6.4 Hz, 2H), 2.71 (t, *J* = 6.8 Hz, 2H), 2.02 (p, *J* = 6.4 Hz, 2H). ^{13}C-NMR (100 MHz, $CDCl_3$) δ 171.0, 169.7, 168.0, 146.2, 136.7, 135.8, 135.2, 134.2, 134.1, 133.5, 130.6, 125.6, 123.6, 122.4, 120.0, 118.3, 40.0, 36.5, 30.557, 23.5. ESI-MS calculated for $C_{22}H_{18}Br_2N_3O_7$ 594.0 ($M+H^+$), observed 593.9 ($M+H^+$).

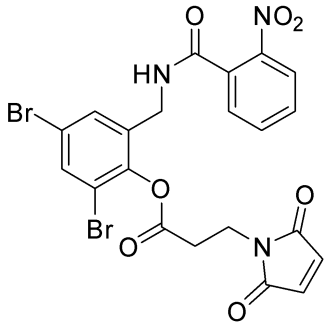

2,4-dibromo-6-((2-nitrobenzamido)methyl)phenyl 3-(2,5-dioxo-2,5-dihydro-1*H*-pyrrol-1-yl)propanoate, 27. Prepared according to the procedure given for the preparation of **24** using *N*-(3,5-dibromo-2-hydroxybenzyl)-2-nitrobenzamide (42.1 mg, 0.098 mmol), 3-(2,5-dioxo-2,5-dihydro-1*H*-pyrrol-1-yl)propanoic acid (24.9 mg, 0.147 mmol), N, N-diisopropylethylamine (52.3 µL, 0.294 mmol), and (Benzotriazol-1-yloxy)tris(dimethylamino)phosphonium hexafluorophosphate (65.0 mg, 0.147 mmol). The crude product was purified by silica gel chromatography to provide 2,4-dibromo-6-((2-nitrobenzamido)methyl)phenyl 3-(2,5-dioxo-2,5-dihydro-1*H*-pyrrol-1-yl)propanoate (7.4 mg, 13.0 % yield). ^{1}H-NMR (400 MHz, $CDCl_3$) δ 8.05 (dd, *J* = 8.4, 1.2 Hz, 1H), 7.69 (d, *J* = 2.4 Hz, 1H), 7.67 (td, *J* = 8.0, 1.6 Hz, 1H), 7.63 (d, *J* = 2.0 Hz, 1H), 7.57 (td, *J* = 7.2, 1.2 Hz, 1H), 7.51 (dd, *J* = 7.6, 1.6 Hz, 1H), 6.67 (s, 2H), 6.42 (t, *J* = 6.0 Hz, 1H), 4.52 (d, *J* 6.0 Hz, 2H), 3.94 (t, *J* = 6.4 Hz, 2H), 3.07 (t, *J* = 6.4 Hz, 2H). ^{13}C-NMR (100 MHz, $CDCl_3$) δ 170.4, 168.8, 166.3, 146.4, 145.8, 135.3, 134.2, 133.8, 132.9, 132.3, 130.6, 128.8, 124.5, 120.4, 120.2, 117.9, 39.1, 33.2, 32.4. ESI-MS calculated for $C_{21}H_{16}Br_2N_3O_7$ 579.9 ($M+H^+$), observed 579.9 ($M+H^+$).

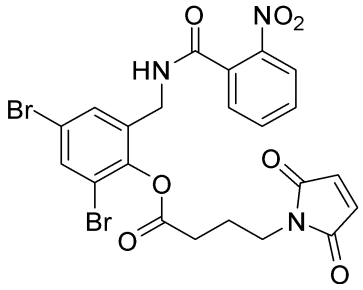

2,4-dibromo-6-((2-nitrobenzamido)methyl)phenyl 4-(2,5-dioxo-2,5-dihydro-1*H*-pyrrol-1-yl)butanoate, 28. Prepared according to the procedure given for the preparation of **24** using *N*-(3,5-dibromo-2-hydroxybenzyl)-2-nitrobenzamide (40.9, 0.095 mmol), 4-(2,5-dioxo-2,5-dihydro-1*H*-pyrrol-1-yl)butanoic acid (23.9 mg, 0.143 mmol), N, N-diisopropylethylamine (39.9 µL, 0.286 mmol), and (Benzotriazol-1-yloxy)tris(dimethylamino)phosphonium hexafluorophosphate (63.2 mg, 0.143 mmol). The crude product was purified by silica gel chromatography to provide 2,4-dibromo-6-((2-nitrobenzamido)methyl)phenyl 4-(2,5-dioxo-2,5-dihydro-1*H*-pyrrol-1-yl)butanoate (7.6 mg, 13.4 % yield). ^{1}H-NMR (400 MHz, $CDCl_3$) δ 8.01 (dd, *J* = 8.0, 1.2 Hz, 1H), 7.70 (d, *J* = 2.4 Hz, 1H), 7.67 (d, *J* = 2.0 Hz, 1H), 7.64 (td, *J* = 8.4, 1.2 Hz, 1H), 7.55 (td, *J* = 8.0, 1.6 Hz, 1H), 7.49 (dd, *J* = 8.0, 1.6 Hz, 1H), 6.75 (t, *J* = 6.0 Hz, 1H), 6.68 (s, 2H), 4.52 (d, *J* = 5.2 Hz, 2H), 3.60 (t, *J* = 6.0 Hz, 2H), 2.68 (t, *J* = 6.4 Hz, 2H), 2.00 (p, *J* = 6.4 Hz, 2H). ^{13}C-NMR (100 MHz, $CDCl_3$) δ 171.0, 170.5, 166.4, 146.5, 146.1, 135.2, 134.2, 133.9, 133.7, 133.1,

132.4, 130.6, 128.9, 124.4, 119.9, 117.9, 39.4, 36.5, 30.7, 23.5. ESI-MS calculated for $C_{22}H_{18}Br_2N_3O_7$ 594.0 ($M+H^+$), observed 594.1 ($M+H^+$). HRMS (ESI-TOF) calculated for $C_{21}H_{18}Br_2N_3O_7$ 593.9506 observed 593.9450.

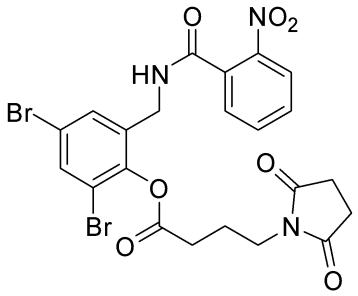

2,4-dibromo-6-((2-nitrobenzamido)methyl)phenyl 4-(2,5-dioxyopyrrolidin-1-yl)butanoate, 29. Prepared according to the procedure given for the preparation of **24** using *N*-(3,5-dibromo-2-hydroxybenzyl)-2-nitrobenzamide (51.2mg, 0.119 mmol), 4-(2,5-dioxopyrrolidin-1-yl)butanoic acid (33.0 mg, 0.179 mmol), N, N-diisopropylethylamine (64.0 µL, 0.357 mmol), and (benzotriazol-1-yloxy)tris(dimethylamino)phosphonium hexafluorophosphate (79.0 mg, 0.179 mmol). The crude product was purified by silica gel chromatography to provide 2,4-dibromo-6-((2-nitrobenzamido)methyl)phenyl 4-(2,5-dioxyopyrrolidin-1-yl)butanoate (44.0 mg, 62.0 % yield). ^{1}H-NMR (400 MHz, $CDCl_3$) δ 8.00 (dd, *J* = 8.4, 1.2 Hz, 1H), 7.69 (s, 2H), 7.63 (td, *J* = 7.6, 1.2 Hz, 1H), 7.54 (td, *J* = 7.6, 1.2 Hz, 1H), 7.49 (dd, *J* = 7.6, 1.2 Hz, 1H), 7.06 (t, *J* = 6.0 Hz, 1H), 4.50 (d, *J* = 6.0 Hz, 2H), 3.55 (t, *J* = 6.4 Hz, 2H), 2.68 (t, *J* = 6.8 Hz, 2H), 2.64 (s, 4H), 1.98 (s, *J* = 6.0 Hz, 2H). ^{13}C-NMR (100 MHz, $CDCl_3$) δ 177.9, 170.6, 166.5, 146.6, 146.4, 135.4, 134.1, 133.8, 133.6, 133.0, 130.6, 129.2, 124.5, 120.0, 118.0, 39.7, 37.6, 31.1, 28.2, 22.8. ESI-MS calculated for $C_{22}H_{20}Br_2N_3O_7$ 596.0 ($M+H^+$), observed 595.9 ($M+H^+$).

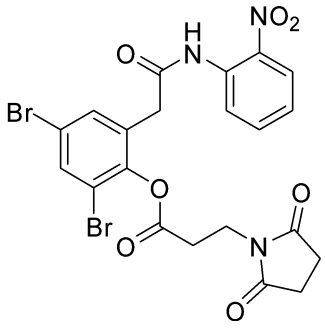

2,4-dibromo-5-(2-((2-nitrophenyl)amino)-2-oxoethyl)phenyl 3-(2,5-dioxopyrrolidin-1-yl)propanoate, 30. Prepared according to the procedure given for the preparation of **24** using 2-(3,5-dibromo-2-hydroxyphenyl)-*N*-(2-nitrophenyl)acetamide (167.7 mg, 0.390 mmol), 3-(2,5-dioxopyrrolidin-1-yl)propanoic acid (100.0 mg, 0.584 mmol), N, N-diisopropylethylamine (210 µL, 1.17 mmol), and (Benzotriazol-1-yloxy)tris(dimethylamino)phosphonium hexafluorophosphate (258.0 mg, 0.584 mmol). The crude product was purified by silica gel chromatography to provide 2,4-dibromo-5-(2-((2-nitrophenyl)amino)-2-oxoethyl)phenyl 3-(2,5-dioxopyrrolidin-1-yl)propanoate (117.4 mg, 51.6 % yield). ^{1}H-NMR (400 MHz, $CDCl_3$) δ 10.31 (s, 1H), 8.65 (dd, *J* = 8.4, 1.2 Hz, 1H), 8.17 (dd, *J* = 8.8, 1.6 Hz, 1H), 7.73 (d, *J* = 2.0 Hz, 1H), 7.64 (td, *J* = 8.8, 1.6 Hz, 1H), 7.57 (d, *J* = 2.4 Hz, 1H), 7.19 (td, *J* = 8.4, 1.2 Hz, 1H), 3.94 (t, *J* = 6.8 Hz, 2H), 3.76 (s, 2H), 3.02 (t, *J* = 6.8 Hz, 2H), 2.72 (s, 4H). ^{13}C-NMR (100MHz, $CDCl_3$) δ 177.0,

168.0, 167.8, 146.2, 136.7, 135.9, 135.3, 134.2, 133.5, 130.6, 125.7, 123.7, 122.4, 120.2, 118.3, 40.3, 34.1, 31.5, 28.1. ESI-MS calculated for $C_{21}H_{18}Br_2N_3O_7$ 581.9 ($M+H^+$), observed 581.8 ($M+H^+$).

F. ^{1}H-NMR and ^{13}C-NMR spectra for all new compounds

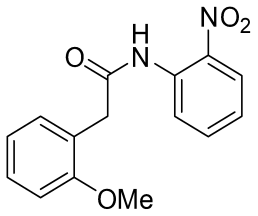

2-(2-methoxyphenyl)-*N*-(2-nitrophenyl)acetamide, 6 ($CDCl_3$)

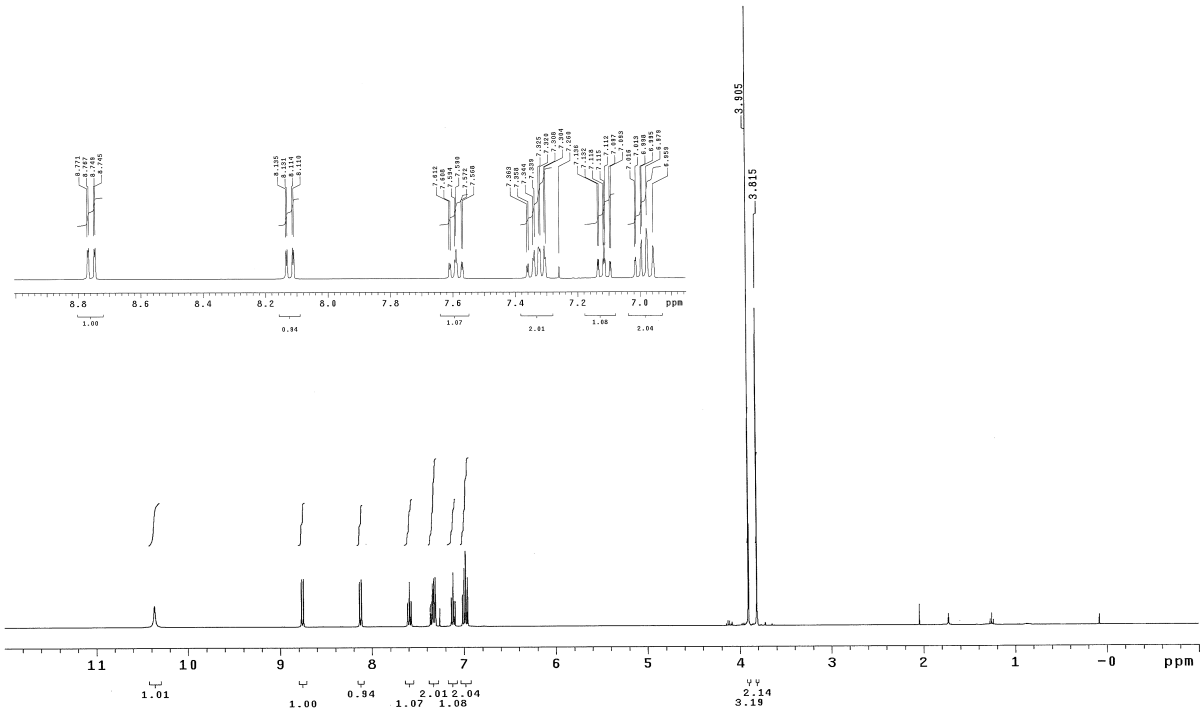

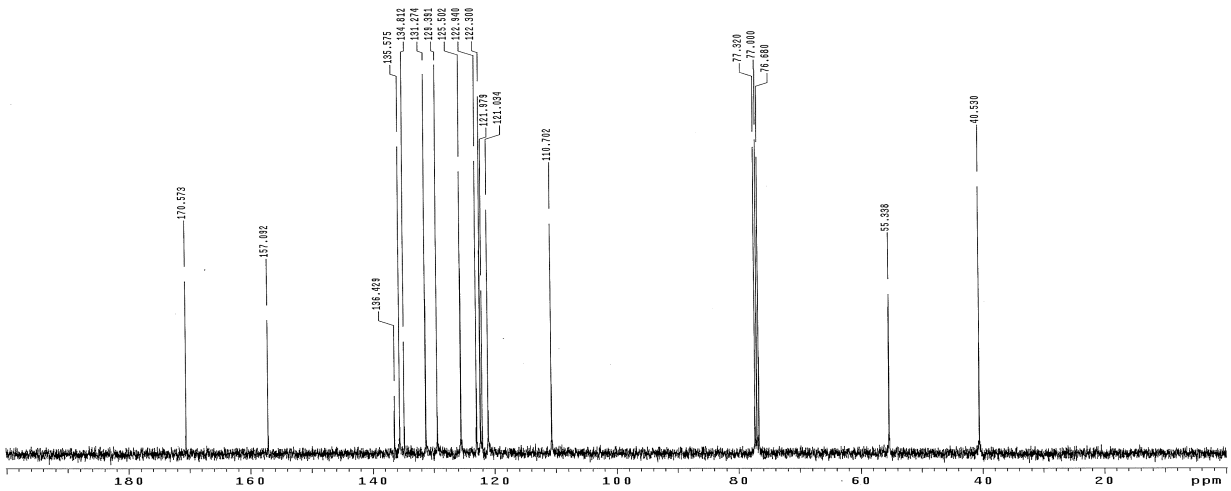

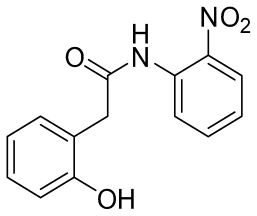

2-(2-hydroxyphenyl)-*N*-(2-nitrophenyl)acetamide, S1 ($CDCl_3$)

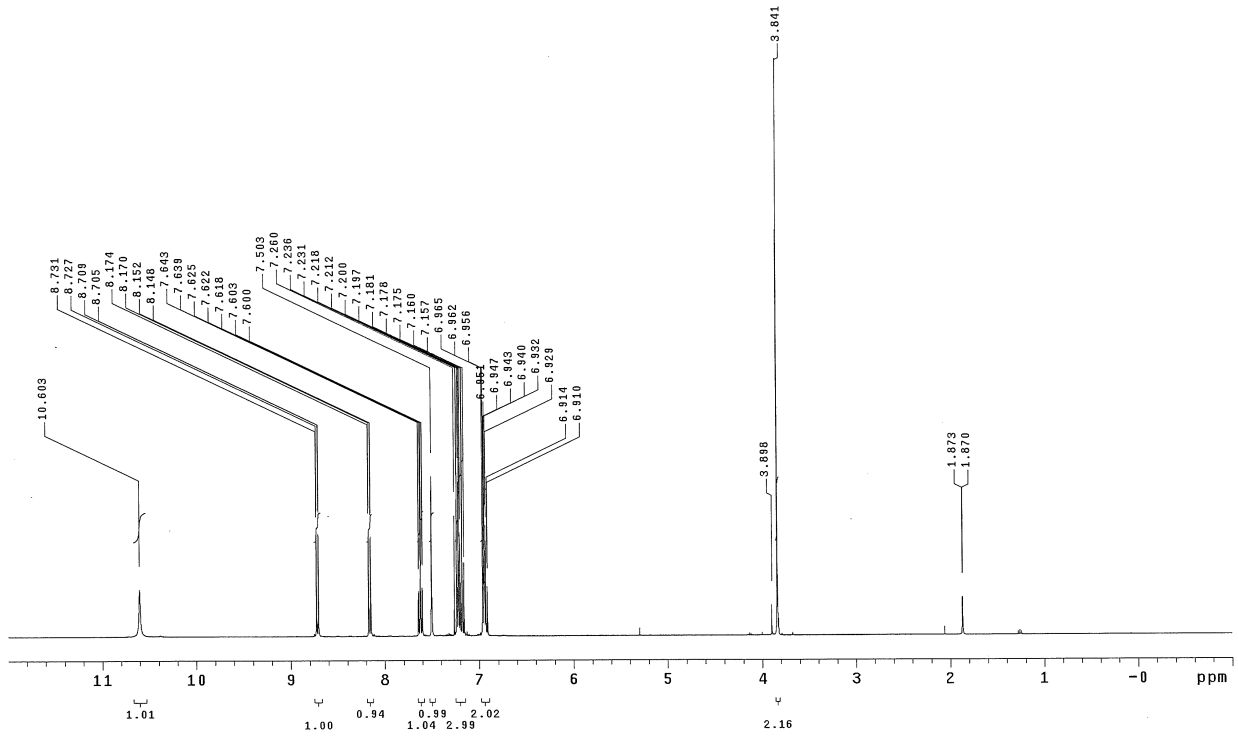

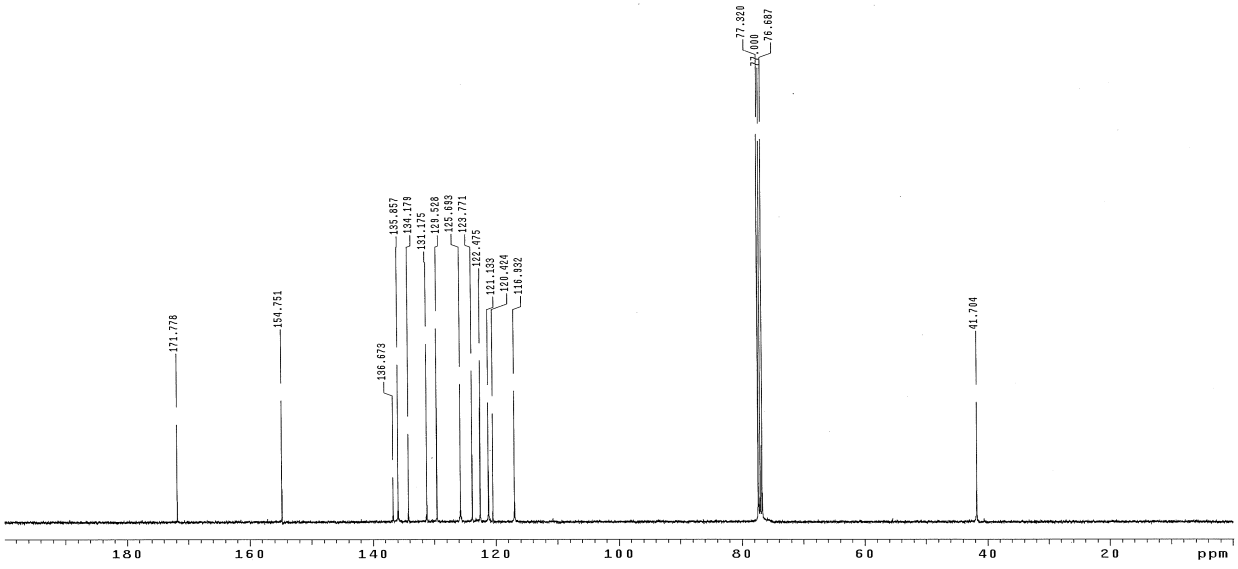

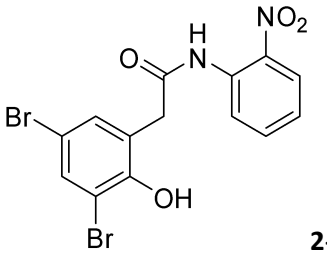

2-(3,5-dibromo-2-hydroxyphenyl)-N-(2-nitrophenyl)acetamide, 7. ($CDCl_3$)

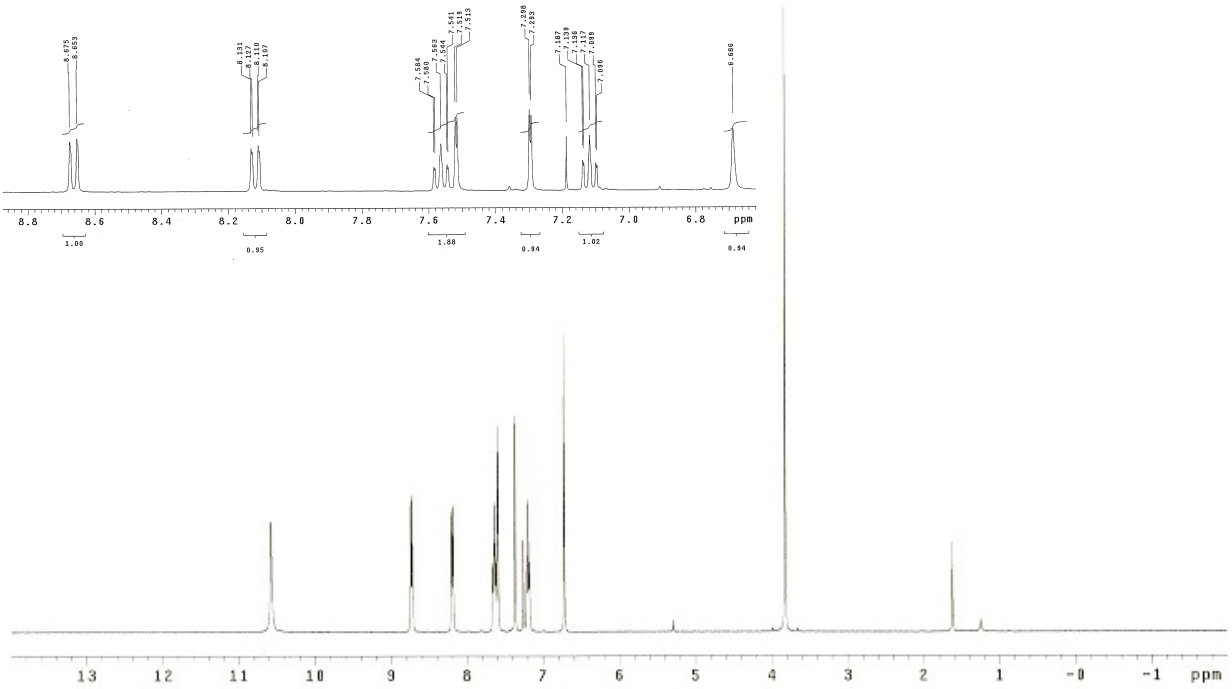

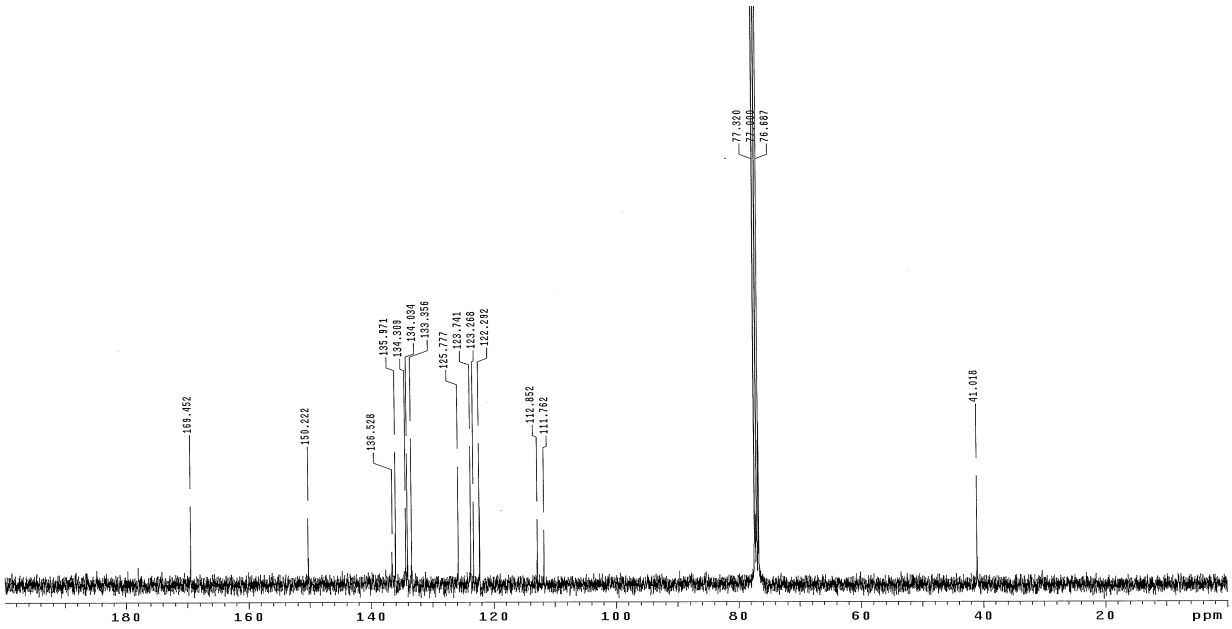

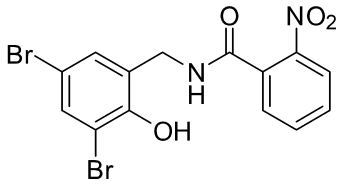

***N*-(3,5-dibromo-2-hydroxybenzyl)-2-nitrobenzamide, 10. (DMSO-d6)**

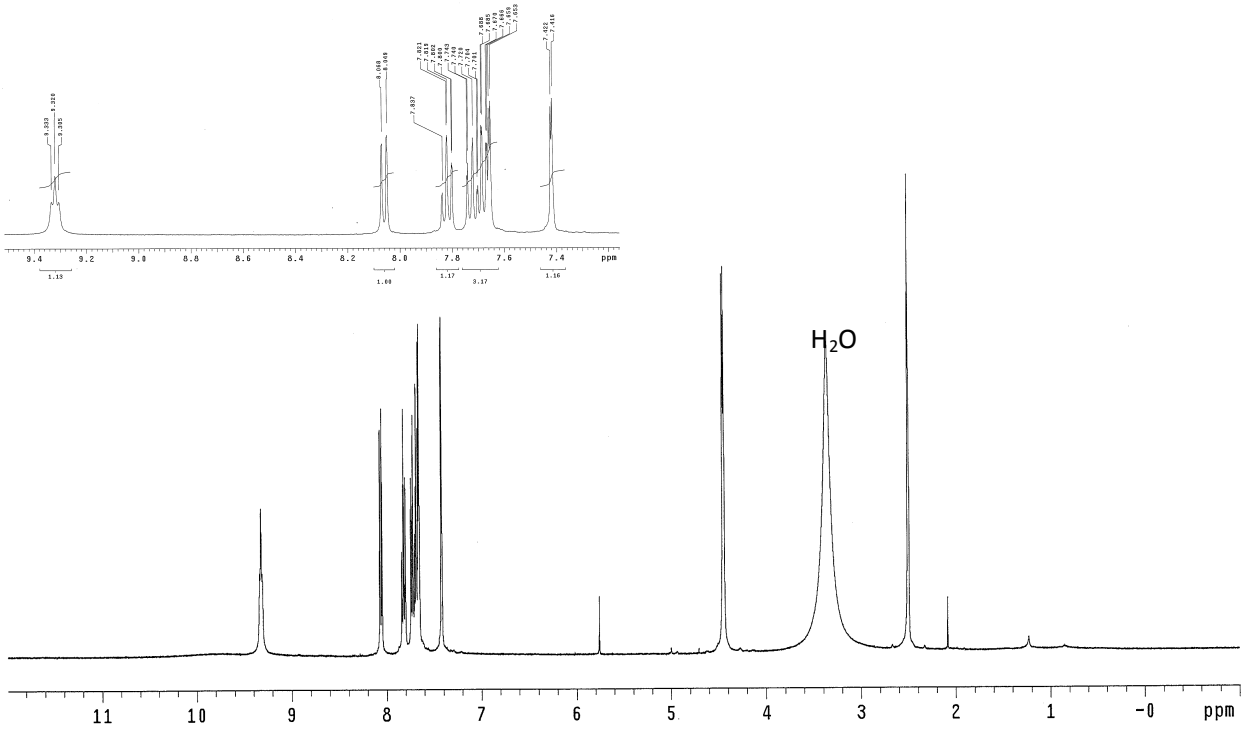

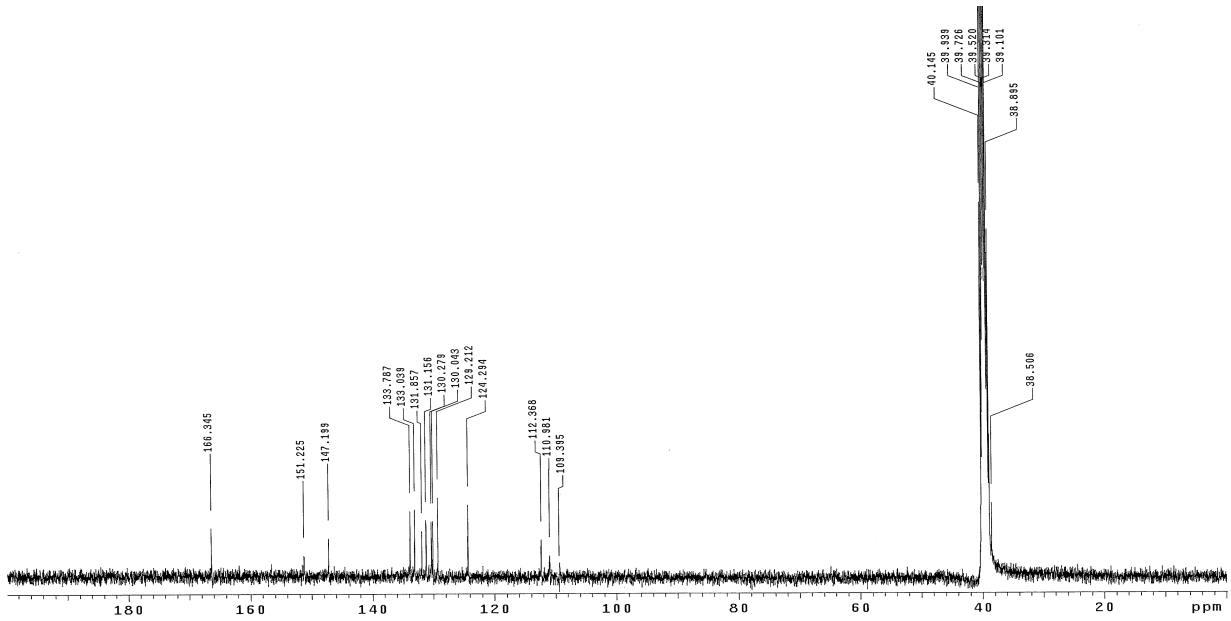

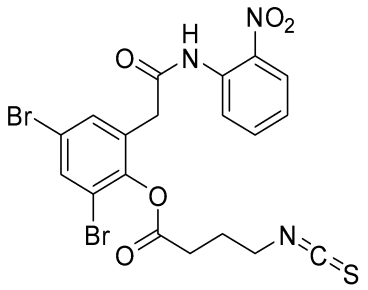

2,4-dibromo-6-(2-((2-nitrophenyl)amino)-2-oxoethyl)phenyl 4-isothiocyanatobutanoate, 11. ($CDCl_3$)

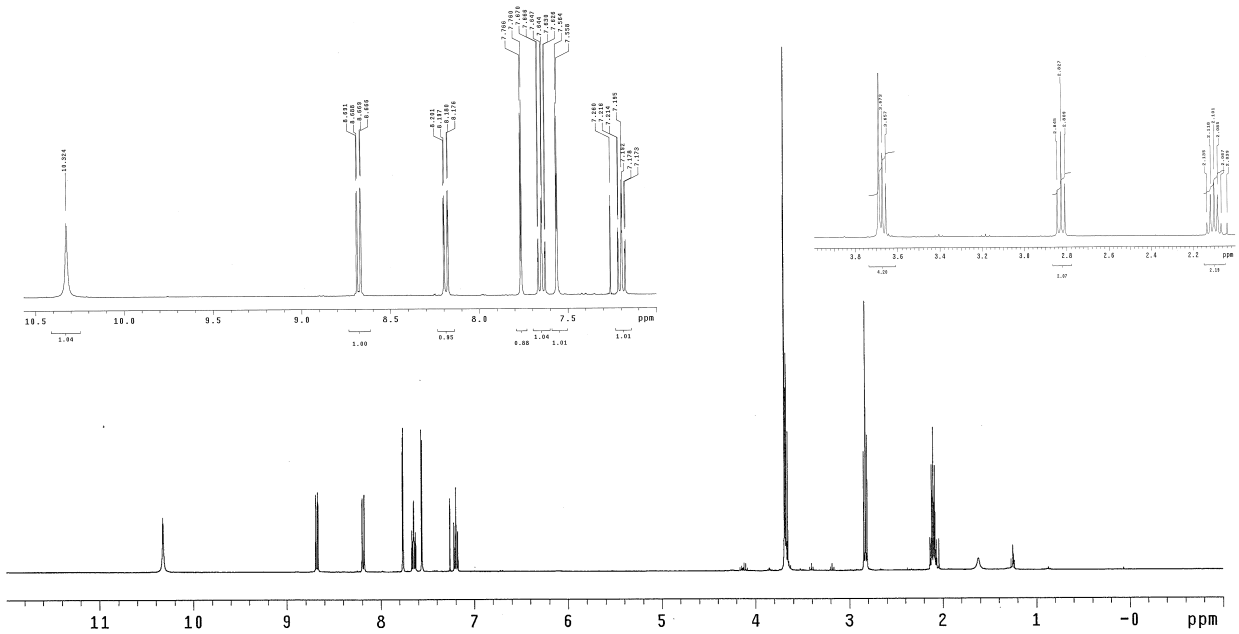

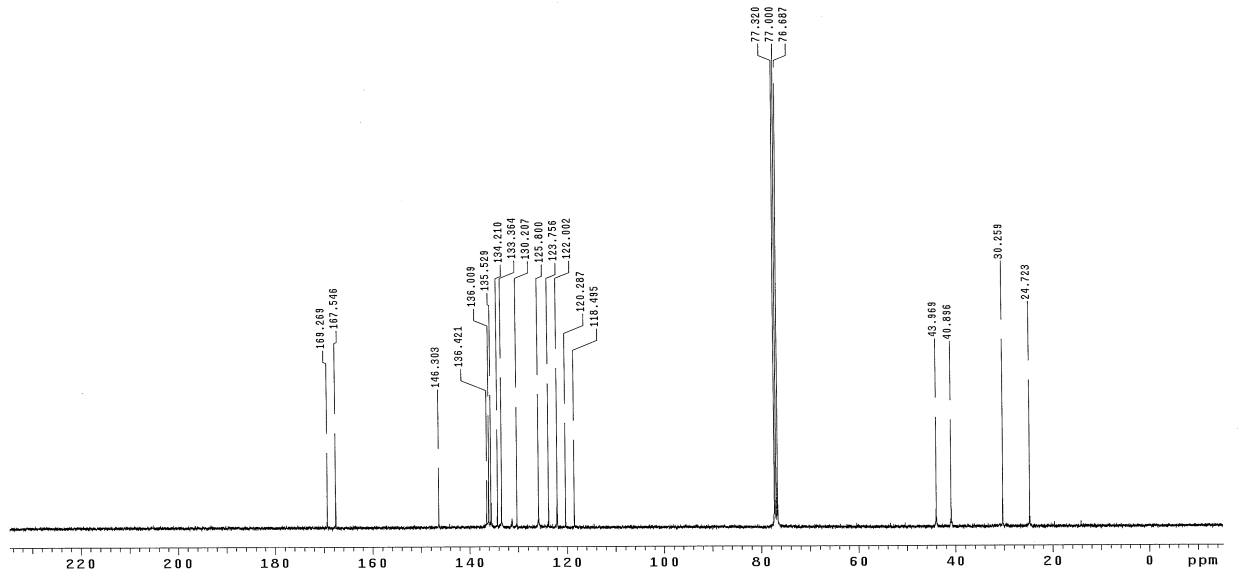

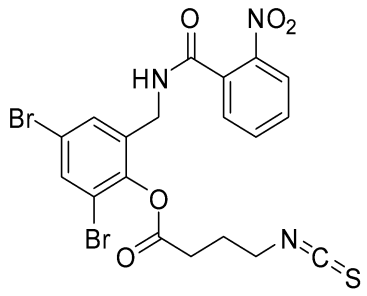

2,4-dibromo-6-((2-nitrobenzamido)methyl)phenyl 4-isothiocyanatobutanoate, 12. (Acetone-d6)

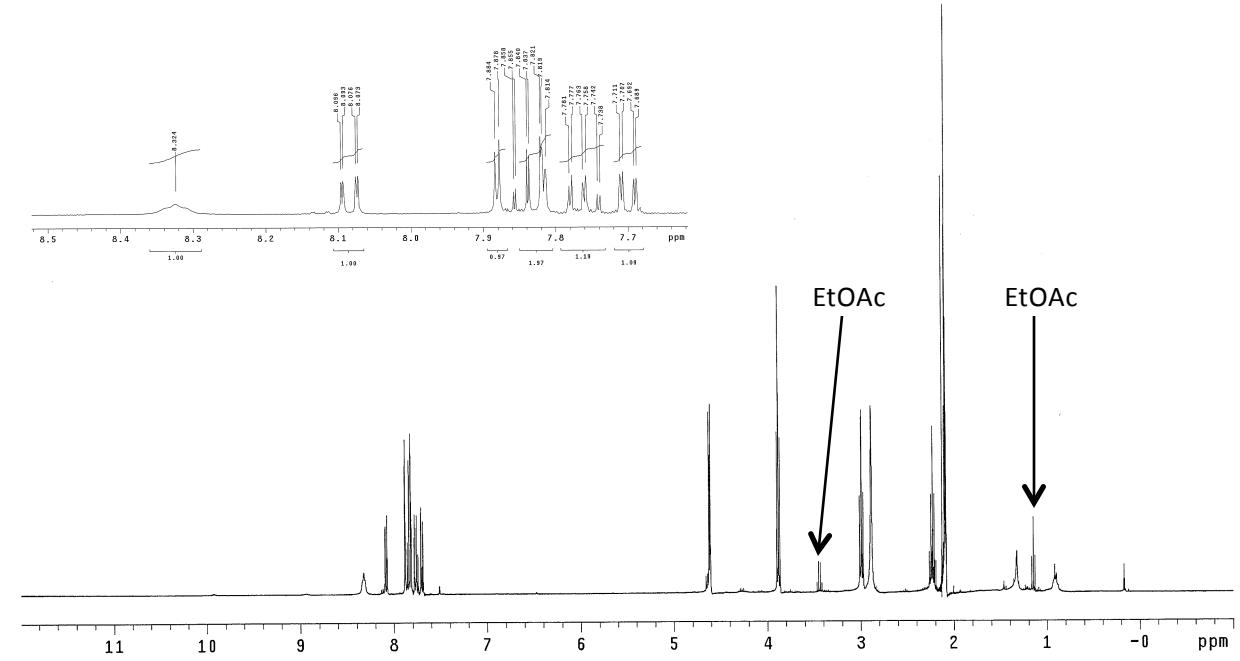

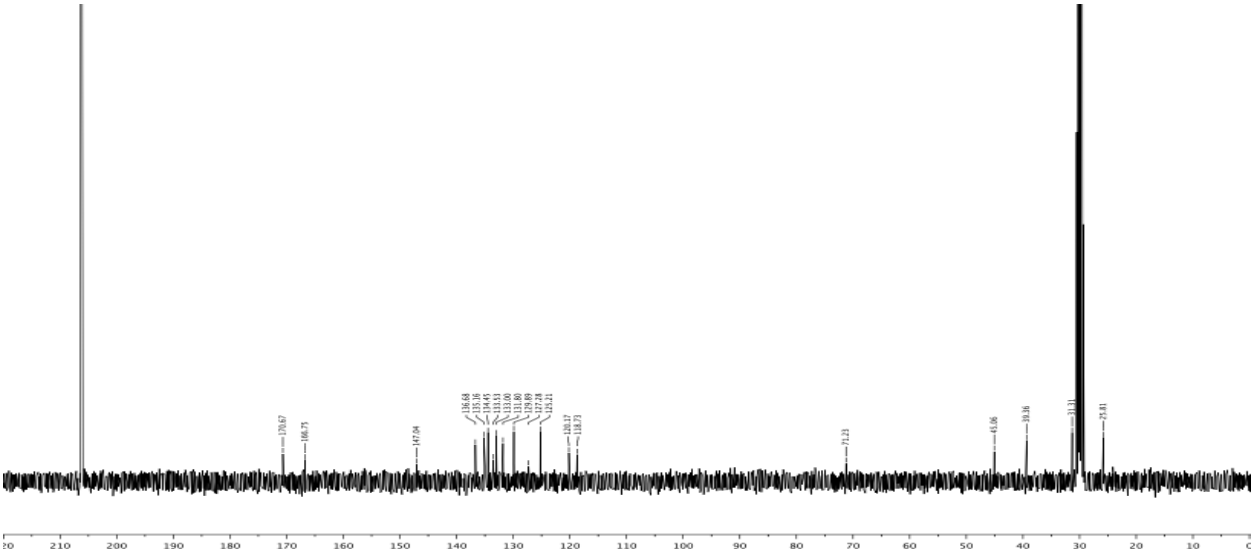

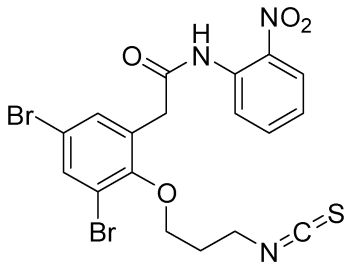

2-(3,5-dibromo-2-(3-isothiocyanatopropoxy)phenyl)-*N*-(2-nitrophenyl)acetamide, 15. ($CDCl_3$)

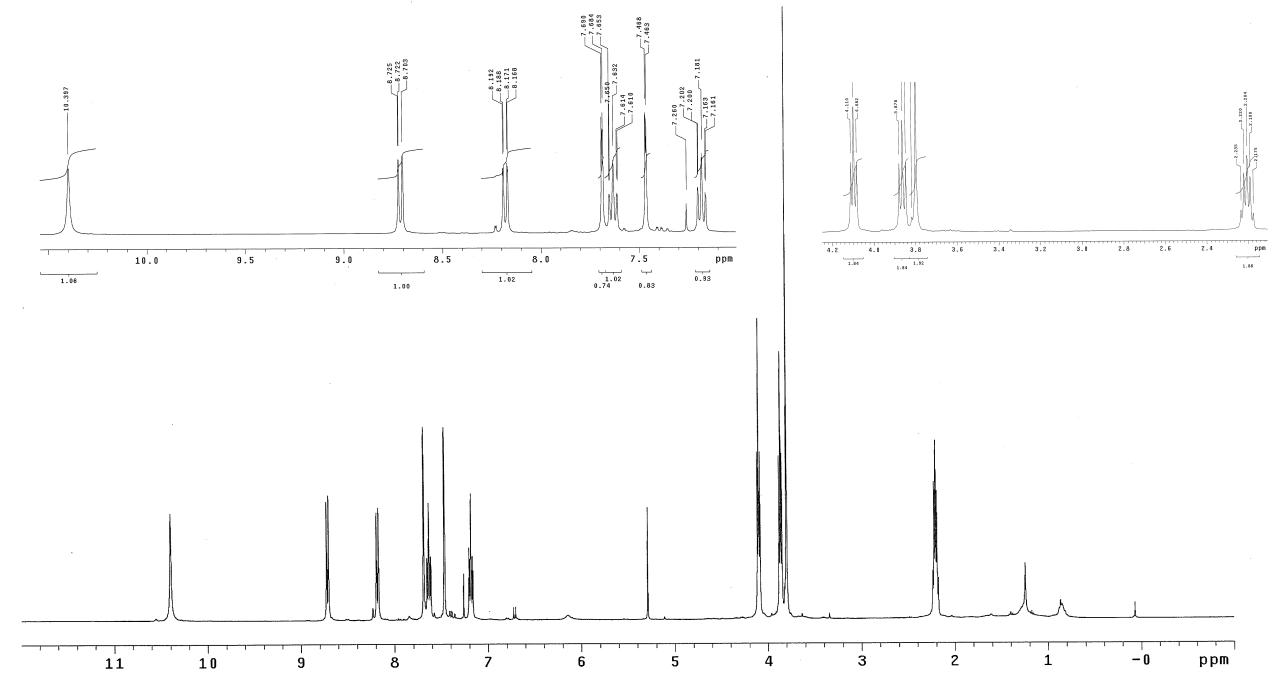

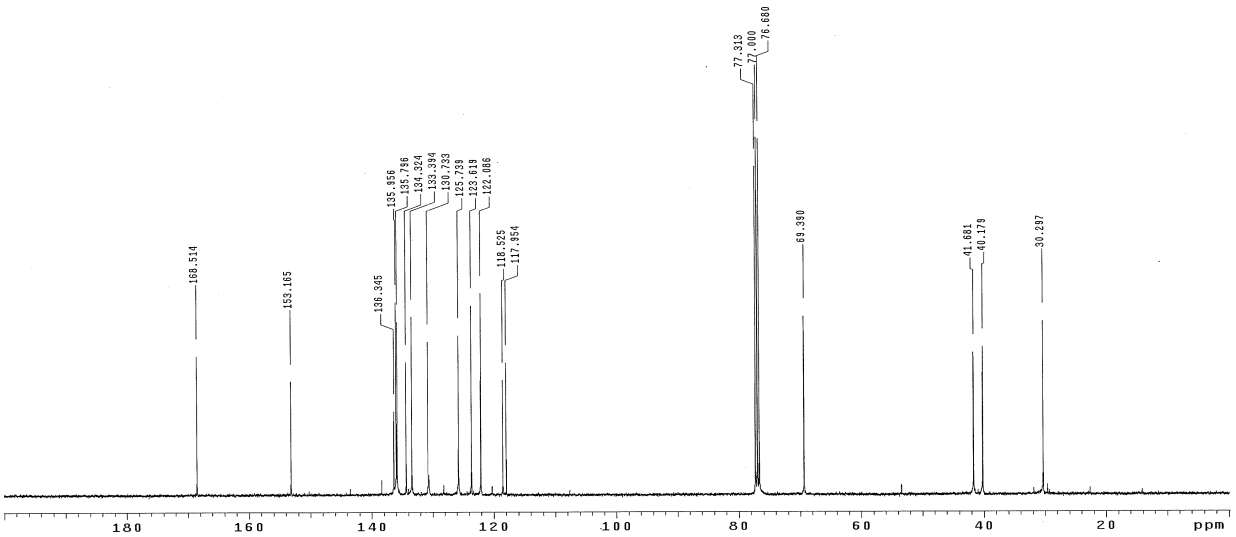

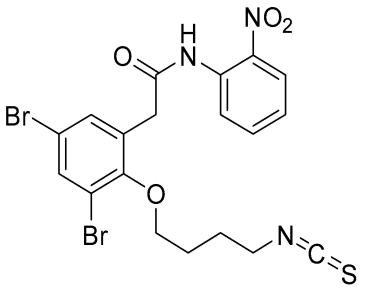

2-(3,5-dibromo-2-(4-isothiocyanatobutoxy)phenyl)-*N*-(2-nitrophenyl)acetamide, 16. ($CDCl_3$)

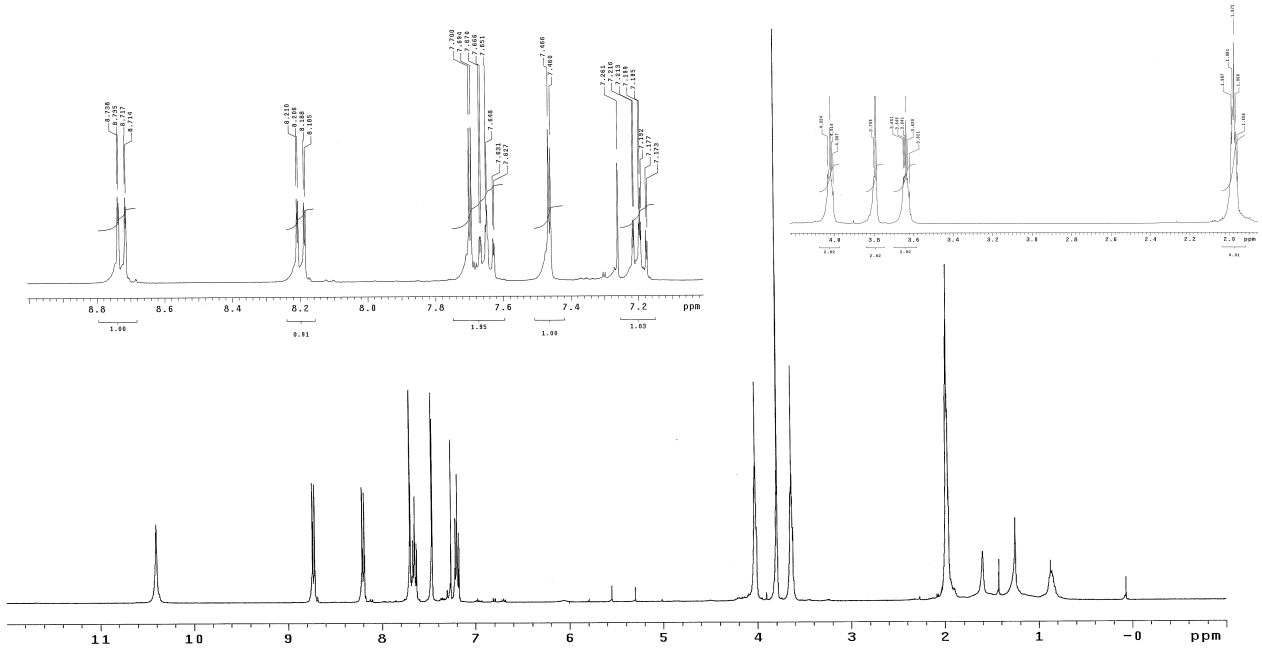

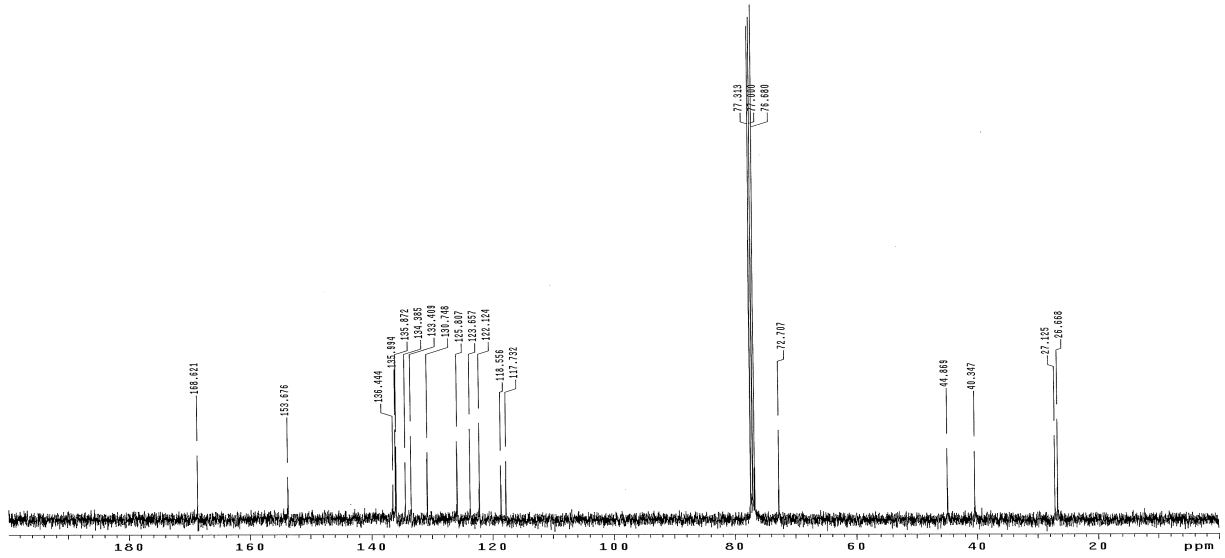

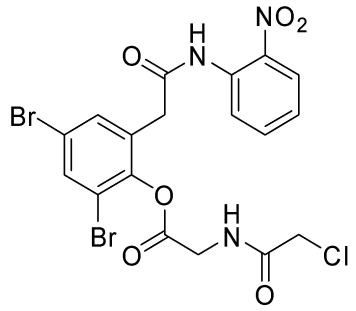

2,4-dibromo-6-(2-((2-nitrophenyl)amino)-2-oxoethyl)phenyl (2-chloroacetyl)glycinate, 17. ($CDCl_3$)

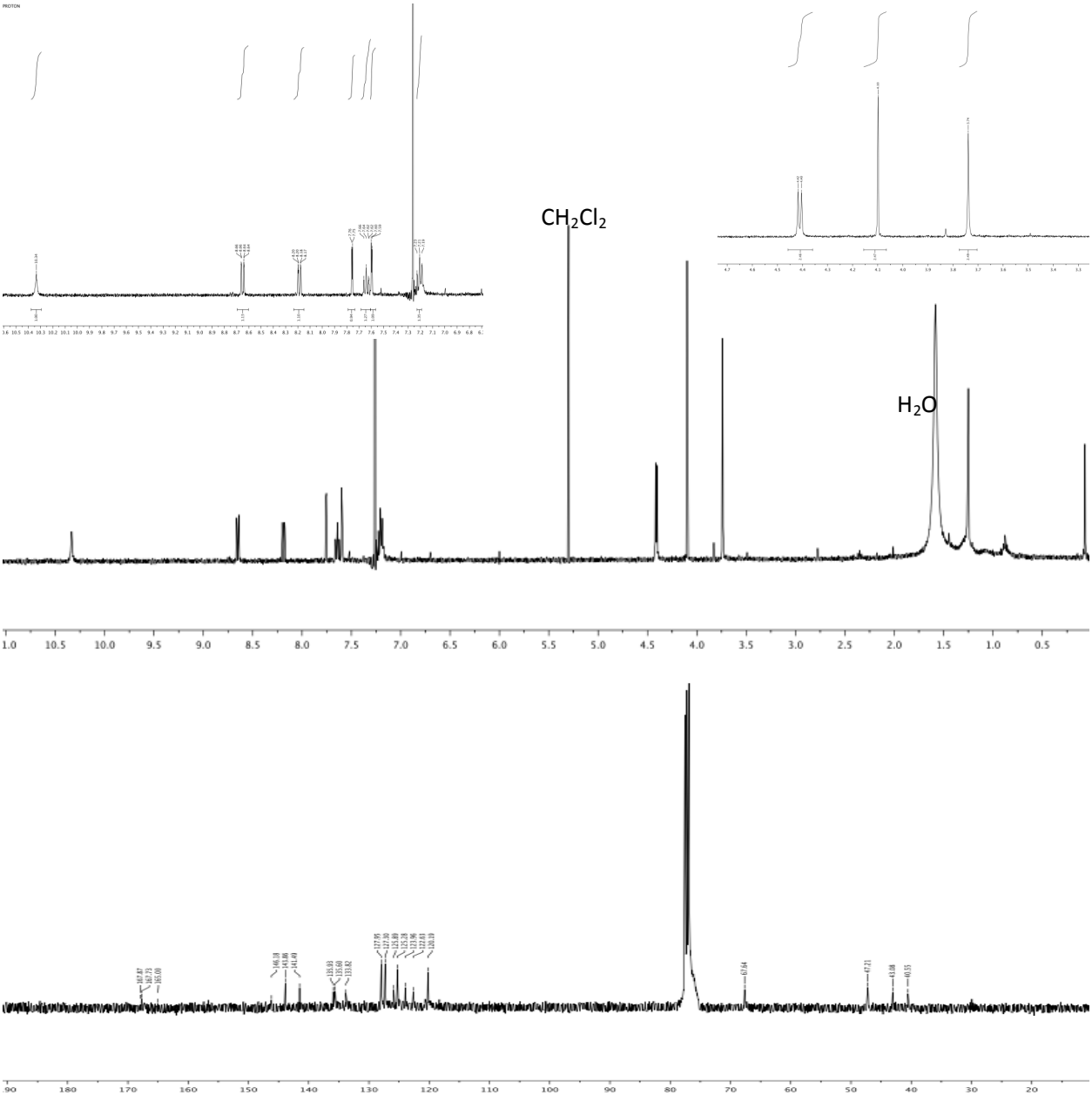

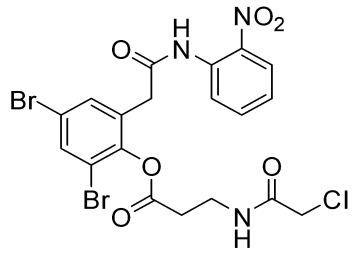

2,4-dibromo-6-(2-((2-nitrophenyl)amino)-2-oxoethyl)phenyl 3-(2-chloroacetamido)propanoate, 18. (^{1}H-NMR in $CDCl_3$, ^{13}C-NMR in DMSO-d6)

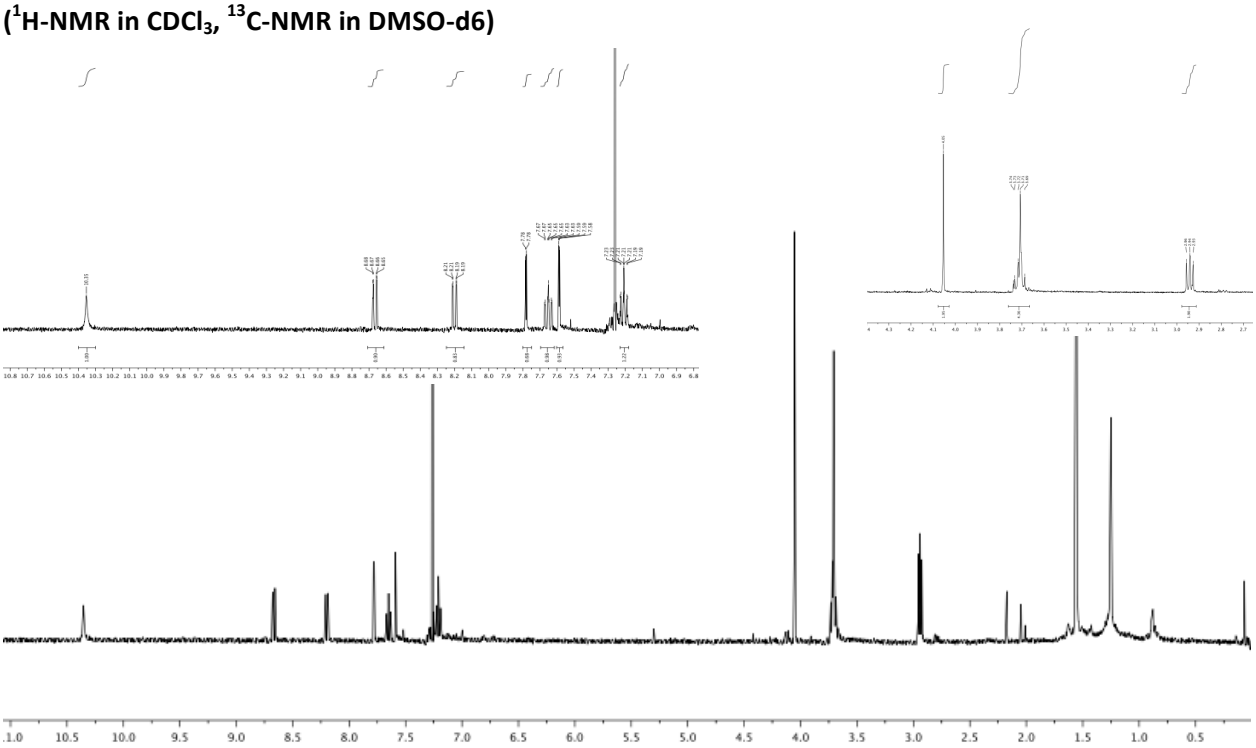

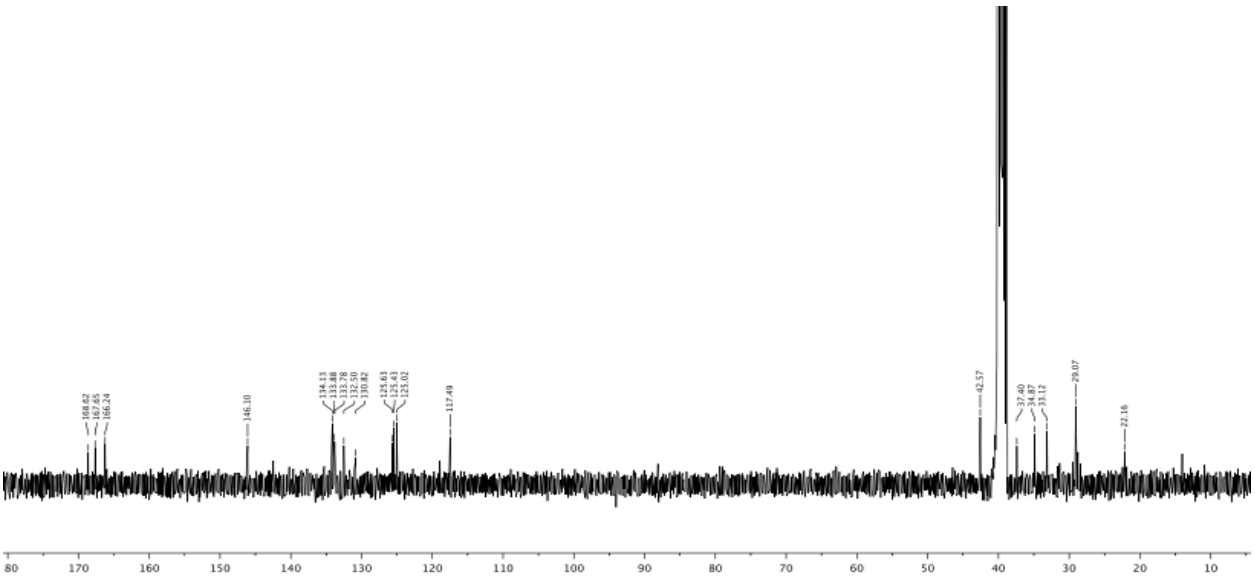

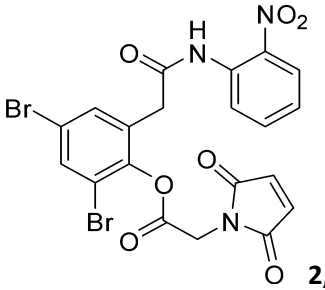

2,4-dibromo-6-(2-((2-nitrophenyl)amino)-2-oxoethyl)phenyl 2-(2,5-dioxo-2,5-dihydro-1*H*-pyrrol-1-yl)acetate, 24. ($CDCl_3$)

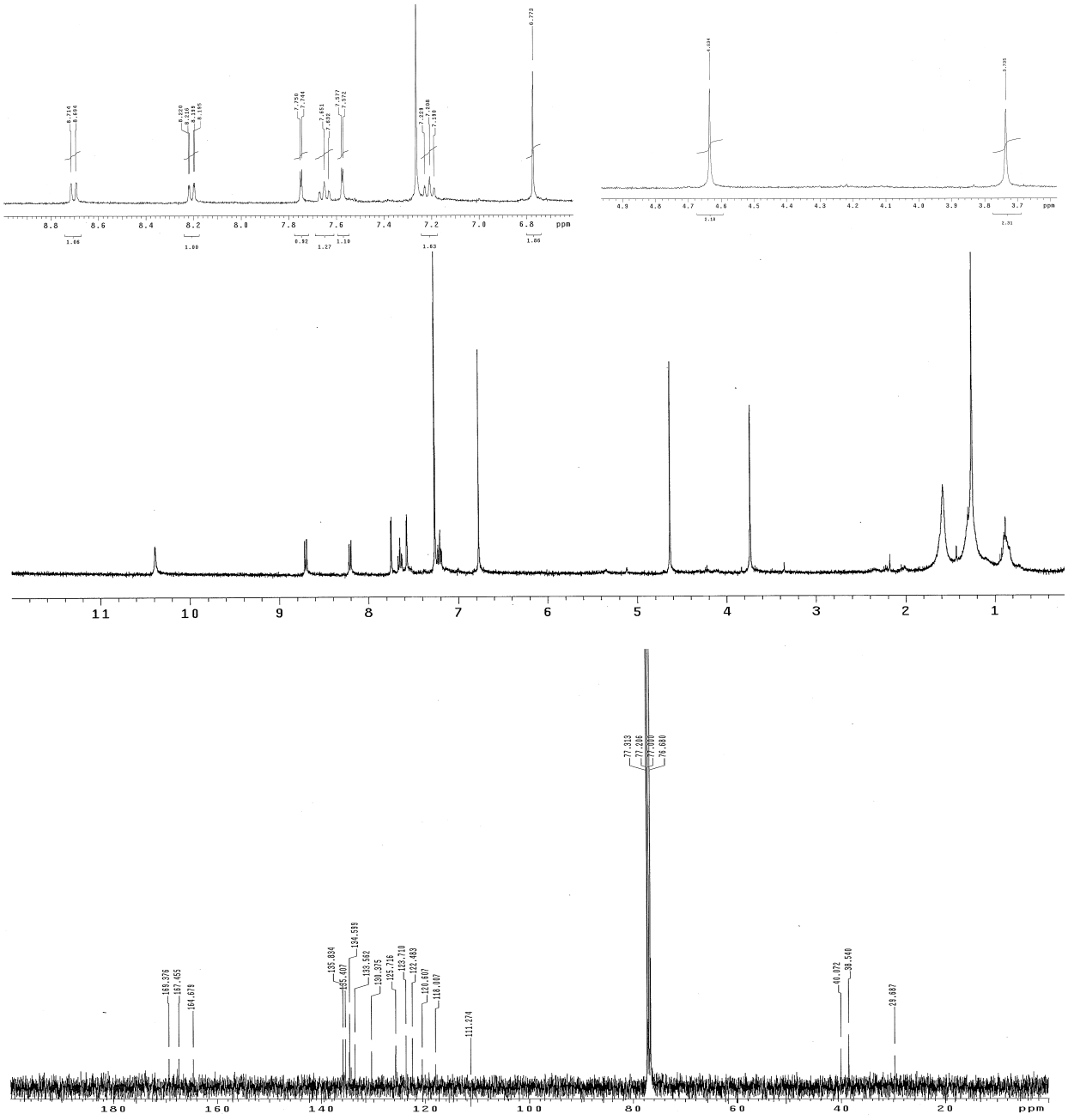

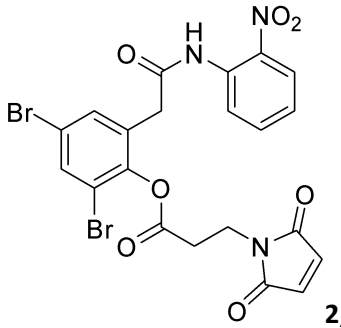

2,4-dibromo-6-(2-((2-nitrophenyl)amino)-2-oxoethyl)phenyl 3-(2,5-dioxo-2,5-dihydro-1*H*-pyrrol-1-yl)propanoate, 25. ($CDCl_3$)

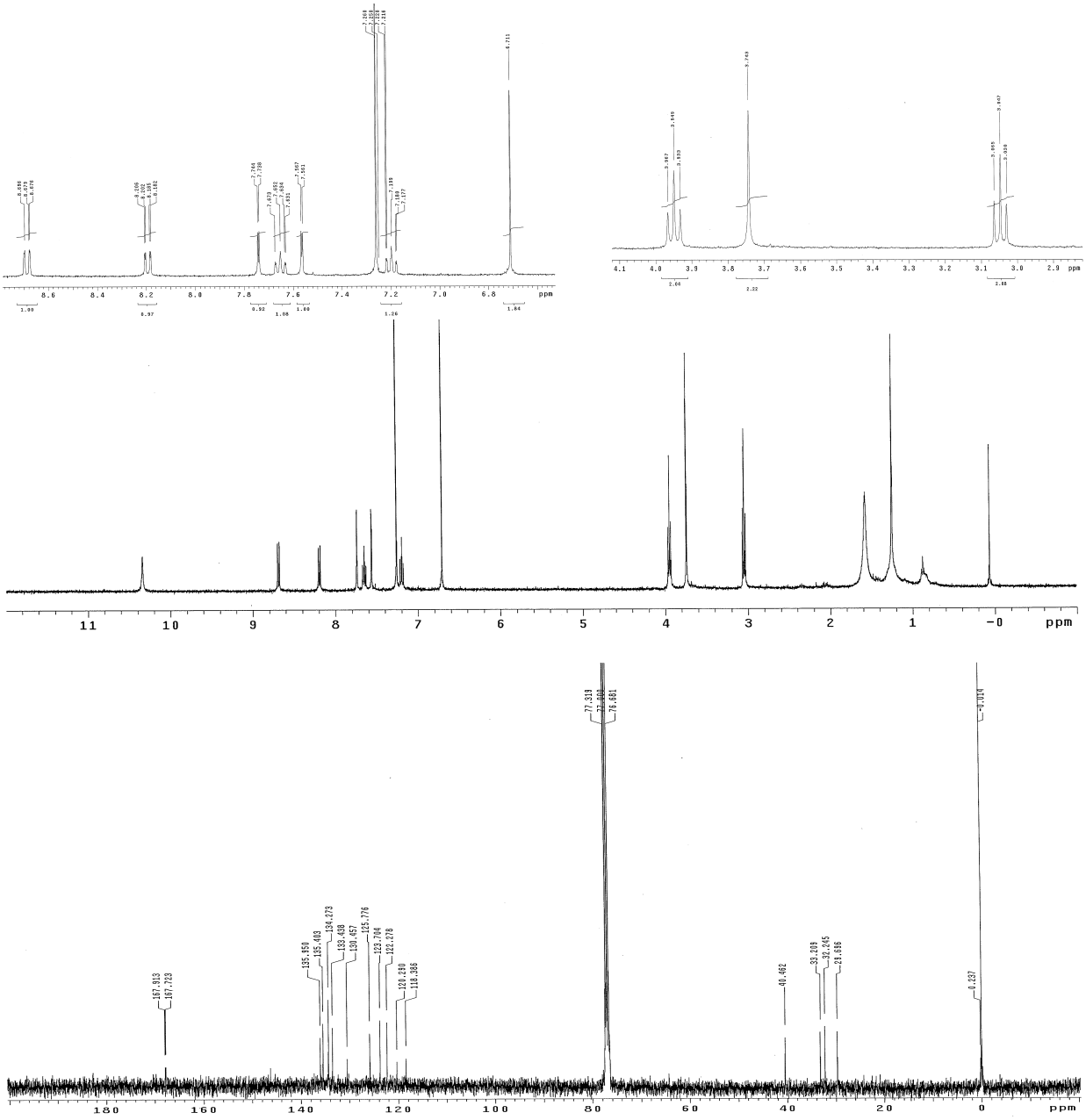

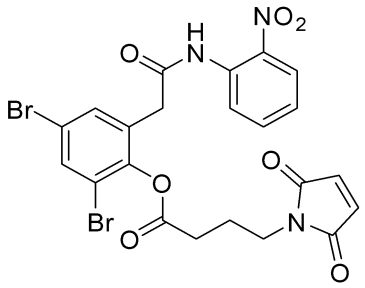

2,4-dibromo-6-(2-((2-nitrophenyl)amino)-2-oxoethyl)phenyl 4-(2,5-dioxo-2,5-dihydro-1*H*-pyrrol-1-yl)butanoate, 26. ($CDCl_3$)

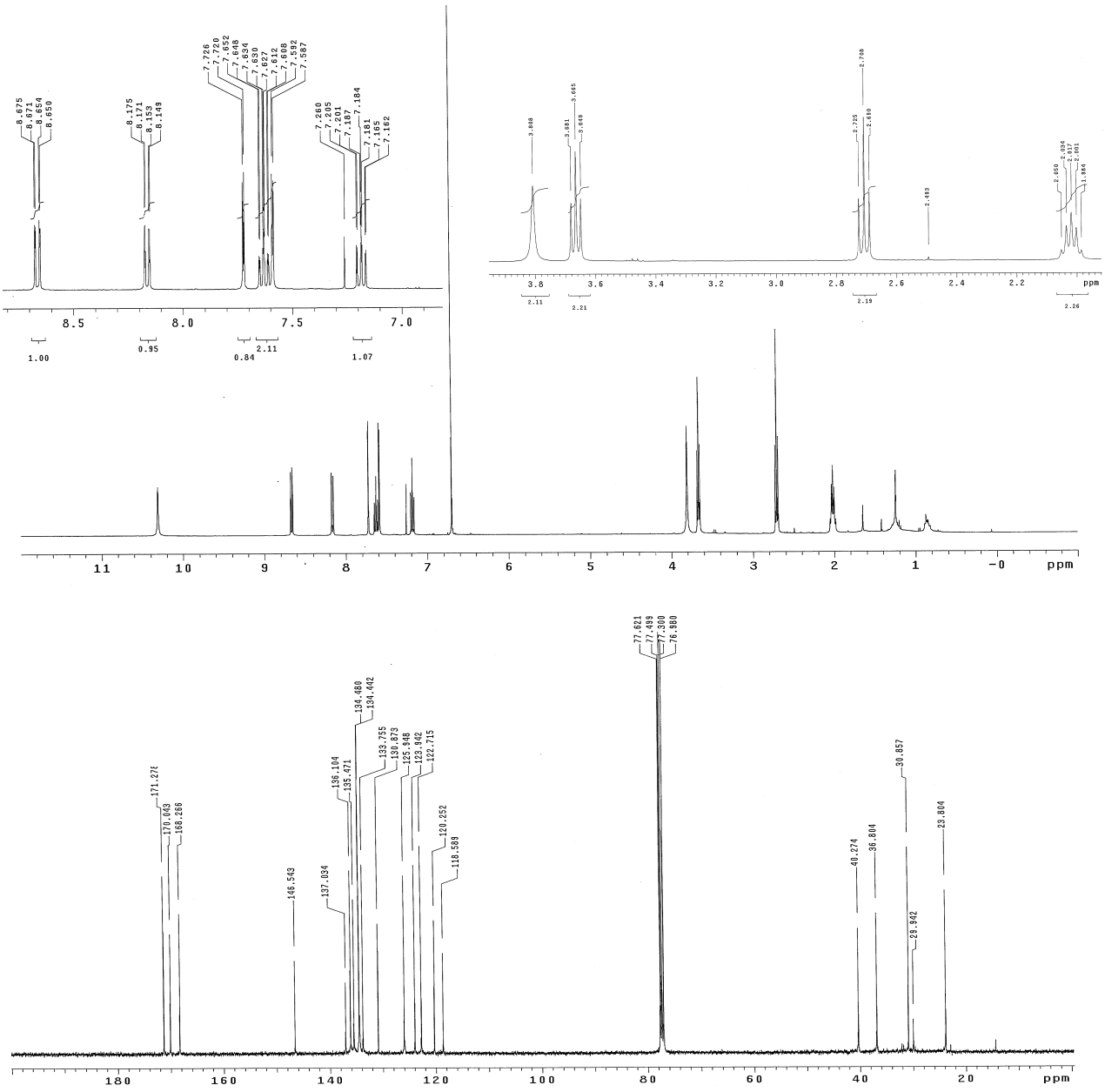

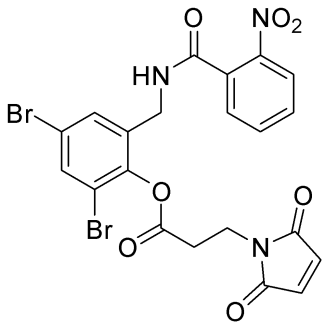

2,4-dibromo-6-((2-nitrobenzamido)methyl)phenyl 3-(2,5-dioxo-2,5-dihydro-1*H*-pyrrol-1-yl)propanoate, 27. ($CDCl_3$)

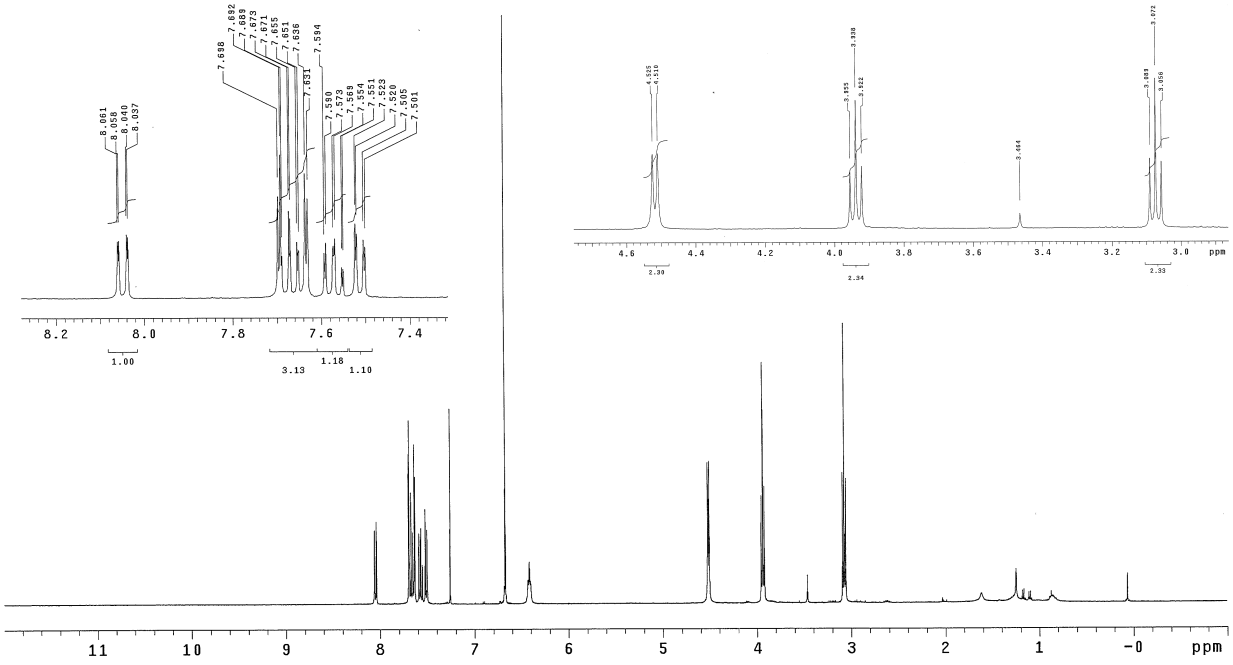

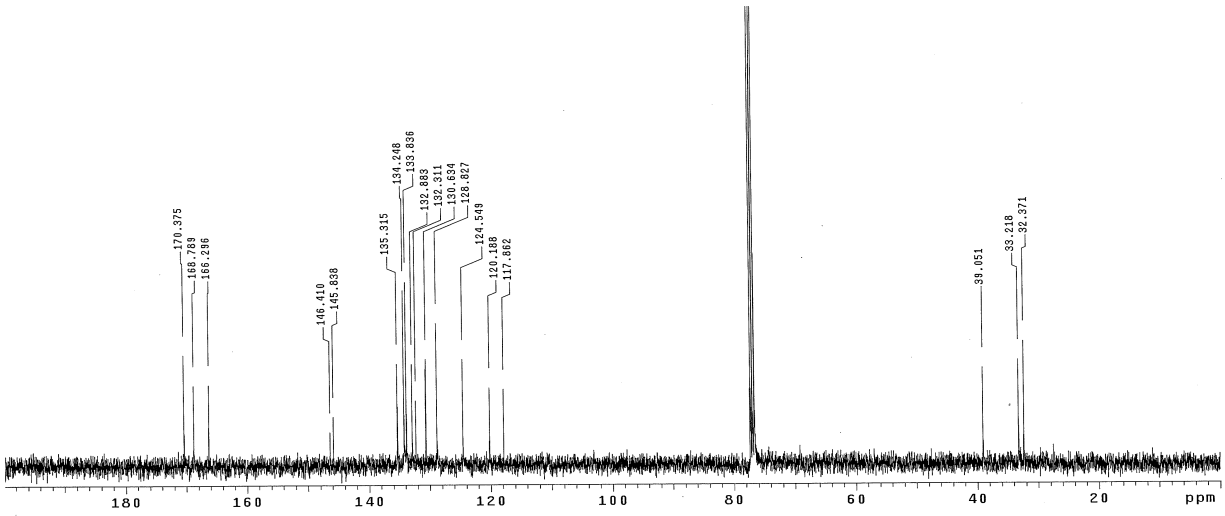

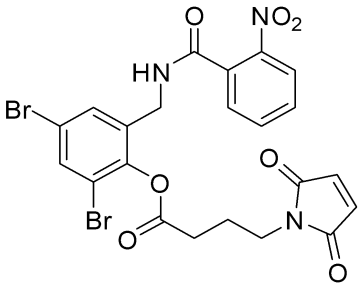

2,4-dibromo-6-((2-nitrobenzamido)methyl)phenyl 4-(2,5-dioxo-2,5-dihydro-1*H*-pyrrol-1-yl)butanoate, 28. ($CDCl_3$)

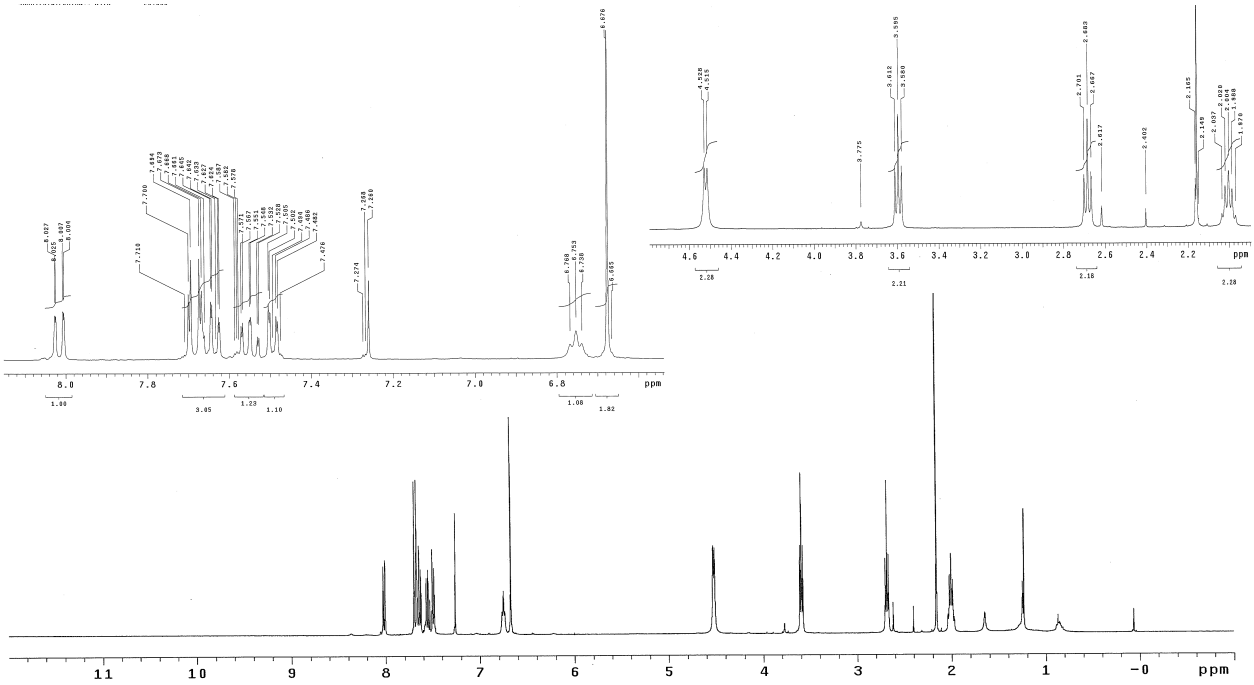

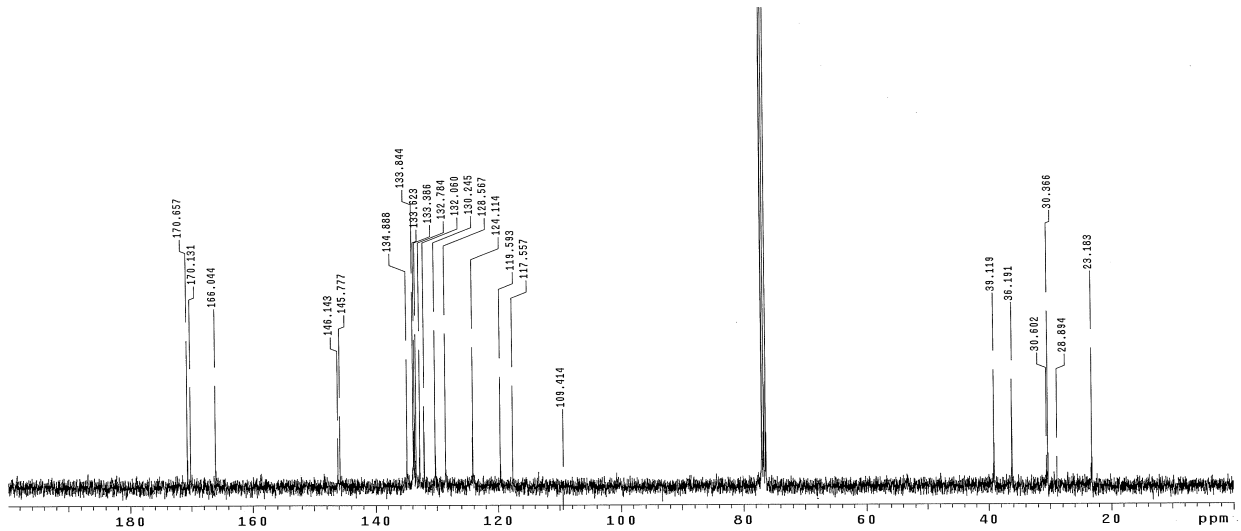

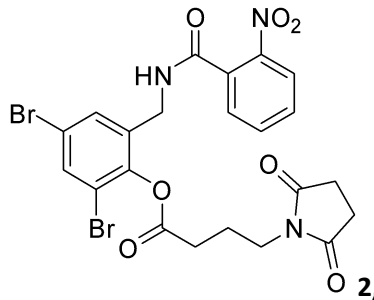

2,4-dibromo-6-((2-nitrobenzamido)methyl)phenyl 4-(2,5-dioxyopyrrolidin-1-yl)butanoate, 29. ($CDCl_3$)

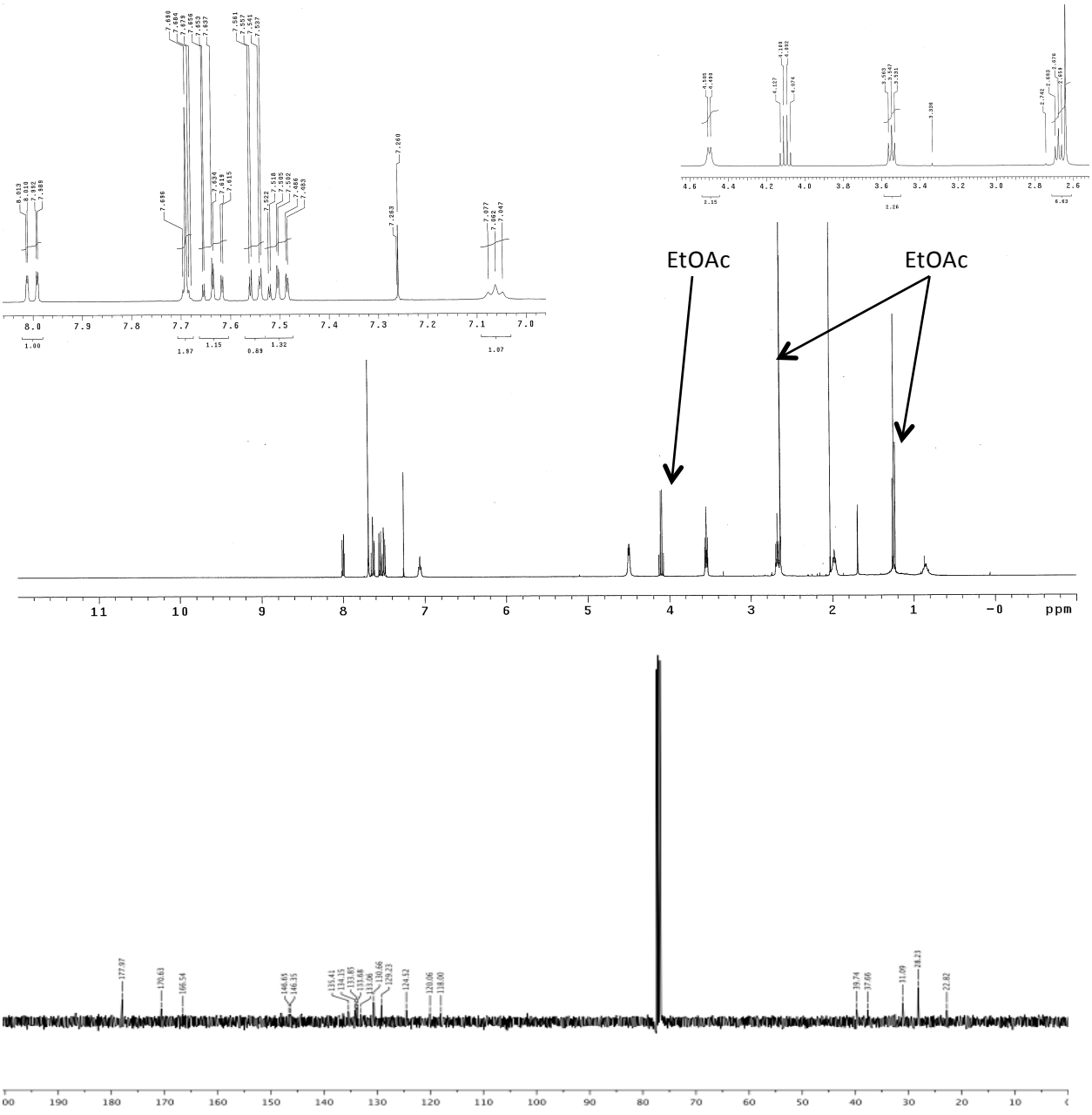

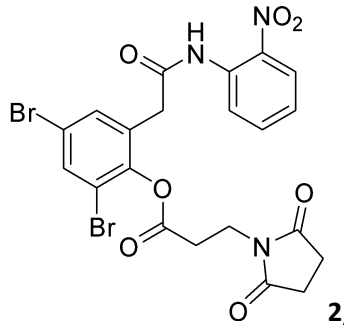

2,4-dibromo-5-(2-((2-nitrophenyl)amino)-2-oxoethyl)phenyl 3-(2,5-dioxopyrrolidin-1-yl)propanoate, 30. ($CDCl_3$)

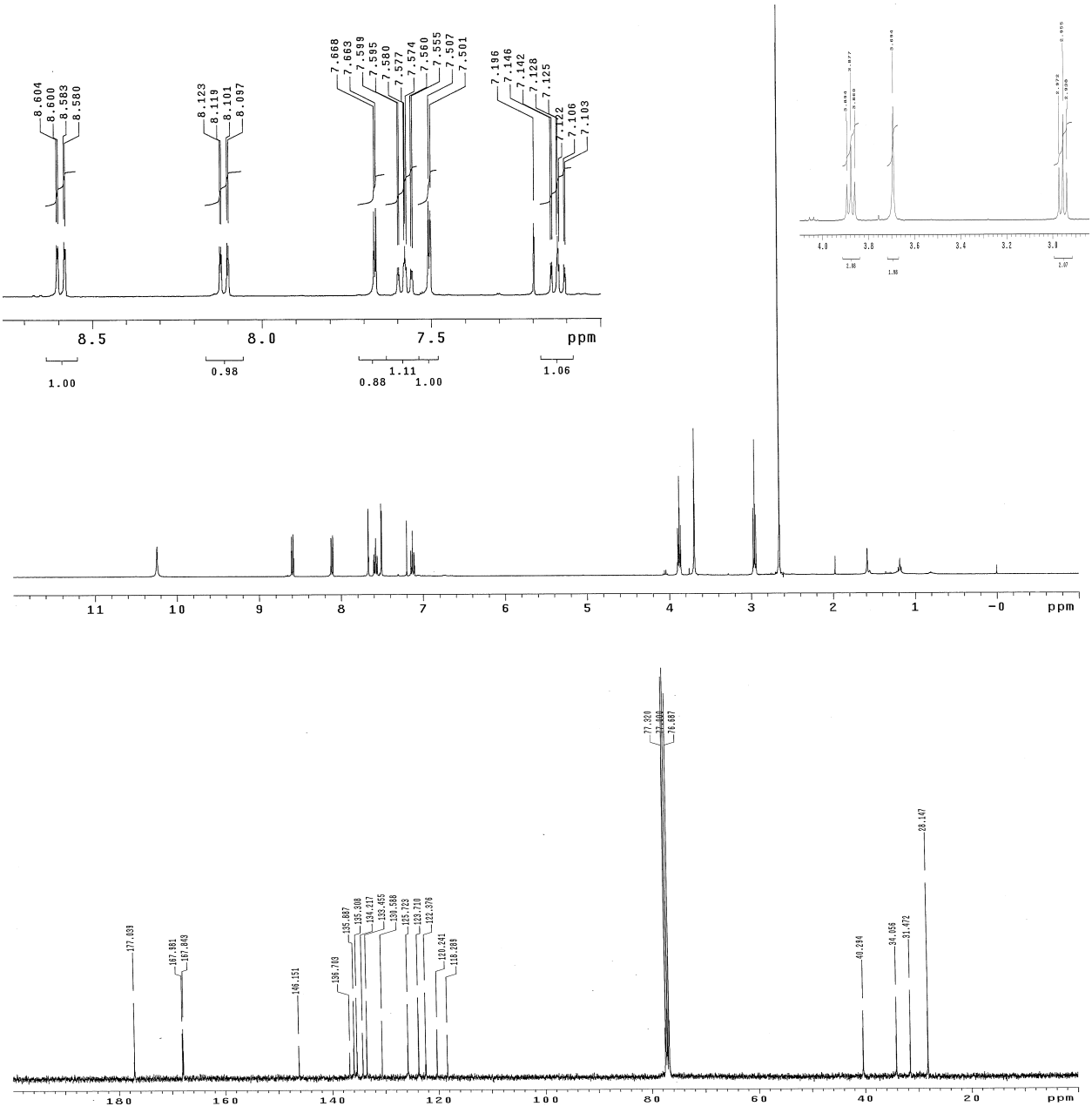

G. Mass Spectra and LC Chromatogram (A_{220}) for all new compounds with tabulated peak integration.

6

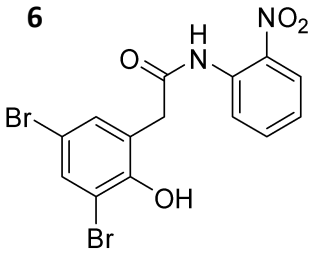

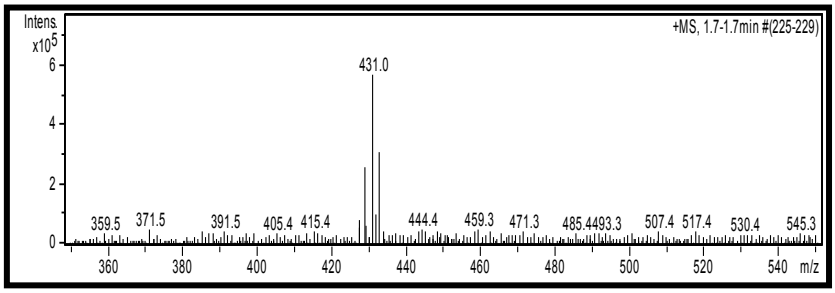

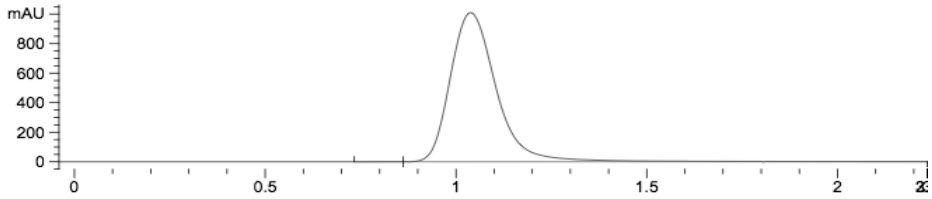

Peak #	RetTime [min]	Type	Width [min]	Area [mAU*s]	Height [mAU]	Area %
1	0.825	BP	0.0592	2.52617	6.51384e-1	0.0299
2	1.039	VB	0.1295	8442.82129	1010.41156	99.9701
Totals :				8445.34746	1011.06294	

9

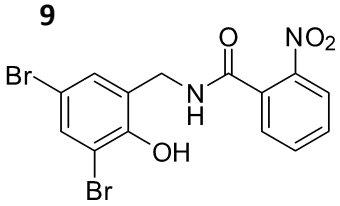

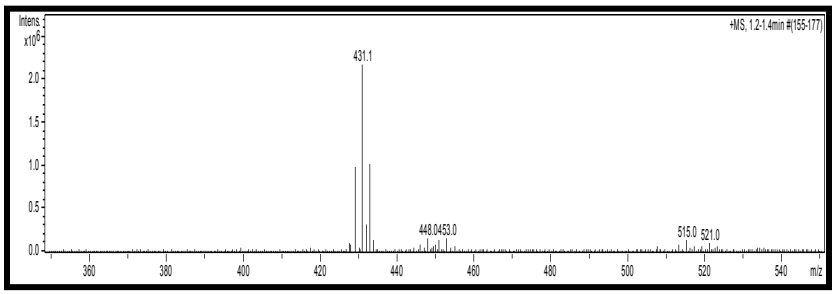

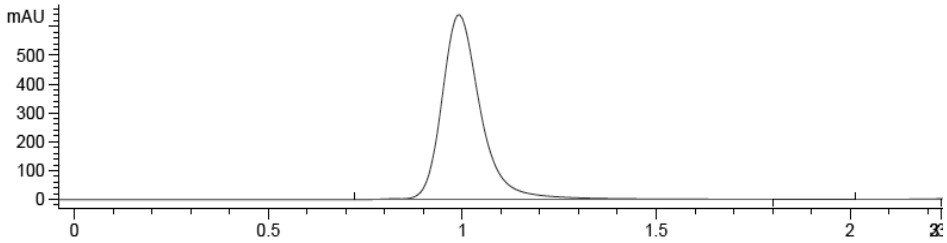

Peak #	RetTime [min]	Type	Width [min]	Area [mAU*s]	Height [mAU]	Area %
1	0.992	BB	0.1059	4504.78418	641.60095	93.8937
2	2.361	BBA	0.8901	292.96429	4.11743	6.1063
Totals :				4797.74847	645.71838	

10

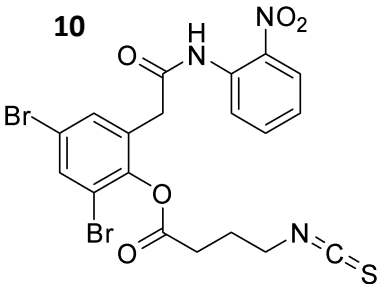

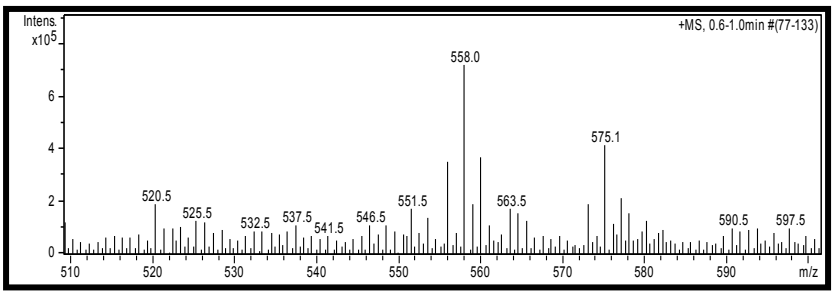

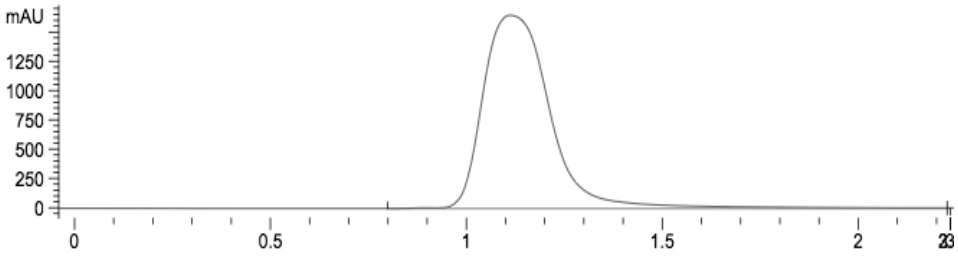

Peak #	RetTime [min]	Type	Width [min]	Area [mAU*s]	Height [mAU]	Area %
1	1.115	PV	0.1887	1.96296e4	1651.35010	96.8843
2	2.538	VBA	0.7550	631.27191	10.94310	3.1157
Totals :				2.02609e4	1662.29320	

11

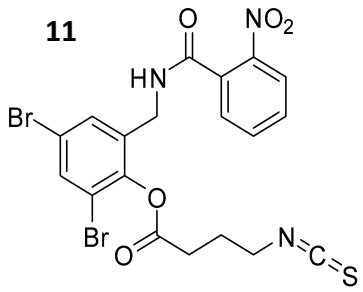

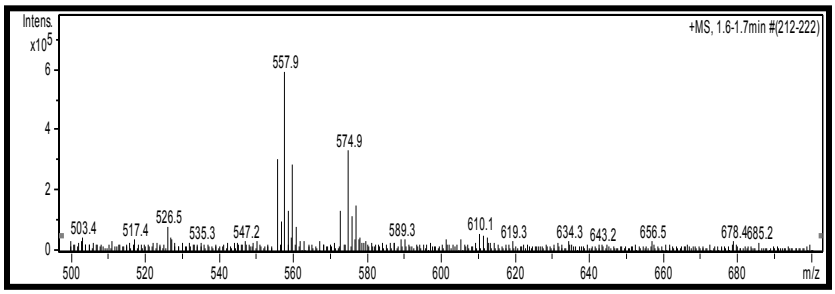

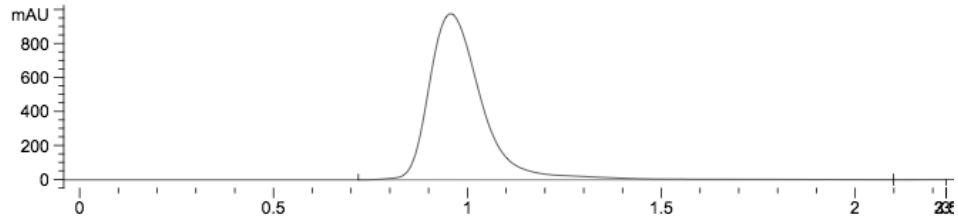

Peak #	RetTime [min]	Type	Width [min]	Area [mAU*s]	Height [mAU]	Area %
1	0.957	PV	0.1451	9144.58984	978.27350	97.8481
2	2.514	VB	0.4033	201.10567	6.60352	2.1519
Totals :				9345.69551	984.87702	

15

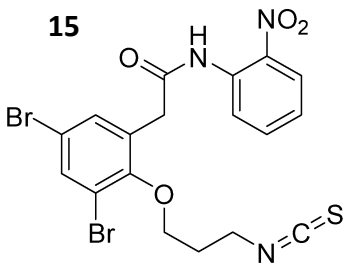

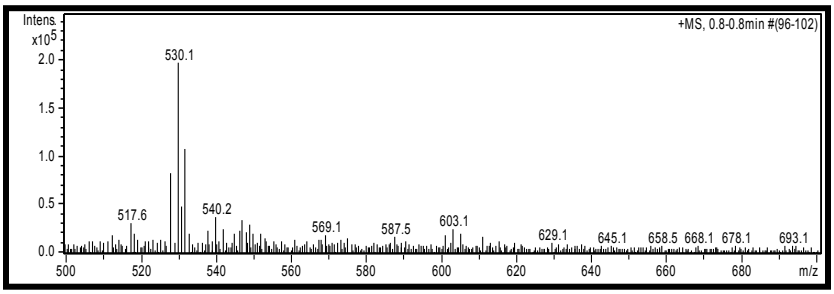

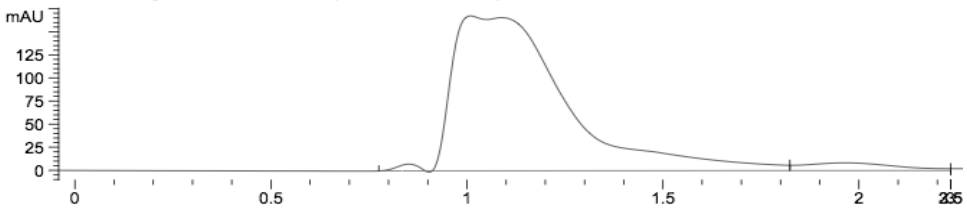

Peak #	RetTime [min]	Type	Width [min]	Area [mAU*s]	Height [mAU]	Area %
1	1.033	PV	0.2651	3367.60474	165.72868	91.8276
2	1.964	VV	0.2489	140.44814	8.49349	3.8297
3	2.609	VB	0.4673	159.26030	4.47401	4.3427
Totals :				3667.31317	178.69619	

16

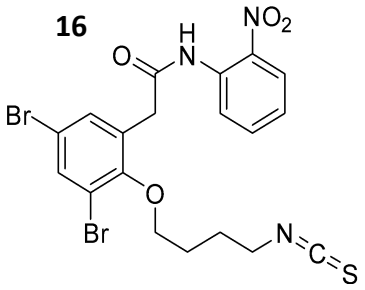

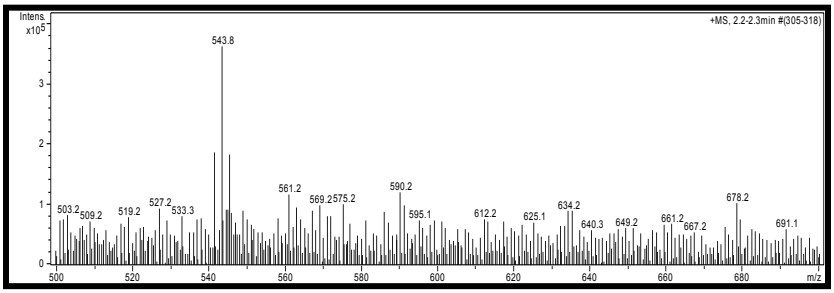

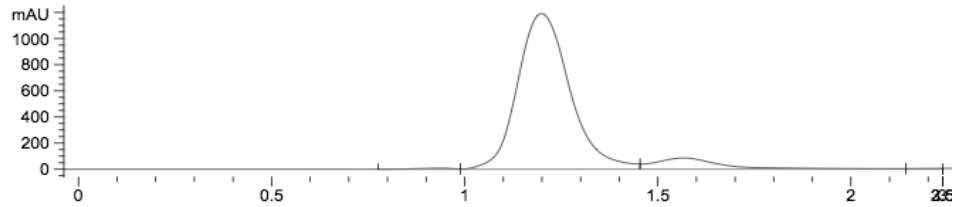

Peak #	RetTime [min]	Type	Width [min]	Area [mAU*s]	Height [mAU]	Area %
1	0.932	BV	0.0942	52.06311	8.41179	0.4178
2	1.199	VV	0.1457	1.12037e4	1191.14478	89.8999
3	1.566	VV	0.1798	1064.02173	86.31525	8.5378
4	2.274	VV	0.2073	104.50057	7.19938	0.8385
5	2.811	VB	0.2178	38.13771	2.42024	0.3060
Totals :				1.24625e4	1295.49142	

17

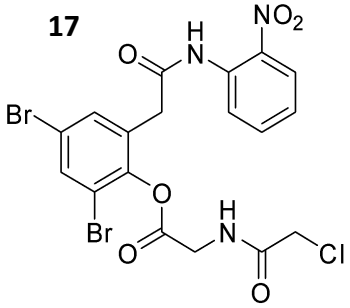

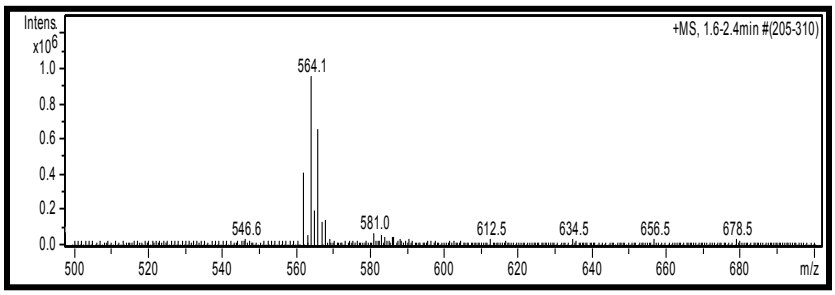

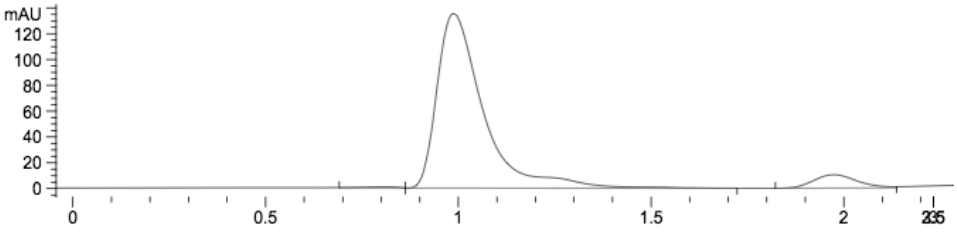

Peak #	RetTime [min]	Type	Width [min]	Area [mAU*s]	Height [mAU]	Area %
1	0.810	BP	0.0935	5.76504	9.15157e-1	0.4739
2	0.989	VP	0.1273	1128.95789	135.35884	92.8049
3	1.974	PV	0.1237	81.76248	10.39786	6.7212
Totals :				1216.48541	146.67185	

18

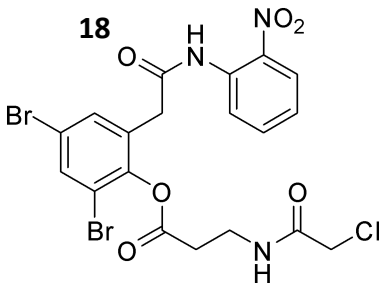

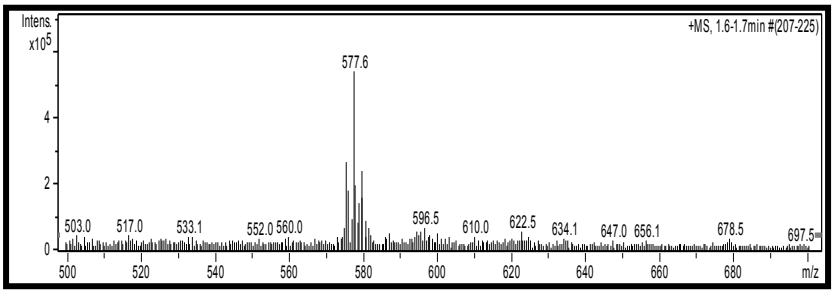

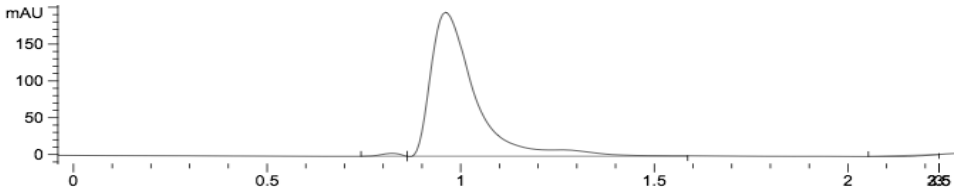

Peak #	RetTime [min]	Type	Width [min]	Area [mAU*s]	Height [mAU]	Area %
1	0.821	PV	0.0553	13.90924	4.12393	0.8456
2	0.963	VB	0.1197	1541.19006	196.00287	93.6918
3	2.329	PB	0.3213	89.85864	3.86405	5.4627
Totals :				1644.95795	203.99085	

24

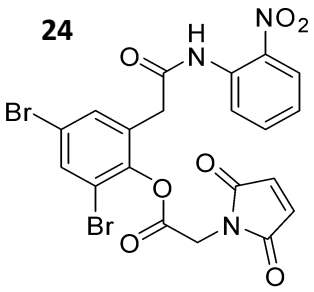

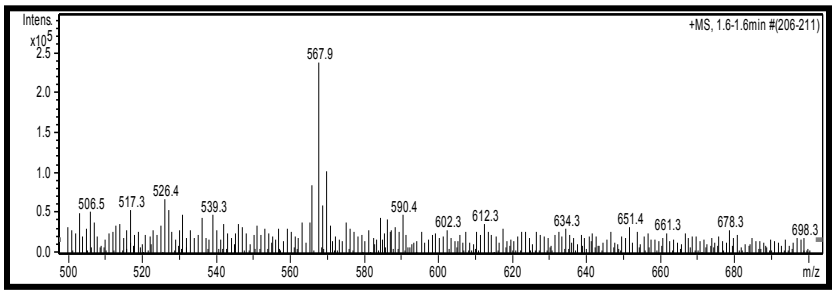

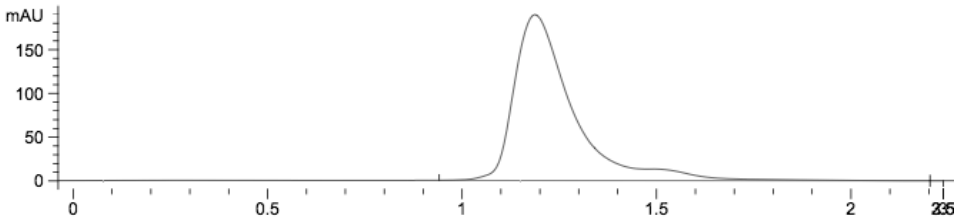

Peak #	RetTime [min]	Type	Width [min]	Area [mAU*s]	Height [mAU]	Area %
1	1.188	BP	0.1562	1984.11047	189.47176	99.2341
2	2.482	VP	0.1380	15.31320	1.68606	0.7659
Totals :				1999.42368	191.15782	

25

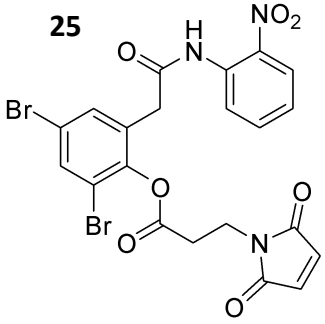

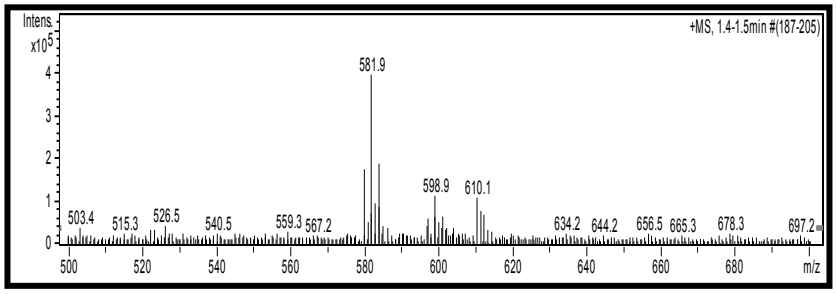

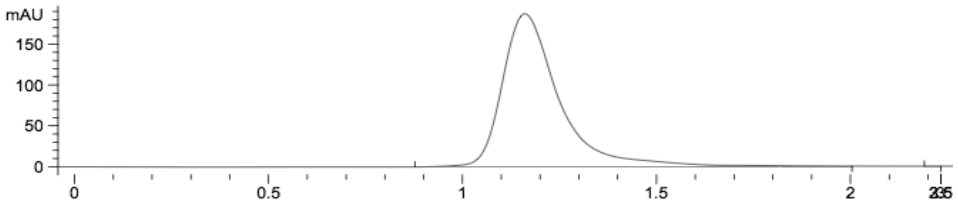

Peak #	RetTime [min]	Type	Width [min]	Area [mAU*s]	Height [mAU]	Area %
1	1.161	BB	0.1531	1914.84656	187.60013	96.7954
2	2.431	BB	0.4305	63.39565	1.89408	3.2046
Totals :				1978.24221	189.49421	

26

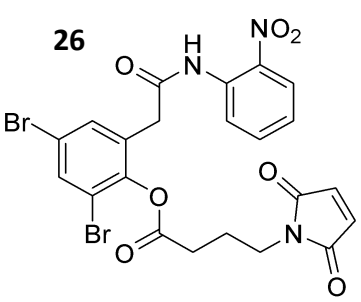

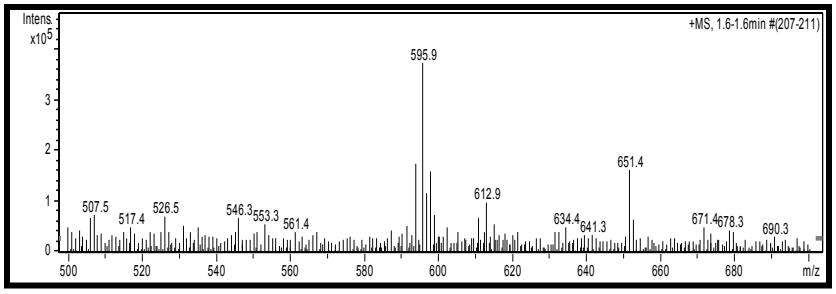

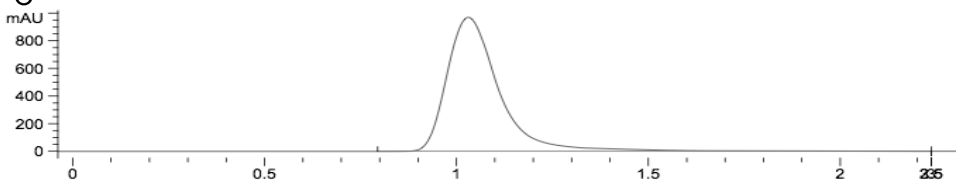

Peak #	RetTime [min]	Type	Width [min]	Area [mAU*s]	Height [mAU]	Area %
1	1.031	BV	0.1436	9118.53906	970.75641	99.6552
2	2.507	VB	0.2239	31.54737	1.93843	0.3448
Totals :				9150.08643	972.69484	

27

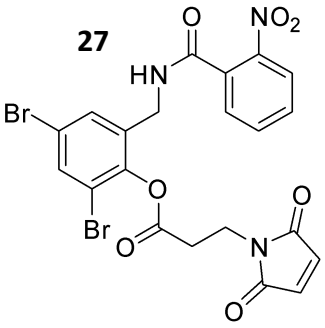

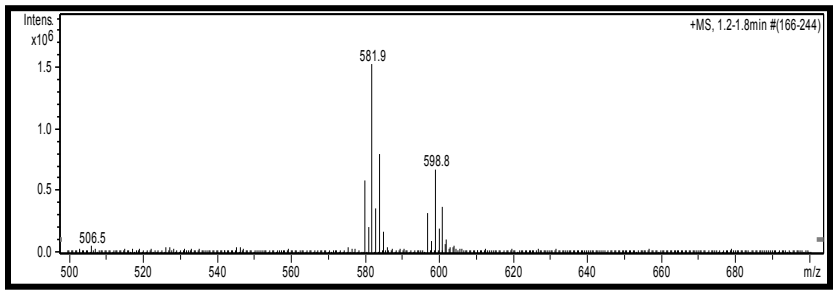

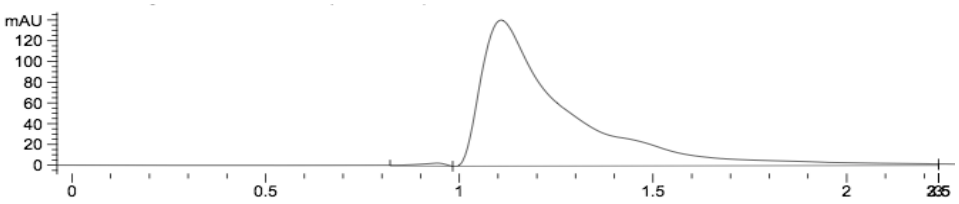

Peak #	RetTime [min]	Type	Width [min]	Area [mAU*s]	Height [mAU]	Area %
1	0.937	BP	0.0774	15.20945	2.88924	0.6974
2	1.109	VV	0.2096	2120.77979	140.90456	97.2456
3	2.486	VB	0.2606	44.86017	2.35166	2.0570
Totals :				2180.84940	146.14546	

28

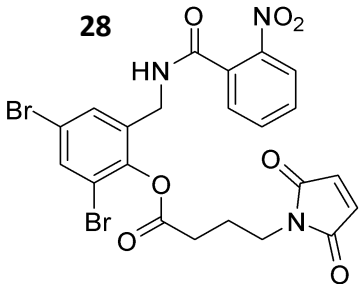

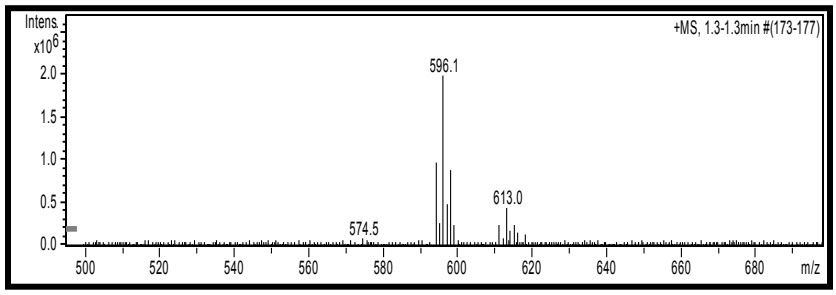

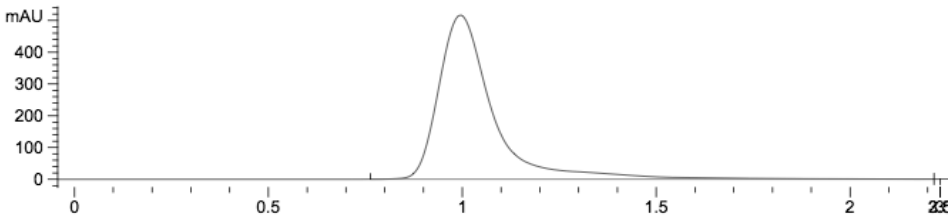

Peak #	RetTime [min]	Type	Width [min]	Area [mAU*s]	Height [mAU]	Area %
1	0.995	BB	0.1447	4990.26562	516.53094	99.4564
2	2.398	BB	0.2188	27.27489	1.75953	0.5436
Totals :				5017.54052	518.29047	

29

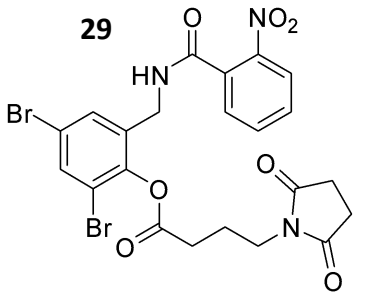

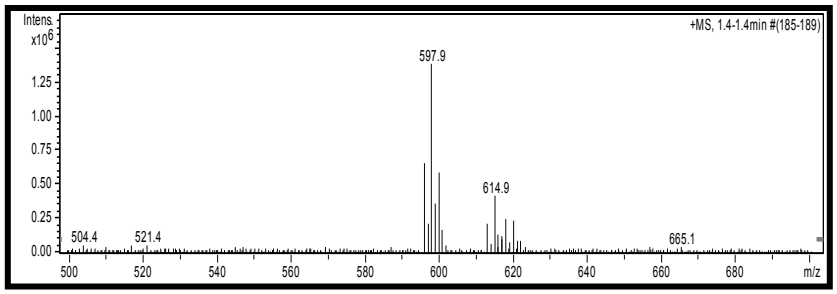

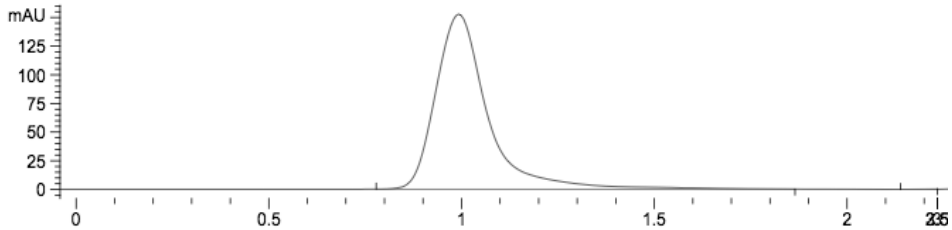

Peak #	RetTime [min]	Type	Width [min]	Area [mAU*s]	Height [mAU]	Area %
1	0.992	BB	0.1438	1437.31592	152.73764	98.6457
2	2.376	PB	0.2265	19.73282	1.24784	1.3543
Totals :				1457.04874	153.98548	

30

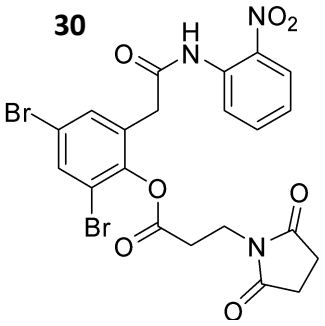

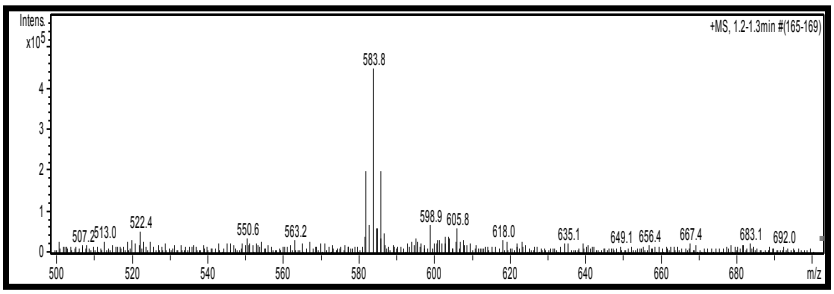

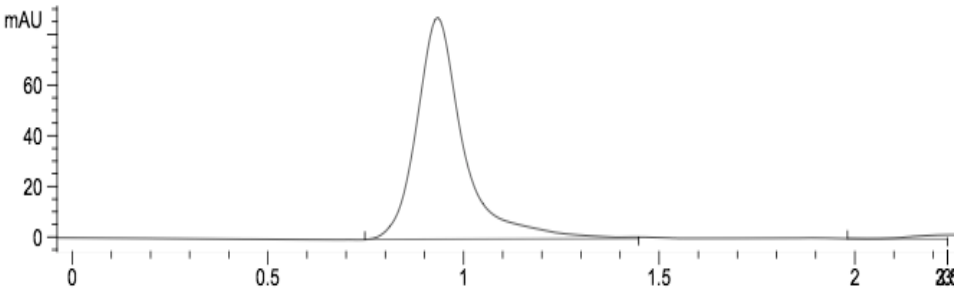

Peak #	RetTime [min]	Type	Width [min]	Area [mAU*s]	Height [mAU]	Area %
1	0.933	PB	0.1231	728.88214	87.56658	91.3557
2	2.440	PB	0.4709	68.96824	1.83333	8.6443
Totals :				797.85038	89.39991	

H. Supporting Discussion.

The recently published crystal structure of TP1 (**2** in the manuscript) complexed to the ligand binding domain of LasR [PDB 3IX4; Zou, Y.; Nair, S. K. Molecular Basis for the Recognition of Structurally Distinct Autoinducer Mimics by the Pseudomonas Aeruginosa LasR Quorum-Sensing Signaling Receptor. *Chemistry & Biology* **2009**, *16*, 961–970] informed the placement of electrophilic functionality in our analog series. The ligand (TP1, **2**) binds in the HSL ligand binding pocket and places the 2-chloro benzoate ester in close proximity to C79 of LasR as highlighted in the following images. In these images the ligand (TP1, **2**) is shown in magenta and the side chain of LasR Cys79 is shown. Measurements are in Angstroms. Images and measurements created using PyMOL.

Side View:

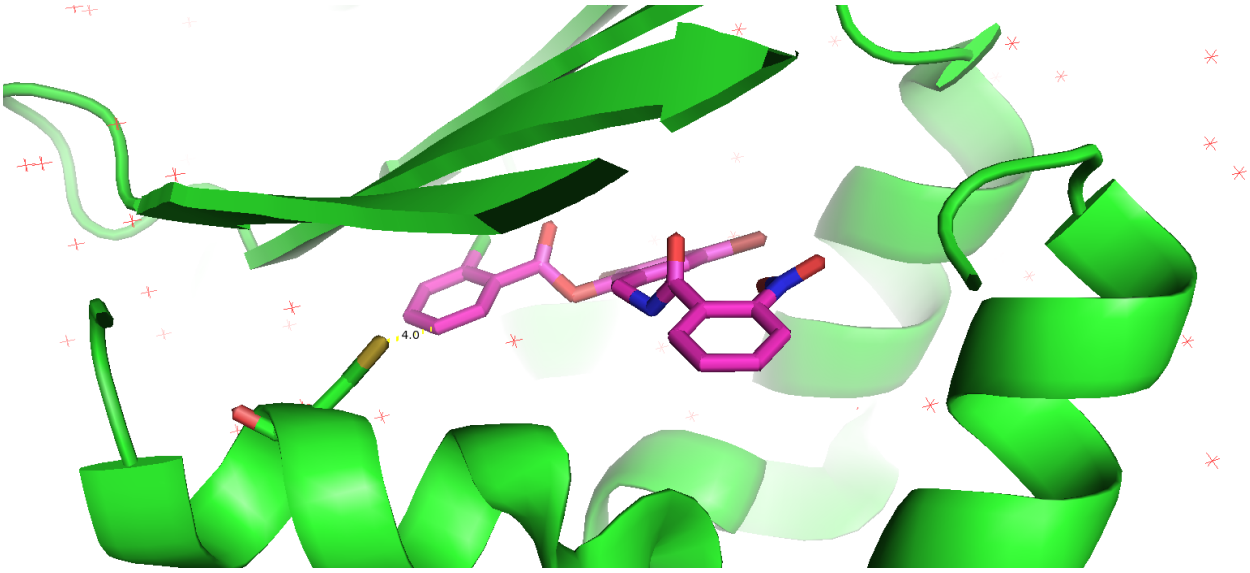

Top View: